Analysis of the Activities of the Inflammatory Cytokine Macrophage Migration Inhibitory Factor on Activation of Endoplasmic Reticulum Stress Responses.

Alistair Gordon Shaw

University of East London
School of Health, Sport and Bioscience

A thesis submitted in partial fulfilment of the requirements of the University of East London for the degree of Master of Research (MRes) in Bioscience
2018

Declaration

I hereby declare that the work presented within this thesis is the result of my own investigation except where a reference has been made to published literature or acknowledgement is made for unpublished research. While registered as a research degree student at UEL, I have not been a registered or enrolled for another award of this university or of any other academic or professional institution.

Alistair Gordon Shaw

Abstract:

The inflammatory cytokine, Macrophage Migration Inhibitory Factor, was initially isolated in the 1970s as a chemokine involved with inhibition of random movement in Macrophages but has also been linked with many other components of the immune system and even foetal development. It is released almost-ubiquitously, during inflammation, with both pro-inflammatory and anti-inflammatory activities. One key regulator of inflammation is the Unfolded Protein Response. during which the Endoplasmic Reticulum within cells regulates protein flux within the ER lumen, especially when that load is beyond the capacity of the ER to successfully process. As part of the UPR response there is a stop in global translation, enhanced transcription and translation of chaperone proteins, increased ER size and capacity and eventually activation of the apoptosis pathways if the protein load does not reduce to a level within the ER's capacity. The UPR is controlled via the transduction proteins, IRE1, PERK and ATF6. Because of the UPR's effect on cellular health and known links to inflammation it was decided to investigate the effects of MIF on UPR activation within cells. Using two different reporter constructs (ATF4.EYFP-N1 or XBP-1.EeYFP-N1) which monitor activation IRE1 and PERK the effects of MIF on UPR activation in HeLa and SH-SY5Y cells was assessed. The observed results show that MIF exerts a marginal suppressive effect on both the IRE1 and PERK between with some variation in the effects of MIF on epithelial (HeLa) or neuronal (SH-SY5Y) origins. This data suggests that MIF may reduce the activation of apoptotic responses within these cells via activation UPR and the PERK pathway through suppression of JNK activity via the noncanonical MIF receptor JAB1. Modulation of UPR responses by MIF would have important downstream effects on the development of auto-inflammatory conditions and neuropathies include Alzheimer's disease due to the suppressed UPRs inability to resolve the pathological protein load.

Contents Page:

List of Figures:

List of Tables:

List of Appendices:

List of abbreviations:

eIF4E-BP1	Eukaryotic Initiation Factor 4E Binding Protein 1
AP-1	Activator Protein 1
APC	Antigen-Presenting Cell
AU	Arbitrary Unit
ATF4	Activating Transcription Factor 4
ATF6	Activating Transcription Factor 6
BiP	Binding Immunoglobulin Protein
CD	Cluster of Differentiation
cDNA	Complementary DNA
CHOP	C/EBP Homologous Protein
CXCR	C-X-C Chemokine Receptor
D-DT	D-Dopachrome Tautomerase
DMEM	Dulbecco's Modified Eagle's Medium
DNA	Deoxyribonucleic Acid
dNTPs	Deoxyribonucleotide Triphosphates
DPBS	Dulbecco's Phosphate-Buffered Saline

EDTA	Ethylenediaminetetraacetic acid
eIF2α	Elongation Initiation Factor 2 Alpha
ER	Endoplasmic Reticulum
ERAD	Endoplasmic Reticulum Associated Degradation
ErDj4	Endoplasmic Reticulum DnaJ-like 4
ERK	Extracellular Signal-Regulated Kinase
ERSE	ER Stress Response Element
eYFP	Enhanced Yellow Fluorescent Protein
FACS	Fluorescently Activated Cell Sorting
FBS	Foetal Bovine Serum
Ig	Immunoglobulin
IL	Interleukin
IRE1	Inositol Requiring Enzyme-1
JAB1	JUN-Activation Domain-binding Protein 1
JNK	JUN N-terminal Kinase
LB	Luria-Bertani Medium
LPS	Lipopolysaccharide
MAPK	Mitogen- Activated Protein Kinase
MFI	Mean Fluorescent Intensity
MIF	Macrophage Migration Inhibitory Factor
mTOR	Molecular/Mammalian Target of Rapamycin
mTORC1/2	mTOR Complex 1/2
NF-κB	Nuclear Factor-κB
OD	Optical Density
ORF	Open Reading Frames
PAMPs	Pathogen-Associated Molecular Patterns
PERK	Protein Kinase R (PKR)-like Endoplasmic Reticulum Kinase
PBS	Phosphate Buffered Saline
PCR	Polymerase Chain Reaction
qPCR	Quantitative PCR
RIDD	Regulated IRE-1 Dependant Decay

RNA	Ribonucleic Acid
RT	Room Temperature
RT-PCR	Reverse Transcriptase PCR
Taq	Thermus Aquaticus
TLR	Toll-like Receptor
TNF	Tumour-Necrosis Factor
TPG	Thapsigargin
TsMIF1	Trichinella spiralis MIF1
UPR	Unfolded Protein Response
UPRE	Unfolded Protein Response Element
XBP-1	X-box Binding Protein 1

Acknowledgements:

My greatest thanks must go to Doctor David Guiliano, my DoS, and who despite my idiosyncratic nature has never given up on me and has be the most helpful, understanding and patient man who has ever had the misfortune to have me cross their path, I cannot be more apologetic or thankful. Thank you. I would be remiss to not thank Mrs Martina Neville and Miss Alessia Taccogna who have both been my friend and my sounding block for at least three years, but also kept me sane and on target. I could not have got here without either of them. I would like to thank Miss Sinosha Paralikar for keeping me company throughout the last months of her own MRes. To all the PhD students at UEL thank you. And finally, I would be extremely remiss to not thank my partner and my parents for keeping me alive. I would have stopped eating 18 months ago without them.

1 Introduction:

1.1 Inflammation:

Complex multicellular organisms, by their nature, have a series of mechanisms to protect against exogenous and endogenous threats to the organism and without these protective measures they would have a brief existence. One of these defences is immune mediated inflammation.

Inflammation is the reaction of a cell, tissue, or organism to a potential source of damage by the release of cytokines (a diverse series of poly-peptide based signallers) that cause a wide variety of different effects. These include: capillary 'leakiness' and the laying down of new blood vessels; the recruitment of tissue resident macrophages, dendritic cells and the adaptive immune system; the repair or renewal of tissue and finally the resolution of the inflammation; that all work through a common set of mediators e.g., nuclear factor kappa-light-chain-enhancer of activated B cells (NF-κB). However, there are at least two 'depths' of inflammation; Acute and Chronic. These 'depths' are not simply phases that inflammation passes through on its way to resolution. (Sugimoto *et al.*, 2016) chronic inflammation will typically follow an acute stage but are discrete events that can occur in any order. Indeed, acute inflammatory responses are more frequently the consequence of infection and wounds that resolve without a chronic phase. In contrast, conditions such as a tumour or autoimmune disease, are more likely present chronic inflammation when the disease is diagnosed.

For the case of infections, dendritic cells, tissue resident macrophages and neutrophils drive inflammation, reacting to the presence of a Pathogen Associated Molecular Patterns (PAMP(s)) via Pathogen Recognition Receptors (PRR). Several PRR families exist, including Toll-Like Receptors (TLR(s)), C-type Lectin Receptors and NOD-Like Receptors. Looking at one family, the TLRs (1-13 in mammals), shows how a constellation of different receptors can lead to the same outcome. The TLR family (except 3 and 10) activate NF-κB signalling via the classical MyD88/IRAK route leading to IκB phosphorylation by IKK/NEMO and therefore Inflammation (Alexopoulou *et al.*, 2001; Jiang *et al.*, 2016)

This activation causes the upregulation of many pro-inflammatory cytokines and chemokines, leading to the onset of inflammation. This picture is complicated somewhat by the fact that NF-κB signalling has been shown to have an anti-inflammatory effect as well as a pro-inflammatory effect, in certain lineages but also at certain times during an inflammatory event (Sugimoto *et al.,* 2016), so that inflammation is, in theory, self-limiting. (Table 1.1).

Table 1.1: A list of prominent immune factors involved in NF-κB regulated inflammation.

Protein	Pro/Anti-Inflammatory	Cell lineages	References
Interferon γ	Pro	T and NK-cells	(Sica *et al.*, 1997)
TNFα	Pro	Ubiquitous	(Collart, Baeuerle and Vassalli, 1990)
IL-1a and b	Pro	Ec, Ma	(Hiscott *et al.*, 1993)
IL-2	Pro	T-cells	(Hoyos *et al.*, 1989)
IL-6	Pro	Ec, Ma and T-cells	(Son *et al.*, 2008)
IL-8	Pro	Ec, Ma	(Sanacora *et al.*, 2013)
IL-9	Pro	T-cells	(Zhu *et al.*, 1996)
IL-10	Anti	Ma, T-cells	(Cao *et al.*, 2006; Hou *et al.*, 2012)
IL-11	Pro	Bone Marrow Stroma	(Bitko *et al.*, 1997)
IL-17	Pro	Bone Marrow Stroma	(Shen *et al.*, 2006)
CD74/Invariant Chain I_I	Pro/Anti	Ma, Dendritic	(Pessara and Koch, 1990)
MHC 1	Pro	Ubiquitous	(Johnson and Pober, 1994)
MIF	Pro	Ubiquitous	(Bloom and Bennett, 1966)

Inflammation is, of course, not just controlled by PRRs. Nor is NF-κB the only inflammatory transcription factor involved; Activator Protein 1 (AP-1) and Interferon Regulatory Factors (IFN family) are also important players in these processes; but all of these can be activated far from the source of the infection due to another important part of the inflammation response: cytokines. These are mostly well categorised but a specific, non-classical cytokine, Macrophage Migration Inhibitory Factor is a known, modulator of many inflammation signals including NF-κB. However despite being one of the first cytokines discovered MIF remains an enigmatic signalling player and many of its observed biological effects have not been fully characterised.

1.2 Macrophage Migration Inhibitory Factor:

1.2.1 History and Structure:

Macrophage Migration Inhibitory Factor (MIF) was discovered in the 1960s when it was identified as proteinaceous factor which inhibited the random migration of macrophages and was associated with delayed hyper-sensitivity (Bloom and Bennett, 1966; David, 1966). However, the protein itself was not characterised until 20 years later when it was finally cloned (Weiser *et al.*, 1989; Bendrat *et al.*, 1997)

Subsequent research has shown that MIF is a pleiotropic cytokine, with much of its effects pro-inflammatory, counteracting the anti-inflammatory action of corticosteroids (Bernhagen *et al.*, 1993; Roger *et al.*, 2005; Fan *et al.*, 2013)and leading to the upregulation of NF-κB, ETS and AP-1. MIF, at first glance, seems to perform some more esoteric functions within organisms, for example the vascularisation of lung tissue in foetus and neonates (Roger *et al.*, 2017). The most obvious effect of MIF on cells is the halting of the random movement of leukocytes through tissues and then acting as a chemoattractant, through CXCR2/CXCR4/CD74 (Klasen *et al.*, 2014), bringing the immune system to the site of the infection/damage. MIF has also been shown to potentiate signals controlling transcriptional regulation of TLR-4 expression. (Roger *et al.*, 2005; Kudrin *et al.*, 2006). This occurs through ETS signalling and takes the form of a positive feedback loop in which more TLR4 production feeds more MIF production.

The crystal structure of MIF which was elucidated in 1996 showed that it can form a homotrimer (Figure 1.1). However, it is unclear whether MIF exists *in vivo* as a homotrimer or as a dimer or monomer as all forms have been identified during *in vitro* biochemical studies. (Sun *et al.*, 1996; Fan *et al.*, 2013; Gordon-Weeks *et al.*, 2015). MIF is encoded by a gene on chromosome 22 and does not share homology with any of the other families of cytokines. However, it does share homology with a second MIF-like protein called D-dopachrome tautomerase (D-DT, sometimes called MIF2) whose gene is also found closely linked to the MIF gene on chromosome 22 (Merk *et al.*, 2012). The MIF promoter contains DNA binding domains for other transcription factors; including AP-1, GATA Family, NF-κB and CREB allowing for its upregulation from a variety of external signals. (Calandra *et al.*, 2003) and unusually has, two different enzymatic activities: oxidoreductase and dopachrome tautomerase (Bendrat *et al.*, 1997; Rosengren *et al.*, 1997). These activities have been shown to have physiological relevance as the knockout of the oxidoreductase has been shown to modulate the damping down of neuronal signalling (Matsuura *et al.*, 2007) and the tautomerase activity has been shown to interact with CD74-CD44 for canonical MIF signalling (Leng *et al.*, 2003).

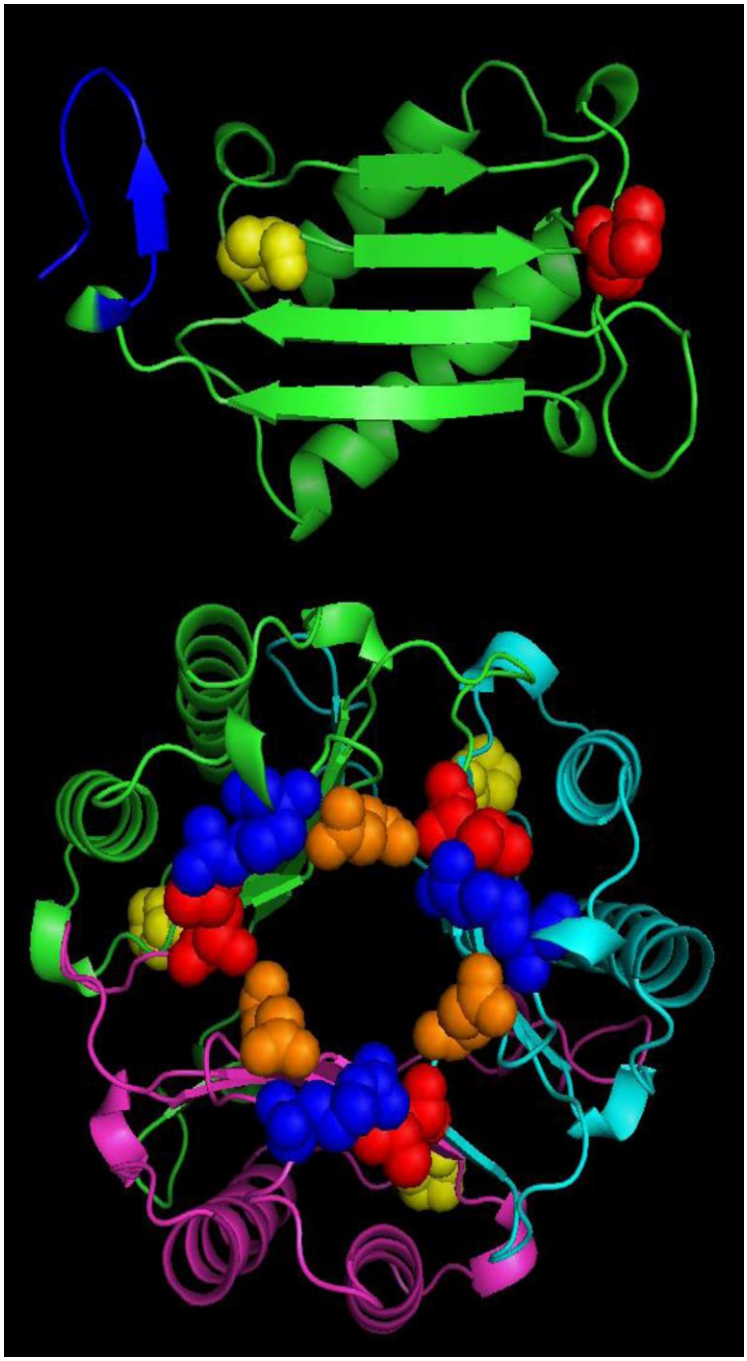

Figure 1.1: **The 3d ribbon structure of human Macrophage Migration Inhibitory Factor (MIF)**. This image is adapted from Gordon-Weeks *et al*., 2015 is two ribbon diagrams for MIF. Ribbon 1 is MIF's monomer. In blue is the oxidoreductase component and the red is the CXCR2 motif. The yellow in the monomer is the tautomerase catalytic site conferred by a proline. Ribbon 2 is the trimer, the back bones of which are coloured cyan, purple, and green. Components shown in the monomer retain their colour.

Another unusual feature of MIF is even though it functions as an extracellular signalling molecule it lacks an N- terminal leader sequence, such as the ER signal peptide. It is not, therefore, completely understood how MIF is secreted out of a cell. However, MIF is produced constitutively and almost ubiquitously in humans (Merk *et al.*, 2009); with MIF being 'rediscovered' in the 90s as a hormone released from the anterior pituitary gland upon sensing LPS, which can lead to toxaemia; as well as epithelial cells, T-cells, granulocytes and macrophages (Bernhagen *et al.*, 1993; Calandra *et al.*, 1994). MIF transcription is not upregulated upon treatment with a PAMP/Cytokine as it is constitutively expressed and stored in vesicles which are released by the cell after receipt of these inflammation signals (Bernhagen et al., 1994).

MIF appears to be well conserved in eukaryotes, with unicellular eukaryotes such as *Plasmodium falciparum* or more 'simple' multicellular animals, such as *T. spiralis* having their own MIF homologue. These other MIF homologues are evolutionarily very distant from the mammalian MIFs (25-46% protein homology, who share a ~95% homology with each other). Interestingly, MIFs from these other eukaryotes have some unique peculiarities and while many share the tautomerase activity (Tan *et al.*, 2001), a large number lack of the oxidoreductase activity, a feature they share with mammalian D-DT/MIF2s (Merk *et al.,* 2012).

1.2.2 Mechanism of MIF's Action:

An open question about MIF is exactly how it performs its functions. Studies have shown that MIF does not always behave like a classical cytokine, able to cause effects by itself, but acts in a secondary capacity modulating other signals (Kudrin *et al.*, 2006). One of the key challenges in characterising the molecular mechanisms of MIF's activities is that it has been postulated that it operates through multiple receptors. These include the extracellular CD74 -CD44 receptor complexes and the CXCR family, (Leng *et al.*, 2003; Leng and Bucala, 2006; Shi *et al.*, 2006; Schwartz *et al.*, 2009) as well as intracellular receptors like JAB-1 (Kleemann *et al.*, 2000) and thioredoxin-interacting protein (TXNIP), (Kim *et al.*, 2017). For its intracellular receptors, cell entry is believed to be mediated through non-receptor mediated endocytosis, but it could also be due to the interaction with Thioredoxin-1 (TRX) (Son *et al.*, 2009). Despite these receptors being identified it has not been elucidated how the MIF-receptor complex imparts effects onto downstream pathways (Kleemann *et al.,* 2000).

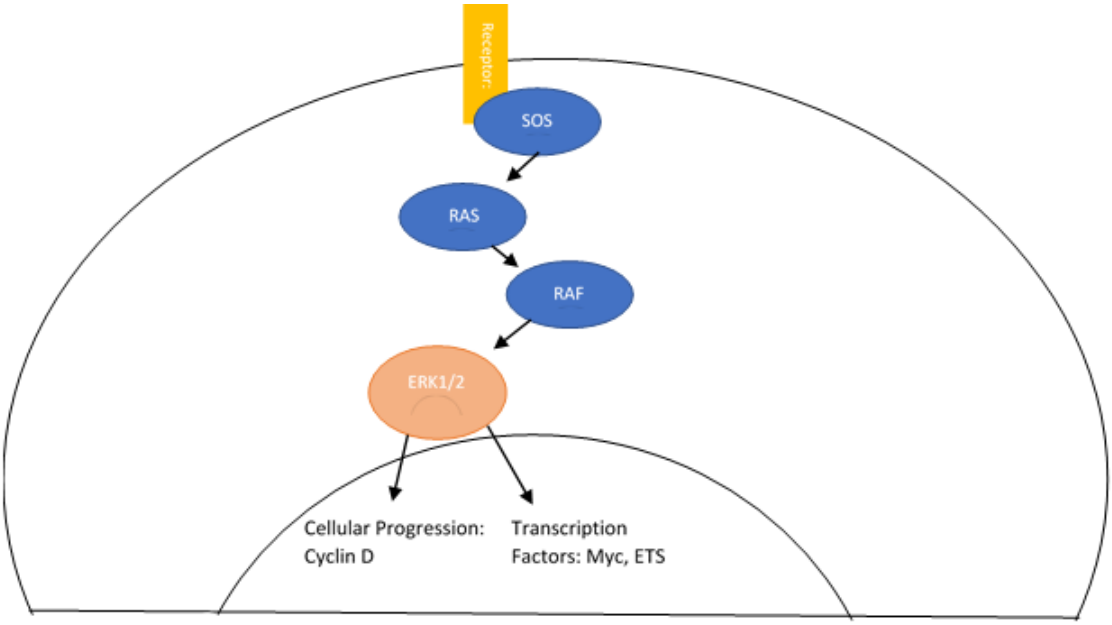

Figure 1.2: **A diagram of the ERK1/2 pathway.** ERK1/2 is a well-defined MAPK signalling pathway that can be briefly stated as: Receptor activation which leads Ras phosphorylation and activation. Ras recruites Raf (Raf-1, B-Raf and A-Raf) that then phosphorylates MEK. Finally the phosphorylation of ERK (1/2) leads to the activation of factors involved in cell cycle progression including cyclin D and transcription factors such as ETS and myc.

What is known though is that MIF signal transduction processes impinges on the Mitogen Activated Protein Kinase (MAPK) pathway (Amin *et al.*, 2003; Lue *et al.*, 2006, 2011). The MAPK signalling pathways are a series of nearly identical chains of receptors, transductors and effectors (Figure 1.2) involved in a wide variety of processes including reception of PAMP and cytokine derived signals. Through the MAPK pathway, MIF is believed to cause many different effects that generally centre on modulating the immune response to a more aggressive clearance of the cause of the MIF release.

One final place the MAPK pathways converge is the Molecular Target of Rapamycin Complexes. These, mTORC1 and mTORC2, are relatively recent discoveries (Gonzalez and Rallis, 2017) but have been shown to have major control on cell survival, reaction to starvation and oxidative stress. It has been shown that active MAPK impingement on the mTORC1, via the phosphorylation of TSC1/2, has the effect of potentiating any other signal entering the mTORC1 path (Carracedo *et al.*, 2008). Indeed, some of those more esoteric functions of MIF such as the lung vascularisation in neonates could be driven by the interaction of MIF and mTORC1 because of mTORC1s downstream effect of causing VEGF up-regulation (Roger *et al.*, 2017).

Another extremely important physiological process within the cell is the control of protein production and folding, especially important for extracellular proteins, and this is controlled by the Endoplasmic Reticulum.

1.3 Endoplasmic Reticulum:

1.3.1 Homeostasis:

The Endoplasmic reticulum (ER) is a series of double membrane sacks called cisternae within eukaryotic cells that bud off the nuclear membrane and remains in proximity to that membrane. The ER has several functions including Calcium (Ca^{2+}) storage and the folding of newly translated nascent soluble or membrane bound proteins destined for secretion or translocation to other organelles within the cell. The ER lumen is a more oxidising environment than the cytosol which allows for more efficient folding and maturation of proteins containing disulphide bonds (Helenius, Marquardt and Braakman, 1992). A third of all nacsent peptides are co- or post-translationally processed in the ER and golgi. Indeed between this and lipid membrane production ER homeostasis is vital for the health of the cell. Recently a number of key studies have established that disruption of ER homeostasis, can have deleterious effects on the organism as a whole giving rise to a variety of pathological conditions many of which are linked to dysregulated inflammatory (Mear *et al.*, 1999; Peeters *et al.*, 2004; Romero-Ramírez *et al.*, 2004; Casas-Tinto *et al.*, 2011; Sha *et al.*, 2011; Gorasia *et al.*, 2015)

To undergo folding in the ER proteins, make their way into the ER in a process called translocation which can occur during the point of translation (Figure 1.3.A). For a peptide to translocate into and translation completed within the ER it requires a N-terminal targeting sequence, or ER signal peptide, which is usually about 15-30 amino acids long, that is recognised by a signal recognition particle (SRP) as soon as the nascent peptide starts to leave the ribosome. This SRP-polypeptide unit, whose translation is temporarily halted due to the docking of the SRP, joins with the cytosolic face of the ER at the translocon sec61 complex (Zimmermann, Müller and Wullich, 2006). At this point the nascent peptide continues being translated whilst being fed into the ER lumen. To complete translation, EDj1 is recruited to sec61, nascent peptides are bound to Binding Immunoglobulin Protein (BiP) a polygamous Heat Shock Protein 70 (HSP70) chaperone, by an ATP-ADP exchange. At this time up to half of all ER processed peptides can be glycosylated by oligosaccharylstransferase, with an oligosaccharide containing mannose units to which a glucose molecule is added by UDP-Glucose Glycoprotein Glycosyl Transferase (UGGT). Once glycosylation occurs the protein enters into the Calnexin/Calreticulin cycle; the removal of mannose from this chain acts as a type of molecular clock the ticking of which causes proteins which failed-to-fold correctly to, eventually, enter the ER Associated Degradation (ERAD) pathway (Tannous, Pisoni and Hebert, 2015; Qi, Tsai and Arvan, 2017)(Figure 1.3.C/Figure 1.3.E). Proteins which have correctly folded are sorted and translocated to their final destinations either within the cell or secreted from the cell via secretory vesicles (Figure 1.3.D).

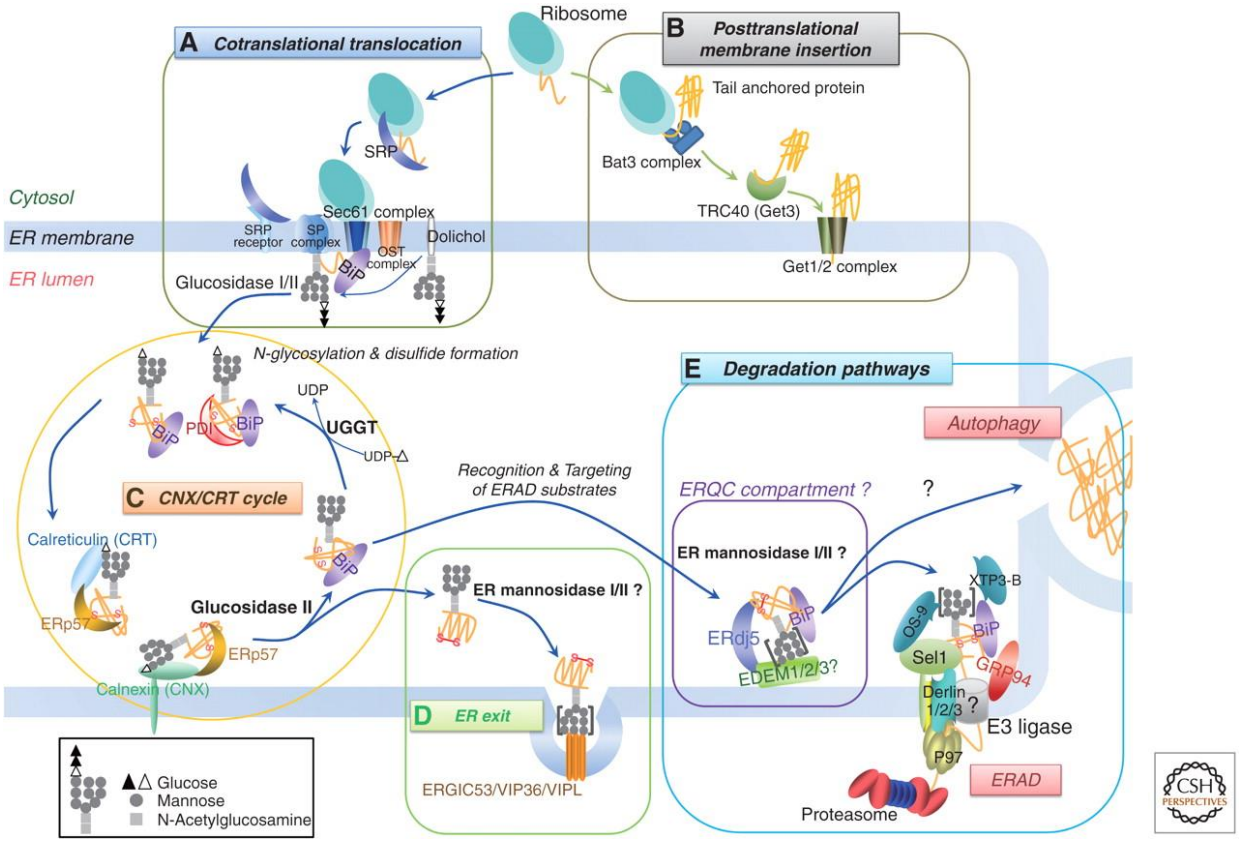

Figure 1.3: **Overview of a Healthy ER.** Image adapted from Araki and Nagata, 2011: The pathways involved with the Translocation (A and B), Folding (C), retrotranslocation (D) and finally, potentially the ER associated degradation of unfolded or misfolded proteins (E).

1.3.2 The Unfolded Protein Response:

On Occasion the ER becomes extremely crowded when there is an accumulation of nascent unfolded or misfolded proteins in the ER lumen (Walter *et al.*, 2015). To ease the concentration of these proteins the Unfolded Protein Response (UPR) is activated. The UPR is a term used to encompass a conserved eukaryote cellular signalling and response system which monitors ER homeostasis. The UPR attempts to recover/promote effective protein folding and recently, it has been shown that components of the UPR are also activated when other types of more generalized cellular stress are encountered such as hypoxic conditions or oxidative stress (Rzymski *et al.*, 2010; Jung-Kang *et al.*, 2017)

When the ER attempts to restore normal conditions via the UPR does so by a). reducing ER protein load, inhibiting general protein translation (Protein Kinase R (PKR)-like endoplasmic reticulum kinase (PERK)), b). increasing the ER's capacity to folding or degrade newly synthesized or misfolding proteins by increasing ER size and chaperone expression (Inositol Requiring Enzyme 1α (IRE1α) and Activating Transcription Factor (ATF6)), and c). removing misfolded protein intermediates by induction of Endoplasmic-reticulum-associated protein degradation (ERAD) components (IRE1α and ATF6). If ER homeostasis is not successfully returned, the cell

will undergo apoptosis via ER stress pathway induced mechanisms activated by C/EBP homologous protein (CHOP) which is controlled by ATF4 translation, long-term activation of XBP-1 and IRE1-JNK signalling pathways which are independent to CHOP (Kato *et al.*, 2012).

It has been shown recently that the fate of the cell during ER stress is determined by the order and timing of UPR component activation events rather than distinct swap of pathways (Walter *et al.,* 2015) with early activiation and inhibition of IRE1α/XBP-1 promoting cell survivial while early activiation of PERK/eIF2a promotes apoptosis.

The UPR is thought to be activated by the dissociation of BiP from the luminal surface of three major effector proteins, the transcription factor ATF6 and two protein kinases: IRE1α (Calfon *et al.*, 2002) and PERK (Figure 1.4). It has been shown that the dissociation of BiP from the UPR effectors occurs when the levels of free BiP drop because of an overload of unfolded protein although it is thought this might not be the whole story as X-Ray crystallography shows dimerised IRE1α contains an MHC fold as the luminal face. This MHC fold seems to allow for a finer control over the dimerization of the IRE1α but also seems to lead to (Bertolotti *et al.*, 2000; Marciniak and Ron, 2006; Gardner and Walter, 2011) oligomerisation. The dimerised IRE1α self-activates and acquires a sequence specific RNAse enzymatic activity after autophosphorylation of the C-terminal kinase domain at S724 (Hetz *et al.*, 2011)The IRE1α RNAse domain then splices an intronic sequence from the mRNA that encodes for a potent bZIP transcription factor known as X-box binding protein 1 (XBP-1). This action removes a 26bp unit that contains a stop codon that prevents the true bZIP protein being produced in normal conditions (Figure 1.4). The spliced(s) XBP-1 (XBP-1s) then upregulates the transcription of genes containing the Unfolded Protein Response Element (UPRE (CAGCGTG)) within their promoters (Mori *et al.*, 1992). Finally, the oligomers of IRE1α can perform Regulated IRE-1 Dependent Decay of mRNA (RIDD) that has been shown to lead to a pro-apoptotic signal via RIG-1 (Maurel *et al.*, 2014; Lencer *et al.*, 2015).

Like IRE1α, PERK also dimerises and activates the kinase by autophosphorylation at the kinase domain at T981. The activated PERK kinase phosphorylates eIF2α preventing the separation of eIF2β from eIF2α sequestering it away preventing the entire eIF2 subunit from being recycled reducing its ability to translate the majority polypeptides produced by the cell and subsequently lowering ER protein load (Clemens, 2001). However, this sequestration leads to the increased translation a subset of stress response transcripts such as the active ATF4 transcription factor because ATF4 contains two upstream open reading frames (uORF) that are bypassed when eIF2 initiated translation is blocked (Figure 1.4) (Vattem and Wek, 2004; Jackson, Hellen and Pestova, 2010). The active ATF4 in turn upregulates the transcription of ATF6, CHOP and HERP. As part of this regulatory loop ATF4 also upregulates the production of GADD34 which

acts to dephosphorylate eIF2α leading to the reactivation of general translation. This occurs both in resolution and apoptosis (Han *et al.*, 2013). Finally, PERK activates Nrf2 (Oxidative response bZIP transcription factor) by phosphorylating Nrf2 allowing it to dissociate from its repressor Keap (Figure 1.4).

The UPRE motif is found within promoters and that is recognised by XBP1. This allows those genes containing it to bypass the dampening of translation caused by the phosphorylation of the α subunit of the Eukaryotic Translation Initiation Factor (eIF2), a major component of ribosomes, by PERK. Such genes include BiP, EDEM, ErDj3-5, GP94, PDI-5 and XBP1 itself (Lee, Iwakoshi and Glimcher, 2003).

ATF6 is a transcription factor that targets the ER Stress Response Element (ERSE) motif (CCAAT(N9)CCACG) in the promotor sequences of chaperone genes (Roy and Lee, 1999). When BiP dissociates from ATF6, the intact ATF6 translocates to the Golgi where it is cleaved by two Golgi resident proteases and the active form travels to the nucleus allowing specific genes, such as extra Calnexin and Calreticulin as well as XBP-1 and the lipid synthesis transcription factor SREBP2, to be transcribed (Okada *et al.*, 2002).

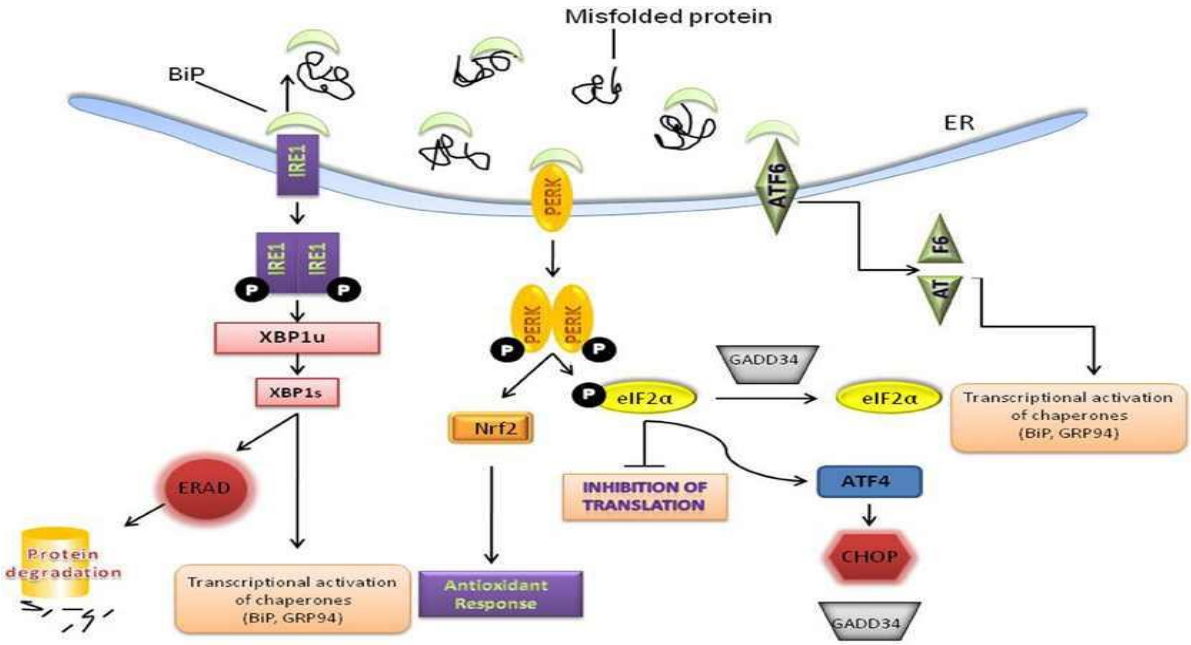

Figure 1.4: **Overview of the Unfolded Stress Response.** Adapted from Brown & Naidoo, 2012: The dissociation of BiP from the luminal surfaces of the three transduction proteins, PERK, IRE1 and ATF6, leads to the Unfolded Protein Response. IRE1 autophosphorylation leads to the translation of XBP-1s and the transcription of chaperone and ERAD proteins. PERK autophosphorylation causes the phosphorylation of EIF2α which inhibits global translation in favour of UPRE and ERSE containing genes. ATF4 is translated due to this inhibition which leads to the translation of CHOP and GADD34. CHOP leads to the activation of apoptosis and GADD34 dephosphorylates EIF2α causing re-initiation of global translation in both resolution and apoptosis. ATF6, after processing in the golgi body, transcribes a similar cluster of genes as XBP1 included BiP ErDj3,4 and 5 and Calnexin/Calreticulin.

As with MIF the UPR does, eventually, talk to mTORC1 and mTORC2 via the suppression of TSC1/TSC2 due to the suppression of ATF6, which leads to the modulation of UPR downstream effects as it has been recently shown that mTOR does in fact affect UPR output; most notably apoptosis and autophagy but also it has been implicated in B-Cell maturation (Appenzeller-Herzog and Hall, 2012). mTOR performs a similar function to the UPR, that of keeping the cell alive. However, mTORC1 works in opposition to the UPR, by causing more protein production due to phosphorylating 4E-BP1, by activating antioxidant pathways and turning on gluconeogenesis. This being said, mTORC1 also reinforces the lipogenesis signal given by the UPR as well as IRE1-JNK pathway and the apoptotic signal that is provided in chronic ER stress as well as the UPR providing more activation potential by ATF6 and CHOP induced AKT activation (although this is cancelled out by IRS1 and mTORC2 in chronic cases) (Appenzeller-Herzog and Hall, 2012).

1.4 Cross talk between MIF and the UPR:

Despite sharing downstream targets including NF-κB and mTOR, it is not known whether MIF can directly affect the UPR signal transducers PERK/ATF4 and IRE1α/XBP1. There are a few crossover points between the MIF signalling pathways and the UPR, including JNK. However, because of these shared downstream targets it is possible that MIF may cause modifications to the standard UPR such as causing the cells to be held in autophagy rather than advancing onto apoptosis.

2.0 Aims:

The aim of this project is to, using chimeric fluorescent proteins transfected into two different cell lines HeLa and SH-SY5s, detect whether the application of MIF causes changes to the initial signal transduction components of the UPR, PERK (ATF4) and IRE1 (XBP1), by co-administering MIF and the UPR inducer Thapsigargin. To perform these experiments chimeric UPR reporter constructs ATF4(1-28).EYFP and XBP-1.EYFP and SH-SY5Y reporter cell lines produced by Prehn lab (Walter *et al.,* 2015) were obtained and characterised. In addition, isogenic HeLa cell clones transfected with the ATF4 reporter construct were also produced and characterized. The results of the UPR reporter cell line experiments were followed by transcriptional analysis of several downstream targets of the UPR using RT-qPCR.

3.0 Methods and Materials:

3.1 Bacterial Culture:

Escherichia coli strains were maintained LB broth (24% tryptone, 12% yeast extract, 24% NaCl) or LB agar (LB broth with 4% w/v agar) with the appropriate antibiotic selection (kanamycin 100 μg/mL). For long term storage the bacterial cultures were stored at -80° in a 20% glycerol stock.

3.1.1 Transformation of *E. coli*:

The UPR reporter plasmids Human p.ATF4/XBP1.YFP-N1, were transformed into chemically competent Top10 using a modified rubidium chloride -based protocol (Inoue et al.,1990).

Top10 were inoculated either directly from frozen stocks or from an overnight LB agar plate 5mls of LB broth is inoculated overnight at 37°C. The following day re-suspend 1.5ml of the overnight in 125ml 2xYT (52% tryptone, 32% yeast extract, 16% NaCl). This is incubated in a shake incubator at 37°C until culture reaches an OD600 0.5-0.7. The culture is pelleted by centrifuging 5000 rpm for 10 minutes at 4°C. Keeping the cells on ice, the pellet is resuspended in 70ml RF1 solution (RF1 100mM RbCl, 50mM MnCl2, 30mM KOAc, and 10mM CaCl2, 15% w/v glycerol, pH5.8). Gently resuspend the cells and incubate on ice for 1 hour. Recentrifuged in previous conditions. Still keeping the cells on ice, resuspend the pellet, removing all the clumps, in 20ml RF2 solution (10mM MOPS, 10mMRbCl, 75mM CaCl2, and 15% w/v glycerol)). Take pre-cooled (-80°C best) cryo-vial tubes aliquot Bacteria and freeze in liquid nitrogen. These are then stored at -80.

3.1.2 Transformation:

These chemically competent bacteria were transformed with the plasmid of choice via heat-shock. To perform heat-shock transformation this the procedure used was this: The frozen aliquot was removed from the -80C and the competent cells thawed and kept on ice. A plasmid DNA that is a maximum of 10% of bacterial volume (10µl in 100µl) is added (dependent on plasmid concentration) and is kept on ice for a minimum of 10 minutes. The aliquot is then placed in a 42° water bath for exactly 45 seconds and immediately placed back on ice for 5 minutes. At the end of five minutes 350µl of LB or 2 x YT broth is added to the aliquot and then incubated at 37 degrees for an hour to help the recovery of the now transformed bacteria. The transformed bacteria were spread on LB agar plates containing the appropriate selection antibiotic and are left overnight in a 37°C Incubator.

3.1.3 Mini/Midi plasmid prep:

Plasmids were purified from transformed bacteria grown overnight in a minimum of 5mls or a maximum of 100mls of LB broth with the appropriate antibiotic. The plasmid extraction was then performed using Qiagen's mini or midiprep system according to manufacturer's protocols with the modifications below. Minipreps are used for small extractions, approximately hundred nanograms of plasmid, compared to midiprep from which a yield of one microgram or more of plasmid can be expected. The minipreps were performed according to manufacturer's protocol (Qiagen). The midipreps were also performed according to the manufacturer's protocol, but with a change to the post P3 wash centrifugation step, spinning once at 25000 rpm for 30 minutes (Qiagen).

3.2: The UPR reporters:

The two UPR reporter constructs, pATF4.EYFP-N1 and pXBP1.EYFP-N1, are derivatives of the pEYFP-N1 Plasmid (Clonetech). These were made and donated for this study by F. Walter and JHM Prehn's (Walter et al., 2015). pEYFP-N1 contains the Enhanced Yellow Fluorescent Protein driven by a CMV promoter. Also contained within the pEYFP-N1 is a neomycin/kanamycin cassette for resistance in both Bacteria and mammalian cells (Figure 3.1)The ATF4.eYFP was created using 280bp of the 5' UTR immediately upstream of the coding region and 84 bp coding for the first 28 amino acids of Human ATF4. It was cloned and the restriction sites XhoI and HindIII was added to allow for cutting into the MCS of the pEYFP. (Figure 3.1.A). The pXBP-1.EYFP-N1 is the full Human pre-splicing transcript of XBP-1 including the splice site and the DNA Binding Domain. The cloned XBP1 was inserted into the pEYFP-N1 plasmid between the XHOL and HindIII cutsites within the Multiple Cloning Site (Figure 3.1.B)

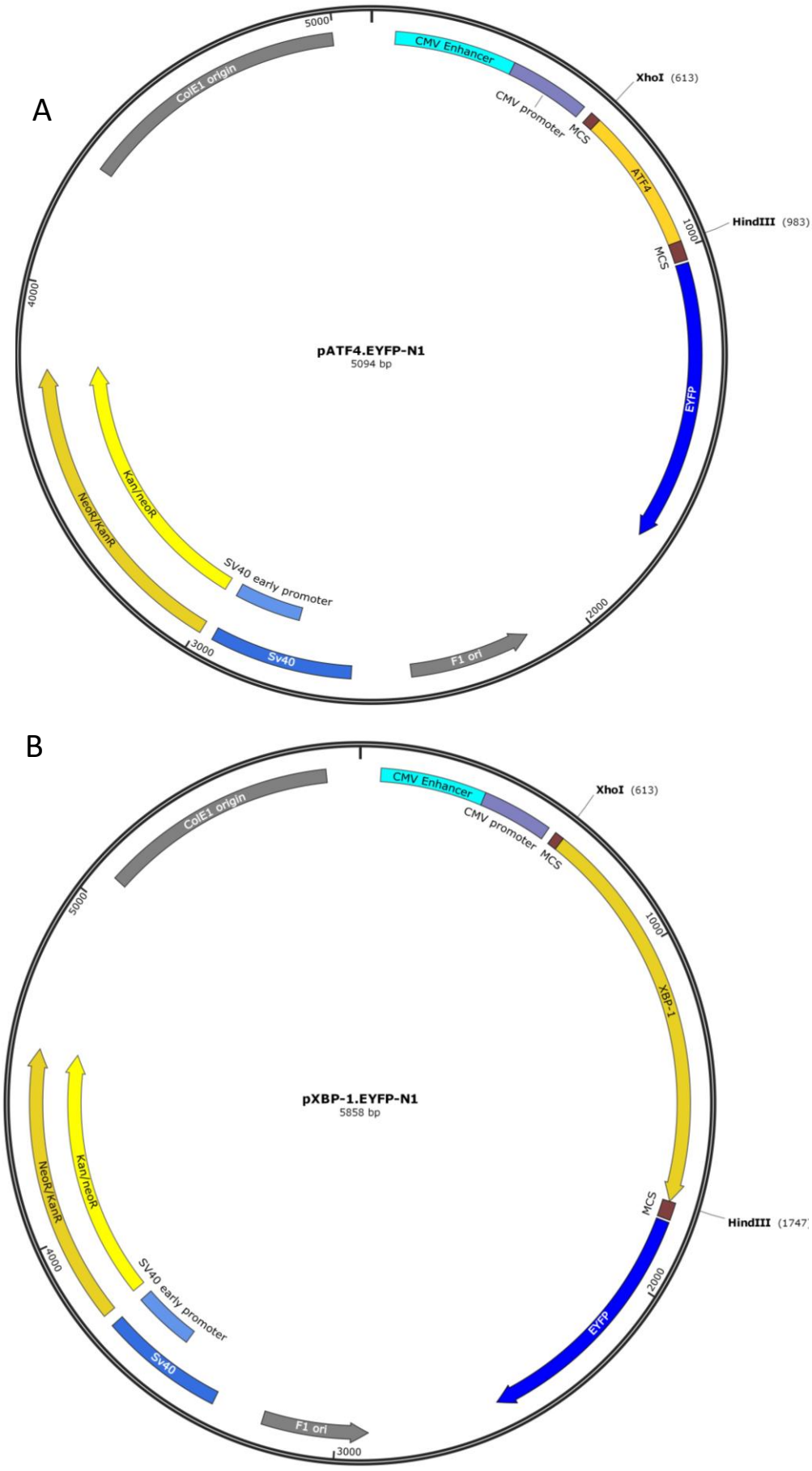

Figure 3.1: **Schematic of the Reporter Plasmid pEYFP-N1** (A) This is the complete ATF4.EYFP-N1, the 360bp insert is between XhoI and HindIII allowing the mRNA to be produced that over runs into the eYFP cassette. (B) This is the complete XBP-1.EYFP-N1. To make this it has the full human which is inserted between XhoI and HindIII allowing the mRNA to be produced that includes the eYFP cassette plus a small linker.

The ATF4.eYFP reporter 5' UTR contains two ORFs that in eIF2α-rich environment are translated in succession because of the quick reacquisition of the ribosome after the end of the uORF1. This does not occur in ER stress conditions, the reacquisition of the 60s component and eIF2 only occurs once it has reached the ORF3 and the protein is translated (Figure 3.2.A).

The XBP1.YFP construct works by IRE1α's RNAse removing a 26nt segment from the mRNA that removes the stop codon from the intron that prevents full translation of XBP1 from occurring (figure 3.2.B).

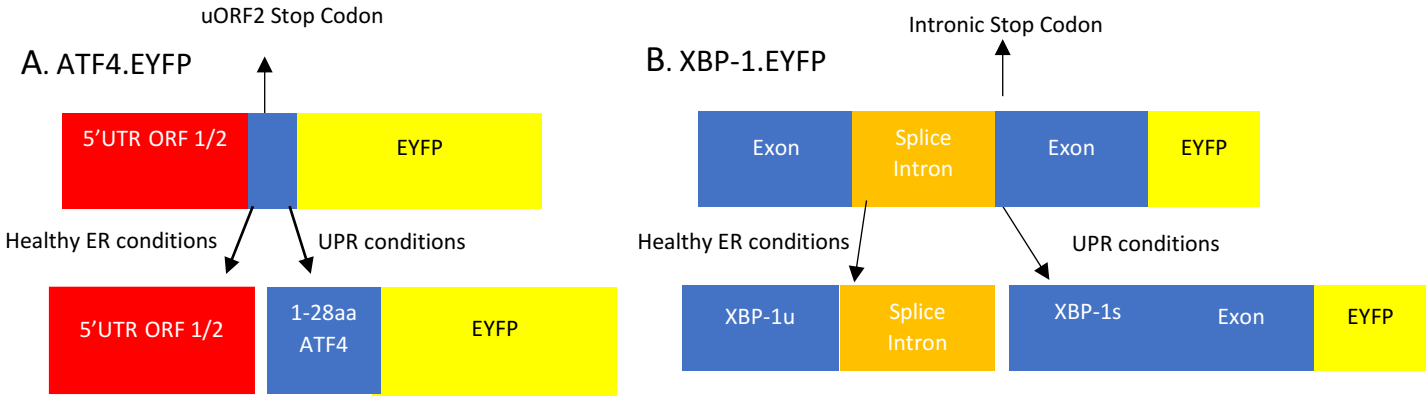

Figure 3.2: **Activating Transcription Factor 4 and X-Box Binding Protein 1 ER Stress reporters constructs**:
(A) ATF4.EYFP reporter: This has two upstream Open Reading Frames (uORFs) that control translation that exist within the 5' untranslated region. uORF2 contains a stop codon that is read when Eukaryotic Initiation Factor 2 (eIF2α) binds to the mRNA within ORF2 after completing the uORF1. Due to the phosphorylation that EIF2α undergoes in ER stress conditions this stop is not read because of the delay in creating the Holoenzyme, because of the sequestering of EIF and, in vivo, ATF4 is translated. This has been taken advantage of and so in the reporter the 5'UTR is attached to YFP via a 28-amino acid linker.
(B) XBP-1.EYFP reporter: This reporter works by utilising the alternative splicing of XBP-1. When classical splicing of the XBP-1 mRNA occurs the stop codon present within the splice site prevents translation of the XBP-1.EYFP. Upon alternative splicing by IRE1 this stop codon is removed so XBP-1 and Yellow is expressed. This XBP-1 is the full transcript so unlike the ATF4 it does have cause downstream effects.

3.3 Mammalian Cell Culture and Chemicals:

The mammalian cells used in this study are HeLas, Human Embryonic Kidneys 293s and SH-SY5s were maintained in complete media (Dulbecco's Modified Eagles Medium (DMEM) supplemented with extra glucose, L-glutamine (Sigma Aldrich) 10% (Hela) or 15% (SH-SY5s) FCS (Gibco), 1% Penicillin/ Streptomycin (Sigma Aldrich)) and grown at 37°C and 5% CO_2. Stocks for both cell lines were made using 90% FCS/ 10% DMSO (Sigma Aldrich) freeing media and stored at -80°C or -170°C. ER stress was induced by Thapsigargin (Sigma Aldrich).

3.3.1 Mammalian Transient Transfection:

To transiently transfect the cells of choice with an experiment specific plasmid, such as the p.ATF4/XBP1.EYFP-N1, the JetPrime DNA and siRNA Transfection Reagent was used according to manufacturer's instructions (Polyplus). Cells were counted and seeded at the density suggested by the manufacturer instructions. For 24 well plates this is ~ 80,000 cells/well but varies depending on well size with a total volume of 0.5 mL of media (Table 3.1).

Table 3.1: Absolute quantity of DNA and Jetprime used to transfect cells

Multi-well plate	**Cells per Well**	**Volume of jetPRIME® Buffer (µl)**	**Total amount of DNA (µg)**
24-well	$1*10^5$	50	0.5
6-well	$1*10^6$	200	2

If the plasmid of choice is wanted to be used at a lower concentration than recommended, then a carrier DNA plasmid pUC18 was used to aid the transfection. This plasmid is added in an amount per well that makes the difference between optimum and required. An example of this is the titration of with the highest level, 0.5µg of with no pUC18 but the lowest 0.125µg containing 0.375µg of the puc18. After the mixing of the JetPrime buffer and the plasmid of choice then it is vortexed and centrifuged in a single speed bench top centrifuge. The JetPrime is then added to the plasmid/buffer mix at a set ratio per well (Table 3.2).

Table 3.2: The Concentration of JetPrime Reagent

Multi-Well Plate	**Volume of jetPRIME® Reagent (µl)**
96-well*	0.2 - 0.3
24-well	1 - 1.5
12-well	1.6 - 2.4
6-well / 35 mm	4 - 6

After the addition of the Jetprime the sample was vortexed, spun once more and then incubated for ten minutes on the bench. After incubation, 50µl of the mixture is added dropwise to each well and incubated for a minimum 4 hours before the media is changed and a minimum of 16 hours before the cells are either treated with drug or processed for analysis by flow cytometry.

3.3.2: Isolation of Mammalian Cell lines stably transfected with UPR reporters:

Transient transfection efficiencies can vary between experiments and can create heterogeneous populations of transfected cells which express different levels of the reporter constructs. To try and overcome some of these experimental limitations we attempted to isolate stable cell lines harbouring XBP-1 and ATF4 ER stress reporter constructs. $1x10^6$ cells were seeded per well in a 6 well plate and transfected with X amount of reporter construct made up to a total of 2 µg with the carrier DNA. Transfected cells were grown in selection free media overnight and then transferred into containing media, G418 (50µg/ml), and grown under selection. Untransfected control cells were used to monitor the activity of the G418 and ensure transfected cells growing through the selection were genuine transfectants. Transfected polyclonal cell lines were expanded under selection, assessed in the ER stress response assays and frozen stocks made in freezing media (90% FCS, 10% DMSO).

3.3.3 Isolation of Single Cell Clones:

To isolate isogenic stably transfected clones for each construct the polyclonal cell lines were diluted to a concentration of 0.5 cells/mL and 200 µL added to each well of a 96 well plate. Cells were grown in selection for a minimum of two weeks until islands of growth could be observed. Clones were then expanded, assessed in the ER stress response assays and frozen stocks made in freezing media.

3.4 Flow Cytometry:

To assess the activity of the ER stress reporter constructs of cells were trypsinized, washed and resuspended in ~350µl of FACS sheath. Levels of cell fluorescence were measured using a FACScelesta (BD Bioscience) with a set gating strategy for each fluorescent marker. For time point experiments the cells were fixed in 3.8% Paraformaldehyde (PFA) 10 minutes then washing 3x in 1xPBS and refrigerated before analysis. FACS data was acquired on Diva (BD Bioscience) and analyzed on FlowJo (BD Bioscience).

3.4.1 Specific Experiment Set Ups:

For most experiments, cells were seeded into a 24 well plate at a concentration of $1x10^5$ cells /well in G418 containing media between 16 and 24 hours before being treated with 150 nM of TPG and/or 250ng/ml of human MIF1 (kindly donated by M.Neville, Guiliano Lab). To test the assess of MIF alone on the reporter constructs cells were treated with a range 31ng/ml - 1500ng/ml of MIF. 150nm TPG as a standard ER stress activation control. Within most experiments all conditions used had three experimental replicates. Most experiments were repeated a minimum of two times. The fluorescence of cells was assessed by FACS at 8 hour and 16 hrs post treatment.

For the time course experiments the standard times analyzed for both constructs were 4, 6, 8, 12, 16 and 24 hours post treatment with the additional timepoints of 36 and 48hrs post-treatment were used for the ATF4 reporter.

3.5 RNA Extraction, Reverse Transcription and Quantitative PCR:

3.5.1 RNA Extraction:

For total RNA extraction $2.5x10^5$ isolated cells were stored in 200-300µl of RNA*later* (ThermoFisher) at -20 until ready to extract using the Isolate II kit (Bioline). Extractions were performed using manufacturer's protocol. Briefly after diluting the RNA*later* and cells with 100ul of PBS the cells were lysed by the addition of 350µl RLY buffer, 3.5µl β-Mercaptoethanol. The lysate was then applied into the isolate II filter and centrifuged for 1 minute at 11000 RCF to remove cellular debris. The 350µl of 70% ethanol is added to the supernatant to allow binding to the column and is mixed by pipetting or vortexing. The lysate solution was then added to the binding column, total volume is 750µl, and centrifuged for 30s at 11000 RCF. 350µl membrane desalting buffer was added to the column and after a 30s centrifugation the DNAse I solution was applied and incubated at room temperature for 15 minutes. To stop the activity of the DNAse I, RW1 wash buffer was added to the membrane and then centrifuged for 30s at 11000 RCF. The column was then washed with 600µl RW2 and 250µl RW2 buffer. Finally, 60µl of RNAse free water is added to the column, whilst on ice, and allowed to permeate the membrane for 5 minutes before centrifugation at 11000 RCF for 1 minute to elute the RNA.

3.5.2 Reverse Transcription:

First strand cDNA was synthesized using the SensiFAST cDNA kit (Bioline) and the manufacturer's protocol: X-X ug of total RNA was used.

Table 3.3: The concentration of RT-PCR reagents

Total RNA or mRNA (up to 1 µg)	*n* µl (15µl total)
5x TransAmp Buffer	4µl
Reverse Transcriptase	1µl
DNase/RNase free-water*	Up to 20 µl

After gently vortexing and centrifugation the samples were placed in the thermocycler (Bio-Rad) and the 1st strand cDNA was synthesized using the following cycling conditions: 25 °C for 10 min, 42 °C for 15 min, 85 °C for 5 min and finally 4 °C indefinite hold. cDNA can be stored at -20°C for long term storage.

3.5.3 Quantitative PCR:

qPCR was performed using the the Bioline SensiFast SYBR High-ROX kit and an AriaMx cycler and analysed on the Mx 1.6 Software (Agilent). Primers for CHOP (5'-GGTCCTGTCTTCAGATGAAAATG-3'; 5'-CTTGGTGCAGATTCACCATTC-3') and ErDj4 (5'-TGGCCATGAAGTACCACCCTGACAA-3'; 5'-TCCACTACCTCTTTGTCCTTTACCACT-3') were taken from Walter et al., 2015. The house keeping gene GAPDH was used as the control for normalization of the results. The GAPDH primers set were designed using the NCBI Primer-Blast tool (https://www.ncbi.nlm.nih.gov/tools/primer-blast/).

To perform the qPCR the cDNA from the previous RT step must be normalised to the lowest concentration of RT products, but recommended no lower than 100ng (as determined by concentration added to the RT reaction). Ten µl of the Sensifast kit 2x premade mix ($Mg2^{+}$, polymerase, SYBR green and ROX) was added to 1µl of each primer and up to 4µl of cDNA per reaction for a total volume of 20µl.

The reaction plate was loaded with the master mixes for each gene, to which the template or control RNA was added no Template and no RT Controls were performed for each set of reactions, After the plate is loaded with template and RNA, it was sealed with a plastic film to prevent evaporation, centrifuged for a 1 minute at 1500rpm to remove air bubbles and placed into the cycler to run through the program. The following cycling conditions were used: 95°C for 2 min, 95°C for 5 sec 60°C for 10 second. After 40 cycles of this 2-step program a melt curve was performed by reading the fluorescence every 0.5°C between 95°C and 60°C and back to 95°C. to check the uniformity of products produced during the PCR.

4.0 Results:

Three commonly used laboratory human cell lines HeLa, Human Embryonic Kidney 293 (HEK 293), and SH-SY5Y (neuroblastoma) were selected for the assessment of MIF treatment on ER stress responses. After initial attempts to optimize transfection of reporter constructs were completed further it was decided to abandon further work with HEK293 cells as there were inconsistencies in responses observed with both the XBP-1.pEYFP-N1 and ATF4.pEYFP-N1reporter constructs and it was not possible to isolate either polyclonal or isogenic clones during the timeframe of the project (see appendix supplementary data and figures S1 and S2).

4.1 Optimization of transfection of the ER stress constructs into HeLa cells:

ER stress reporter plasmid constructs XBP-1.pEYFP-N1 and ATF4.pEYFP-N1 received from J.M Prehn lab (Walter *et al.*, 2015) were transiently transfected into the HeLa cells after they were seeded into 24 well plates (Figures 4.1 and 4.2). To identify optimal transfection conditions each construct was titrated into the cells with DNA concentrations ranging from 0.125 - 1µg of DNA per $1x10^5$ cell were left for 24 hours to allow reporter expression and their mean florescent intensities measured at 16 hrs after treatment with 150nM Thapsigargin (TPG).

HeLa cells were successfully transfected with the XBP-1 reporter construct and at 16 hours the HeLas (Figure 4.1) showed a consistent titration dependant response to a fixed dose of TPG. After TPG treatment there is an increase in the number of the eYFP positive cells relative to the vehicle transfected cells. The MFI of the positive cells (Figure 4.1.D) for both untreated and treated increases between 0.125µg and 0.25µg then plateaus after 0.25µg. It is of note that the maximum MFI never reaches beyond 250 AU in any conditions tested. We speculate this may be a result of toxic or auto-regulatory effects of the XBP-1.eYFP fusion protein.

Analysis of the kinetics of the ER stress reporter constructs was performed by monitoring eYFP levels in 150nM TPG treated HeLa cells over a 24 hr (XBP1) or 36 hr (ATF4) time course. For the XBP-1.pEYFP-N1 reporter there was a steady increase in the number of eYFP positive cells (5 to 25%) peaking at 16 hrs post treatment (Figure 4.2.B). However, while there was a clear and sustained increase in the number of eYFP positive cells there was only a transient increase in the MFI of eYFP positive cells (~2x untreated cells) that peaked 8 hr post treatment with TPG (Figure 4.2.D).

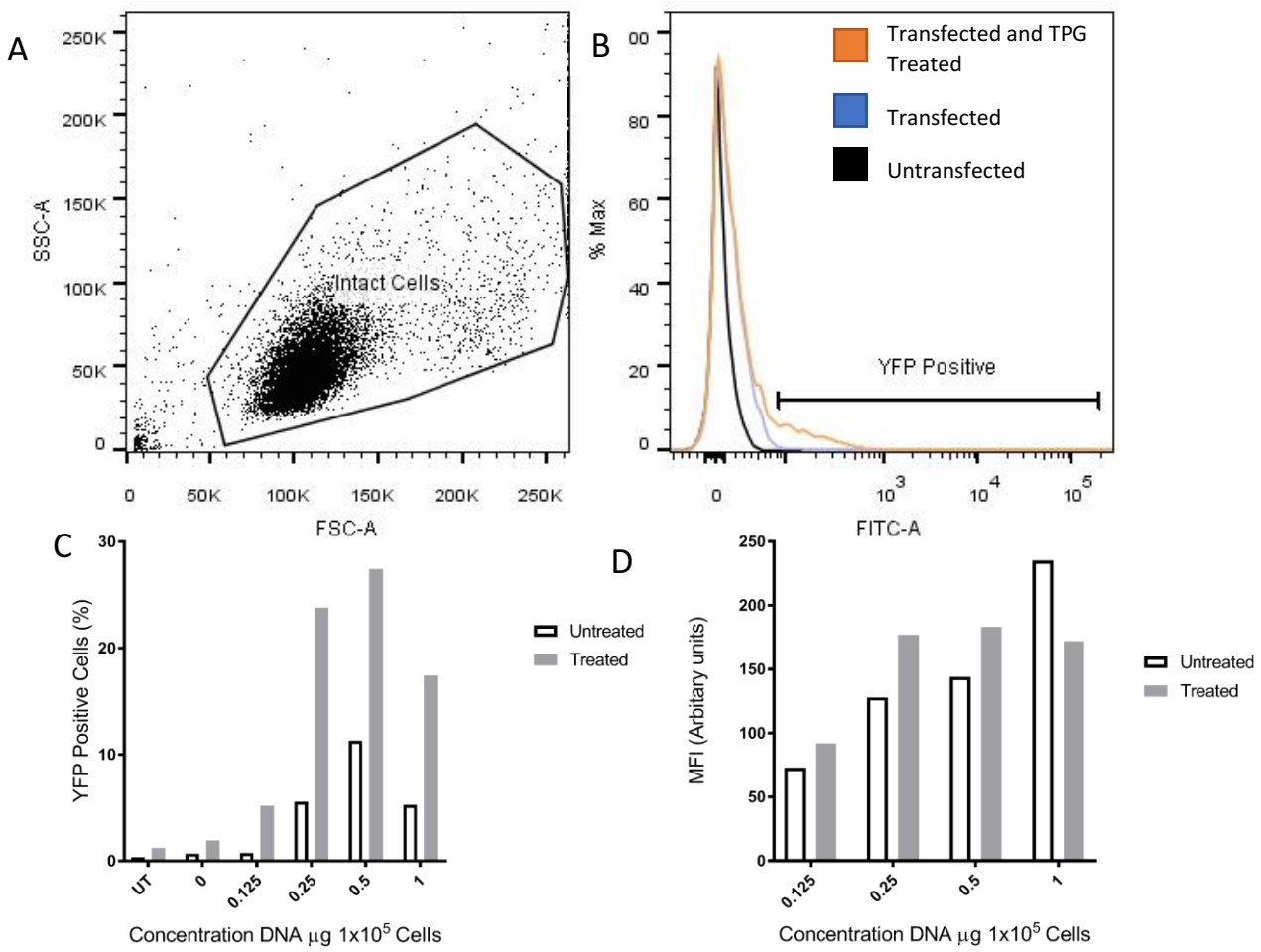

Figure 4.1: **Optimisation of HeLa Cells Transiently Transfected with Different Doses of XBP1.eYFP Transcriptional Reporter.** HeLa cells were seeded 24 hrs before transfection with the XBP-1.pEYFP-N1 reporter construct and treatment with 150 nM TPG. Sixteen hours after treatment cells were collected fixed and analysed by FACS. (A) Intact cells gate was set on the dot plot. Intact cells were then assessed for levels of eYFP. (B) The eYFP positive gate was set so that less than 0.1% of the untransfected cells fell within the gate. The histogram shows representative results using 0.25 ug reporter DNA/10^5 cells. (C) The graph shows the percent of eYFP positive cells 16hrs after treatment with TPG in Hela cells transfected with a range of reporter plasmid DNA concentrations (ranging 0.125- 1µg DNA/5x10^4 cells, UT: Untransfected cells). (D) The changes in the MFI of the eYFP positive cells is also shown (N=1).

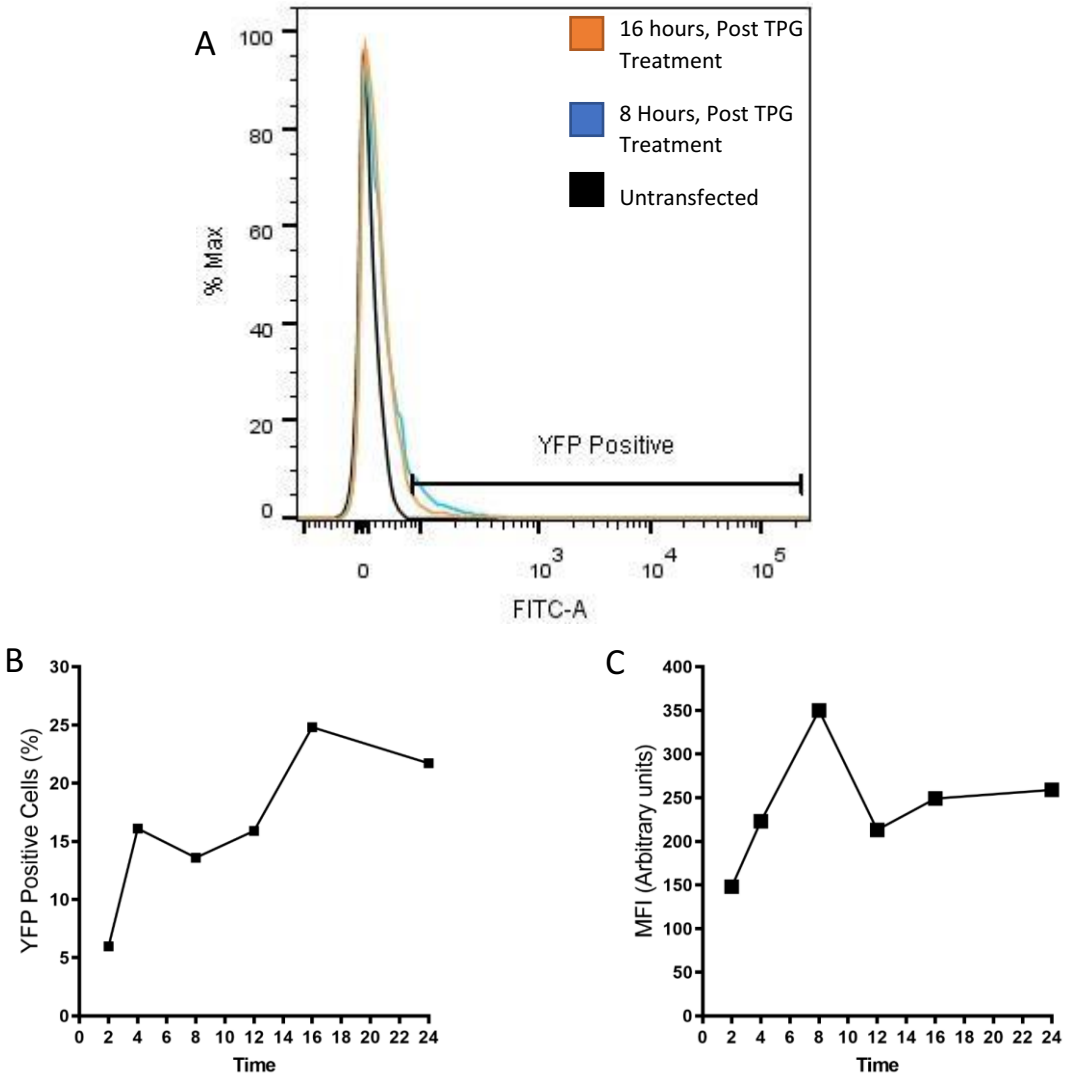

Figure 4.2: **The Activation of the XBP-1.eYFP Transcriptional Reporter over Time in HeLa cells after Treatment with TPG.** Hela cells were seeded 24 hrs before transfection with 0.5 µg/1x10^5 cells the XBP-1.pEYFP-N1 reporter construct and treatment with 150 nM TPG. Cells were analysed by FACS 2, 4, 6, 8, 12, 16 and 24 hours post-treatment. Intact cells were assessed for levels of eYFP expression. (A) The eYFP positive gate was set so that less than 0.1% of the untransfected cells fell within the gate. (B) The change in percent eYFP positive cell. (C) These cell's MFI was assessed in TPG treated cells over a 24 hour time course (N=1).

HeLa cells were also transfected with ATF4.pEYFP-N1 (Figure 4.3). However, while there was correlation between the amount of DNA transfected into the cells and the number of eYFP positive cells this was not consistent with changes in the MFIs of the cells after treatment with TPG (Figure 4.3.C and D). The only exception to these observations were the cells transfected with 0.125 µg DNA per $1x10^5$ cells. These cells showed both an increase in the number of eYFP positive cells and MFI of eYFP positive cells after TPG treatment (Figure 4.3C and D).

The ATF4.pEYFP-N1 reporter construct showed a bimodal peak in the percent of eYFP positive cells over the 36 hour time course at 4 and 18 hrs post-treatment increasing from 15% (0) to 55% at (18 hrs) post-treatment (Figure 4.4.B). The MFI of the eYFP positive cells also peaked 18hrs post-treatment (Figure 4.4.D).

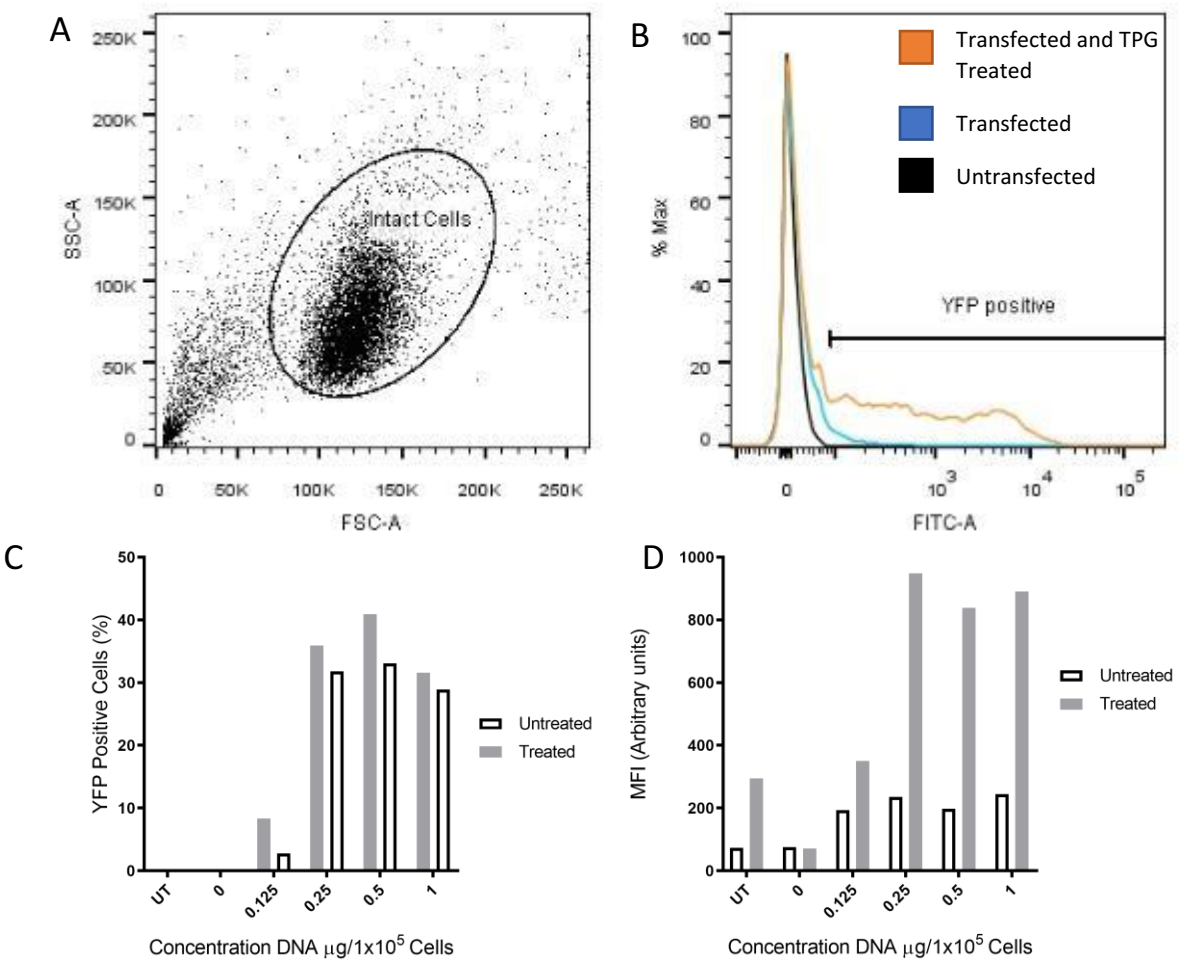

Figure 4.3: **Optimisation of HeLa Cells Transiently Transfected with the ATF4.YFP Transcriptional Reporter.** HeLa cells were seeded 24 hrs before transfection with the ATF4.pEYFP-N1 reporter construct and treatment with 150 nM TPG. Sixteen hours after treatment cells were collected fixed and analysed by FACS. (A) Intact cells gate was set on the dot plot. Intact cells were then assessed for levels of eYFP. (B) Intact cells were assessed for levels of eYFP. The eYFP positive gate was set so that less than 0.1% of the untransfected cells fell within the gate. The histogram shows representative results using 0.25 ug reporter DNA/10^5 cells. (C) The graph shows the percent of eYFP positive cells 16hrs after treatment with TPG in HeLa cells transfected with a range of reporter plasmid DNA concentrations (ranging 0.125- 1µg DNA/$5x10^4$ cells, UT: Untransfected cells). (D) The changes in the MFI of the eYFP positive cells is also shown (N=1).

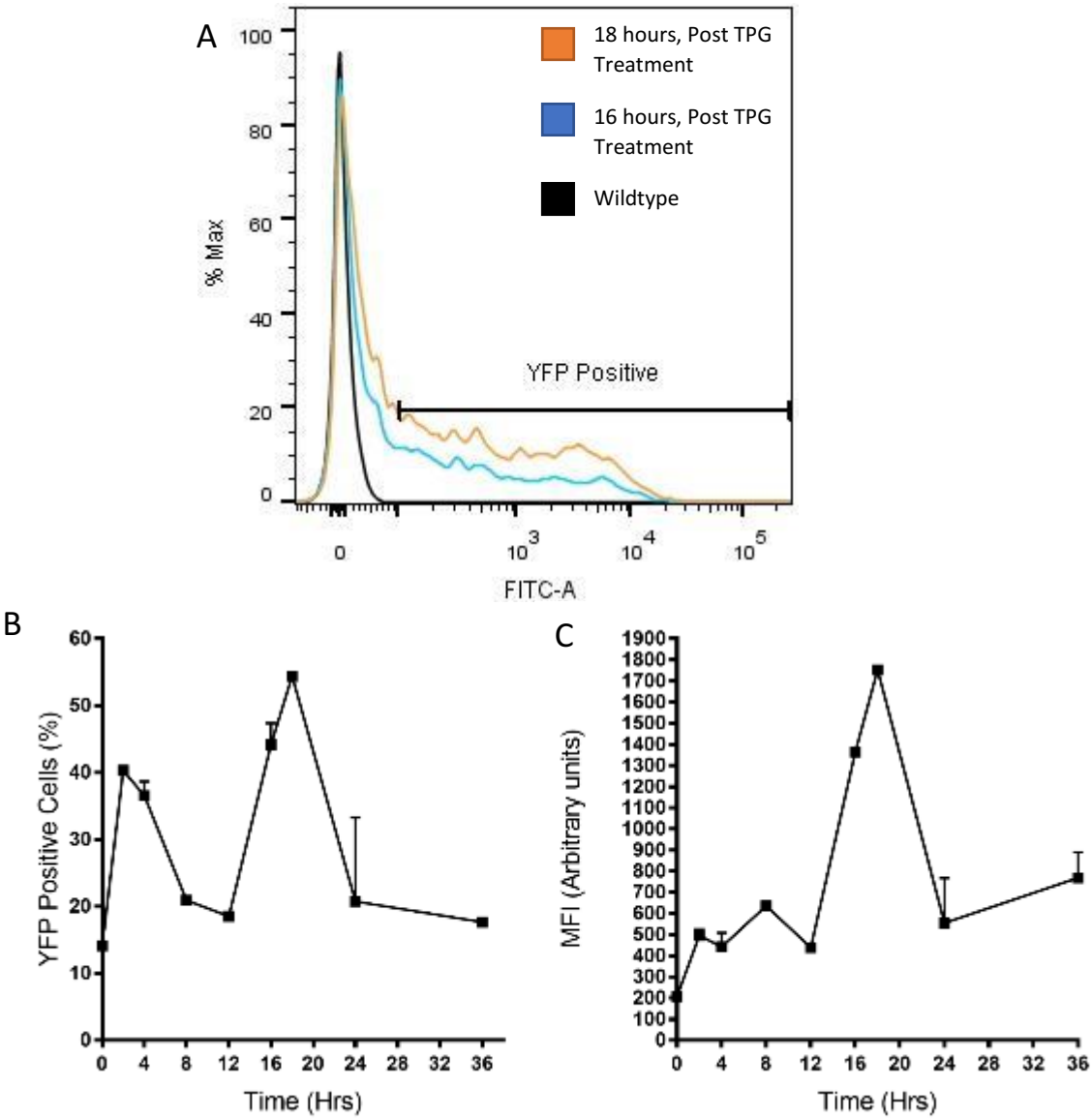

Figure 4.4: **The Activation of the ATF4.eYFP Transcriptional Reporter over Time in HeLa cells after Treatment with TPG.** HeLa cells were seeded 24 hrs before transfection with 0.5 µg/5x10^4 cells the XBP-1.pEYFP-N1 reporter construct and treatment with 150 nM TPG. Cells were analysed by FACS 2, 4, 6, 8, 12, 16, 24 and 36 hours post-treatment. Intact cells were assessed for levels of eYFP expression. (A) The eYFP positive gate was set so that less than 0.1% of the untransfected cells fell within the gate. (B) The change in percent eYFP positive cells and (C) their MFI was assessed in TPG treated cells over a 24 hour time course (N=1).

4.2: Assessment and Characterisation of Stably Transfected SH-SY5Ys:

Upon receipt of the monoclonal SH-SY5Y ER stress reporter cells from the Prehn lab (Walter et.al 2015) they were tested to determine their sensitivity and specificity to ER stress inducers after storage and transport. This was performed by seeding the cells into a 24 well plate, at $5x10^4$ cells/well, then 24 hours later treating them with 375nM, 750nM, 1500nM or 3000nM TPG. The rational for testing doses of TPG within this range for the SH-SY5Y was based on the previously published working concentration used by Walter *et al.* (2015) and it was not known if the cells would respond to lower concentrations of this drug.

The cells were harvested and fixed with 3.8% PFA 8 hours after TPG treatment. Wildtype SH-SY5Ys were used as controls to set the gates for intact and eYFP positive cells. The SH-SY5Ys did not fix particularly well, leading to lower numbers of intact cells when compared to HeLa cells (data not shown).

While the ATF4.eYFP-N1 transfected SH-SY5Y monoclonal cell line (subsequently referred to as WATF4-SH-SY5Y) responded all the doses of TPG with an increase both the percent of eYFP expressing cells and the MFI after treatment (Figure 4.5.B and C) there was no clear dose responsiveness in the conditions tested (Figure 4.5.B). Based on this initial data it was decided that in future experiments 150nM of TPG would be used for the next series of experiments to minimize toxicity and provide similar experimental conditions used with the HeLa cells and in subsequent RT-qPCR assays. However, examination of FACS results of the cells treated with 3mM TPG indicates that this concentration was potentially used in Walter *et. al.* because it activates apoptotic pathways in these cells (Figure 4.5.C).

Unfortunately, the XBP-1.eYFP-N1 transfected SH-SY5Y cells provided by the Prehn lab (subsequently referred to as WXBP1-SH-SY5Y), did not respond well to any concentration of TPG tested (Figure 4.6.B and C) the cells showing a 0.5% increase in eYFP positive cells (Figure 4.6.B). In light of these difficulties wild-type SH-SY5Y were transfected with the XBP-1.eYFP-N1 plasmid and a new polyclonal line containing this reporter construct isolated in parallel with the isolation of a HeLa polyclonal cell line transfected with the same construct.

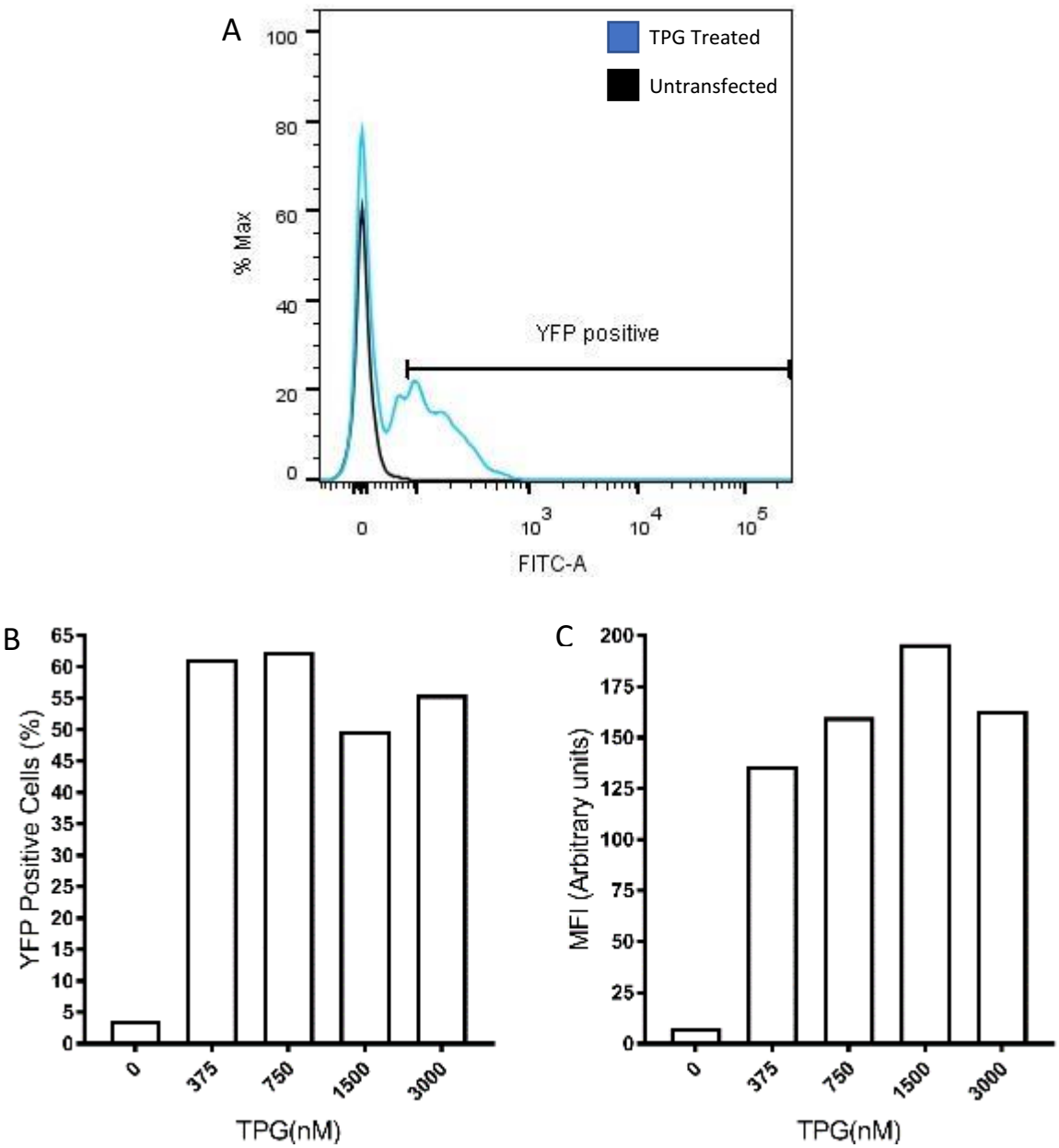

Figure 4.5: **Assessment of Sensitivity and Specificity of the WATF4-SH-SY5Y Reporter Cell Line.** Cells were seeded and allowed to recover for 24 hrs before treatment with a range of concentrations of TPG. Cells were collected fixed and analyzed by FACS 16 hours after treatment. Intact cells were assessed for levels of eYFP. (A) The eYFP positive gate was set so that less than 0.1% of the untransfected cells fell within the gate. (B) The changes in percent eYFP positive cells and (C) their MFI was assessed over drug titration series. While the cells responded well to TPG there was no correlation between drug concentration and the number of eYFP positive cells or their MFI (N=1).

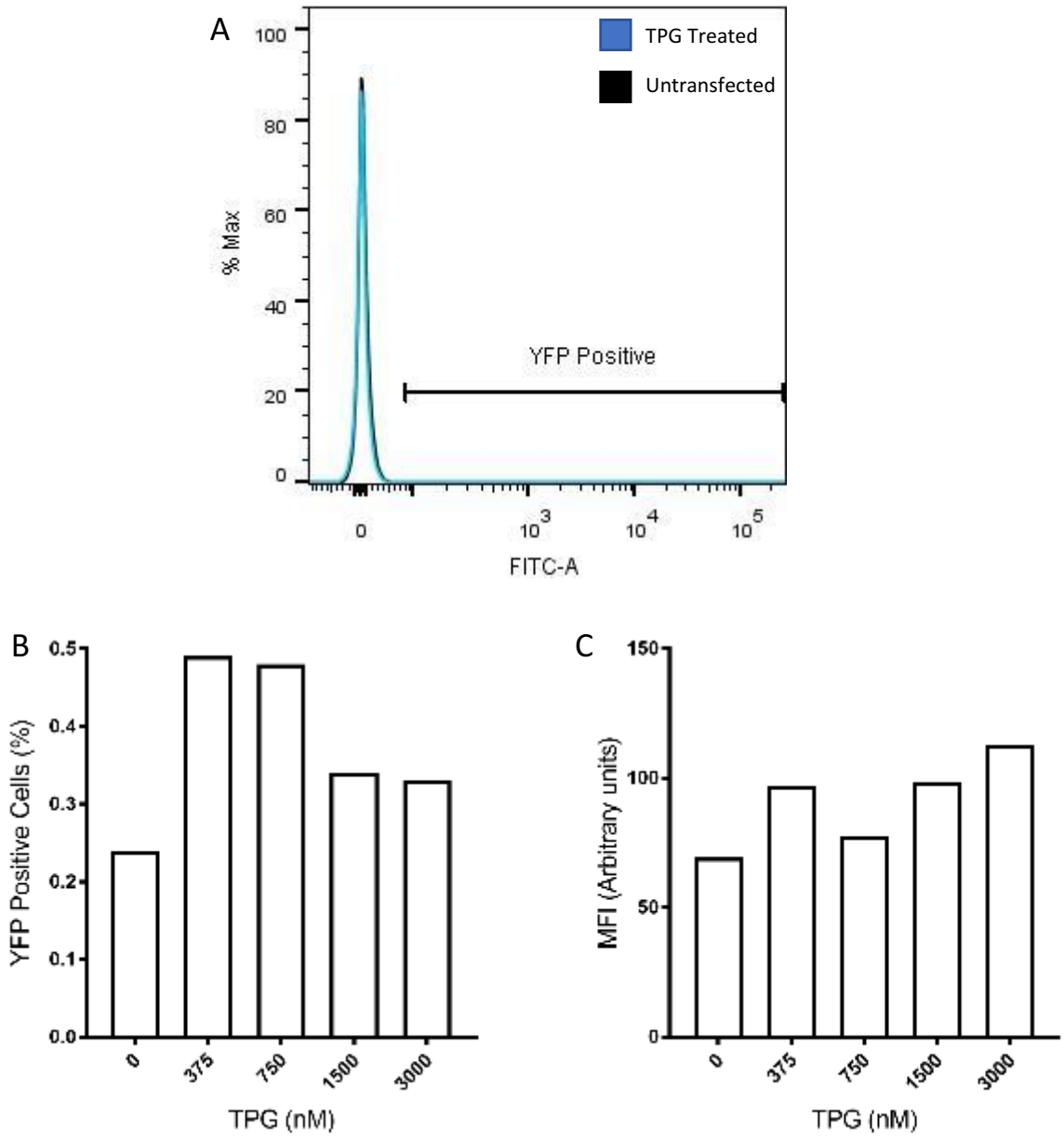

Figure 4.6: **Assessment of Sensitivity and Specificity of the WXBP1-SH-SY5Y Reporter Cell Line.** Cells were seeded and allowed to recover for 24 hrs before treatment with a range of concentrations of TPG. Cells were collected fixed and analyzed by FACS 16 hours after treatment. Intact cells were assessed for levels of eYFP. (A) The eYFP positive gate was set so that less than 0.1% of the untransfected cells fell within the gate. (B) The changes in percent eYFP positive cells and (C) their MFI was assessed over drug titration series. The WXBP-1-SH-SY5Y reporter cell line did not show significant responses to TPG and there was no correlation between drug concentration and the number of eYFP positive cells or their MFI (N=1).

4.3: Isolation of Polyclonal and Isogenic ER Stress Reporter HeLa and SH-SY5Y Cell Lines:

After performing our initial studies in both the HeLas and the SH-SY5Y cells it was decided that new stably transfected cell lines were required to improve the consistency of the data so both cell lines were transfected with the XBP-1.pEYFP-N1 and ATF4.pEYFP-N1 reporters and polyclonal lines selected using G418. Once stable polyclonal lines were isolated, we attempted to further isolate isogenic clones for each cell line and construct.

4.3.1: Isolation of Polyclonal HeLa and SH-SY5Y ER Stress Reporter Cell Lines:

A polyclonal HeLa cell line transfected with the ATF4.eYFP-N1 reporter was successfully isolated and subsequently used to produce an isogenic monoclonal cell line harbouring this construct (Figure 4.7).

However, it was not possible to isolate an equivalent stable polyclonal cell line transfected with the XBP-1.eYFP-N1 reporter construct. HeLa cells transfected with this reporter either did not survive G418 selection, did not show consistent or high levels of EYFP expression or lost expression of EYFP during long term culturing. Fortunately, the SH-SY5Y cells transfected with the XBP-1.eYFP-N1 reporter were able to survive G418 selection and responded to TPG treatment.

Producing a stable polyclonal HeLa cell line stably expressing the XBP-1.eYFP-N1 proved extremely problematic initial attempts (Figure 4.8) resulted in a polyclonal cell line (ASXBP1-HeLa-PC1) which showed no activity to the drug. A second cell was made (ASXBP1-HeLa-PC2) which showed some activity in response to the TPG treatment (Figure 4.8.A). However, it is not dose dependant (Figure 4.8.B) and only a small number of cells showed any expression of eYFP with the TPG concentrations tested (~8% of intact cells). However, these cells gained expression subsequent rounds of passaging where a larger percentage (30-40%) of the cells responded to TPG by expressing eYFP (Figure 4.8.D and E). This cell line was used in the subsequent experiments testing the effects of MIF on XBP-1 activation but required higher concentrations of TPG for clear responses (700nM) when compared to the HeLa ATF4.eYFP-N1 reporter.

The SH-SY5Y XBP-1.eYFP-N1 polyclonal line (ASXBP1- SH-SY5Y-PC1) responded to TPG treatment showing a dose dependant response rising from 17% to 23% eYFP positive cells within the intact cell gate (Figure 4.9). Unfortunately, despite several attempts it was not possible to isolate isogenic TPG responsive monoclonal lines derived from either the ASXBP1-HeLa-PC2 or ASXBP1- SH-SY5Y-PC1 polyclonal cell lines.

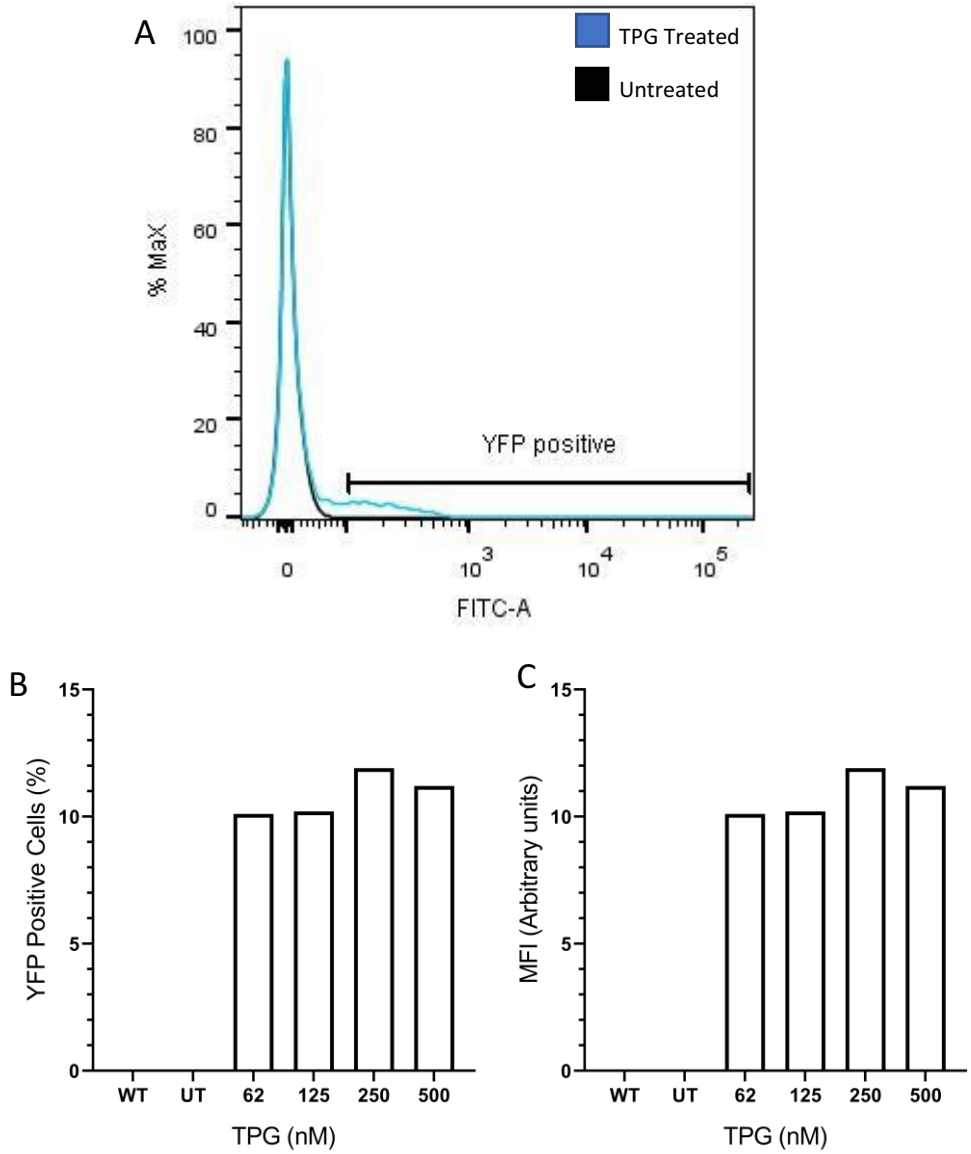

Figure 4.7: **Isolation of a ASATF4-HeLa Polyclonal Cell Line**. HeLa cells transfected with ATF4.eYFP-N1 were selected with G418 for at least three passages The outgrowing resistant cells were seeded and allowed to recover for 24 hrs before treatment with a range of concentrations of TPG. Cells were collected fixed and analyzed by FACS 8 hours after treatment. Intact cells were assessed for levels of eYFP. (A) The eYFP positive gate was set so that less than 0.1% of the untransfected cells fell within the gate. (B) The responses to TPG observed in the ATF4-HeLa-PC1 lines are shown in changes in eYFP positive cells and (C) the changes in the MFI of eYFP positive cells (N=1).

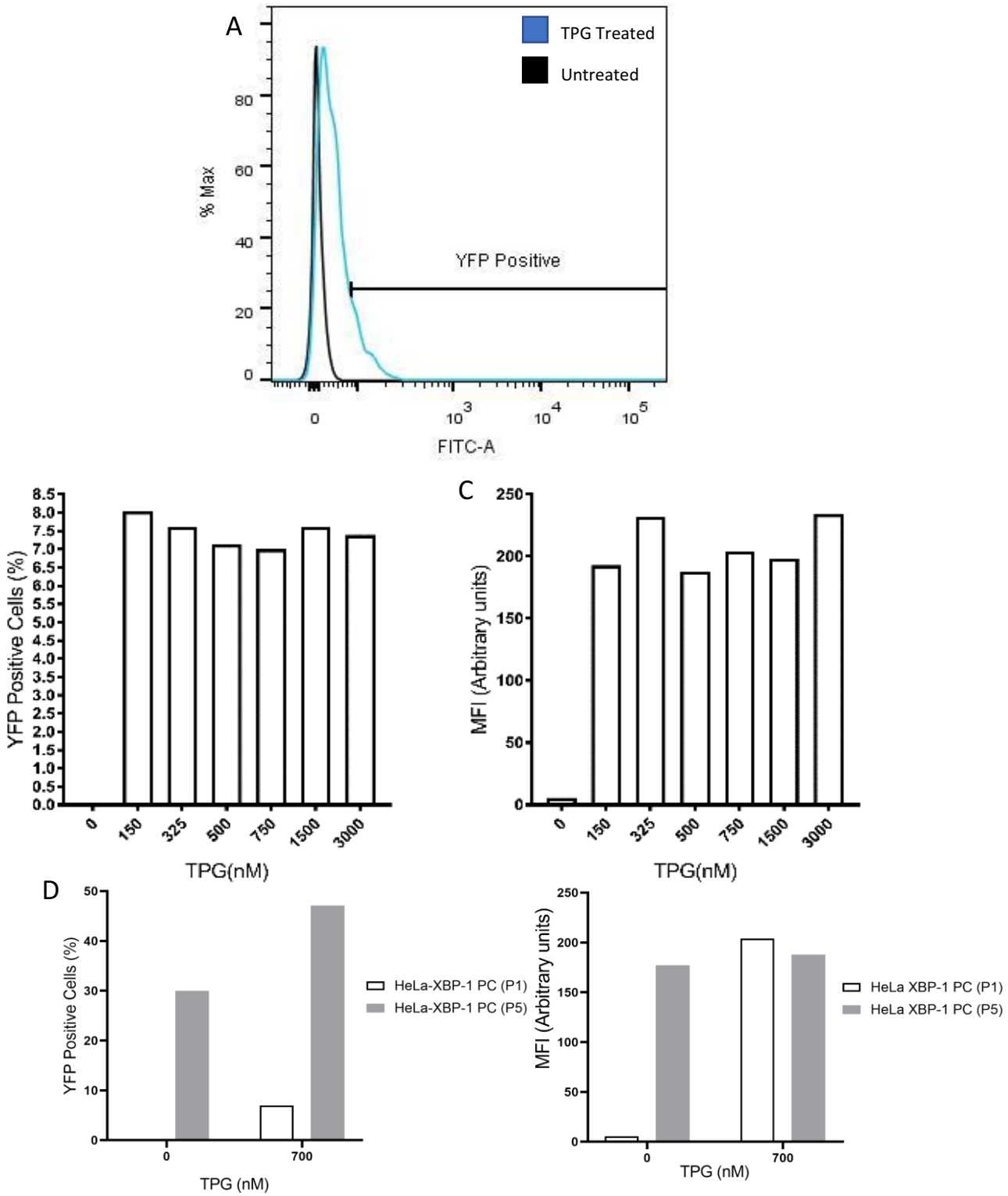

Figure 4.8 **Isolation of a ASXBP1-HeLa Polyclonal Cell Line**. HeLa cells transfected with XBP-1.eYFP-N1 were selected with G418 for at least three passages The outgrowing resistant cells were seeded and allowed to recover for 24 hrs before treatment with a range of concentrations of TPG. Cells were collected fixed and analyzed by FACS 8 hours after treatment. Intact cells were assessed for levels of eYFP. (A) The eYFP positive gate was set so that less than 0.1% of the untransfected cells fell within the gate. The responses to TPG observed in the ASXBP1-HeLa-PC2 lines are shown in (B) changes in eYFP positive cells and (C) the changes in the MFI of eYFP positive cells. (D and E) ASXBP-1-HeLa-PC2 expressed with more intensity as more passages. occurred, the difference between the cells at initial testing and usage (N=1).

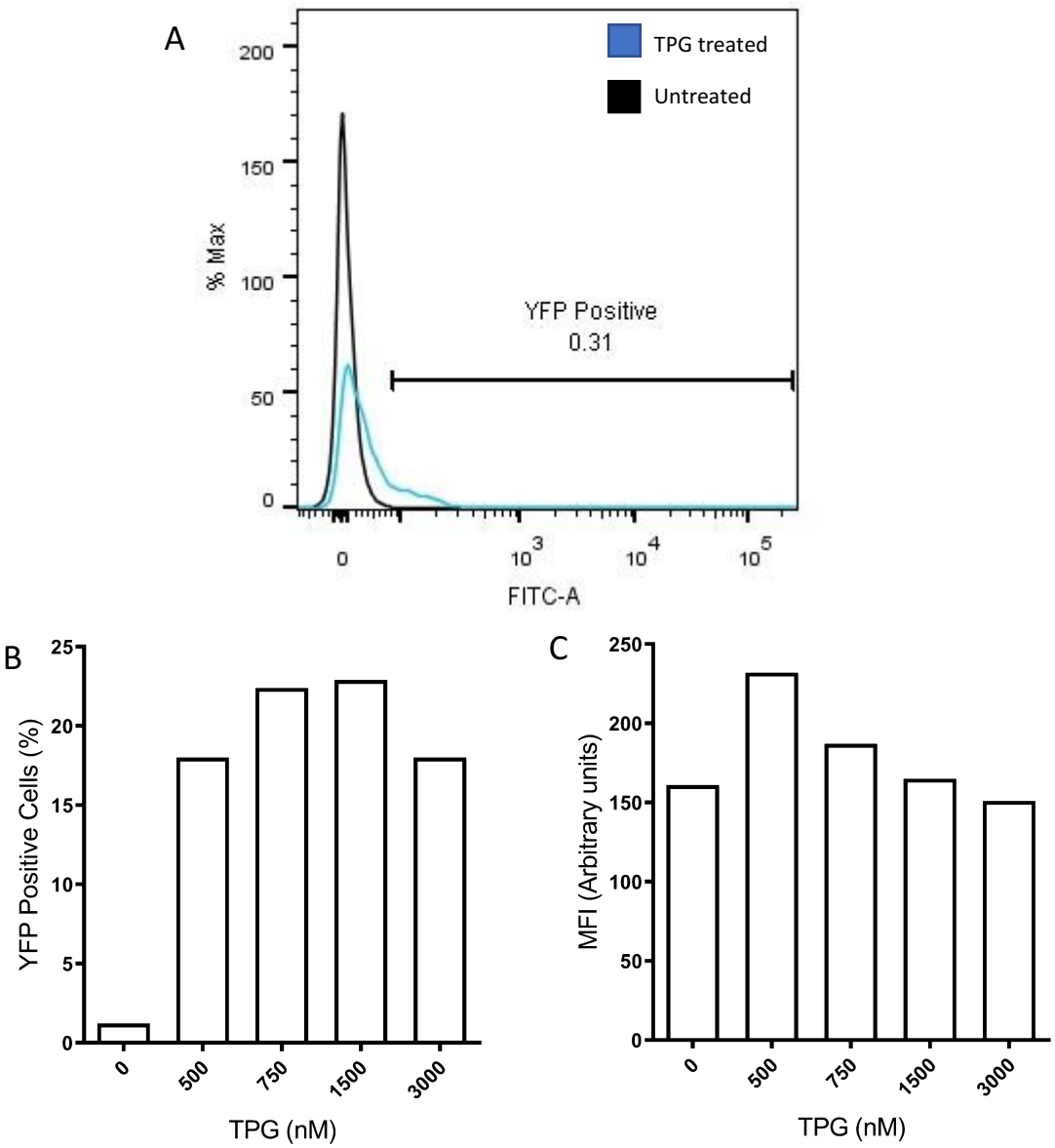

Figure 4.9 **Isolation of a ASXBP1-SH-SY5Y Polyclonal Cell Line**. SH-SY5Ys cells transfected with XBP-1.eYFP-N1 were selected with G418 for at least three passages The outgrowing resistant cells were seeded and allowed to recover for 24 hrs before treatment with a range of concentrations of TPG. Cells were collected fixed and analyzed by FACS 8 hours after treatment. Intact cells were assessed for levels of eYFP. (A) The eYFP positive gate was set so that less than 0.1% of the untransfected cells fell within the gate. (B) The responses to TPG observed in the ASXBP1-SH-SY5Y-PC1 (C) and the changes in the MFI of eYFP positive cells (N=1).

4.3.2: Isolation and Characterisation of Monoclonal Isogenic HeLa Cells Expressing ATF4.pEYFP-N1:

Isogenic monoclonal Hela cells containing an active ATF4.pEYFP-N1 reporter were isolated by taking HeLa cells transfected with ATF4.eYFP-N1 construct, passaging them three times under G418 selection and then seeding them into a 96 well plate at ½ a cell per well plate. After about two weeks wells with obvious cell growth (colonies) were seeded into indivdual T-25 flasks and expanded. Ten clones were successfully isolated and tested for the presence of the of an active ATF4.pEYFP-N1reporter construct. Most of the clones showed no background eYFP expression and no response to TPG (Figure 4.10B and C). However, one clone (D5) showed some background eYFP expression and responded to a range of TPG concentrations (150-3000nM) 8 hrs post treatment (Figure 4.10A). A time-course analysis was performed on this cell line, subsequently called ASATF4-HeLa-Isogenic Clone 1 (ASATF4-HeLa-ASATF4-HELA-IC1), using 150nM TPG which showed that in comparison to the transiently transfected cells (Figure 4.11) it had a delay in the peak in eYFP expression (24 hrs vs 16 hrs) and a steady increase in the MFI of the cells over the entire timecourse (Figure 4.11). Unlike the transiently transfected HeLa cells which have a fluorescence maxima of 10^4au (Figure 4.3) the ASATF4-HELA-IC1 ATF4 isogenic clone (ASATF4-HELA-IC1) shows a narrower range of activation intensities with no fluorescence detected above 10^3au.

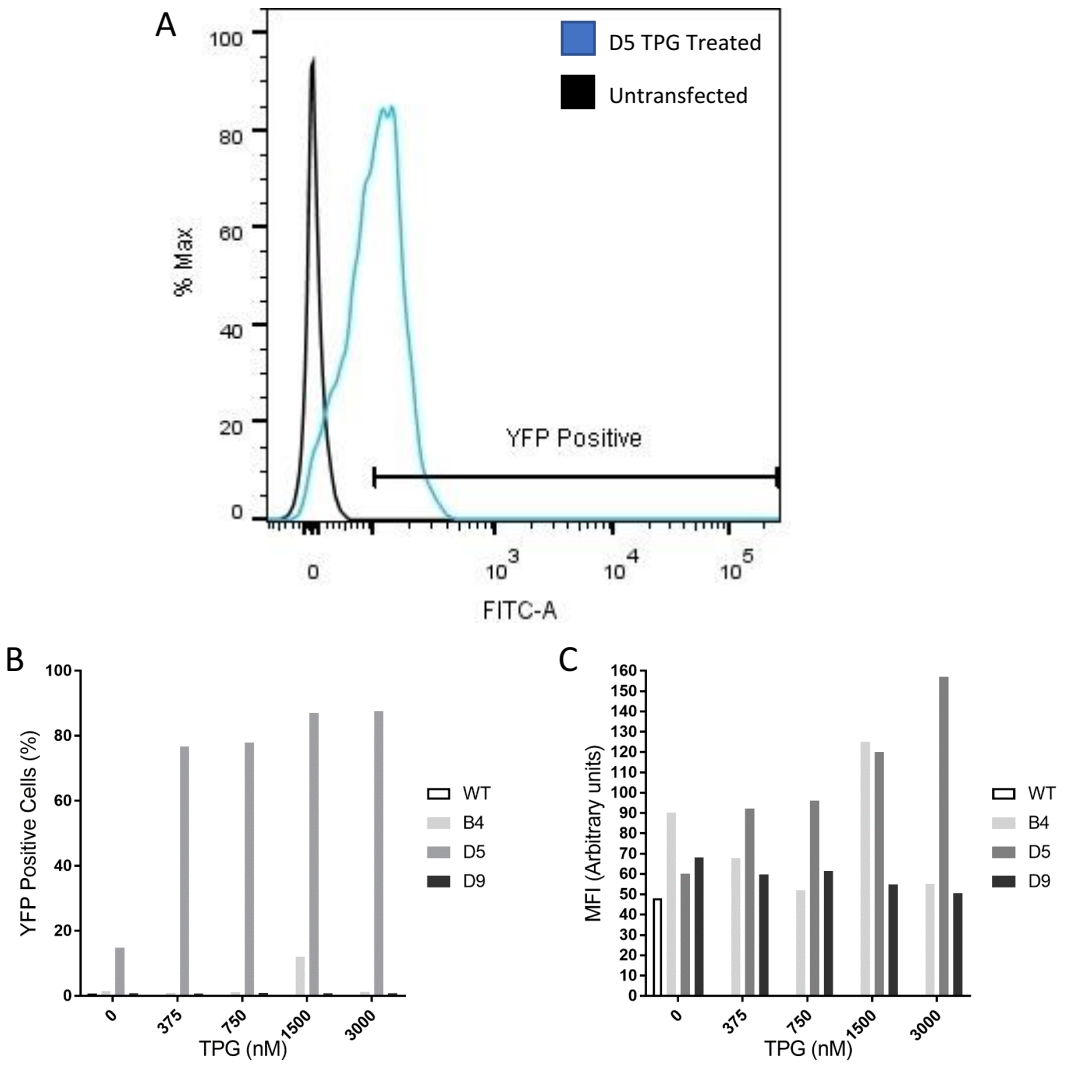

Figure 4.10: **Isolation and Characterization of Single Cell Isogenic HeLa Cells Transfected with the ATF4.pEYFP-N1 Reporter Construct.** The clones B4, D5 and D9 seeded into a 24 well plate and allowed to recover for 24 hrs before treatment with a range of concentrations of TPG. Cells were collected fixed and analyzed by FACS 8 hours after treatment. Intact cells were assessed for levels of eYFP. (A) The eYFP positive gate was set so that less than 0.1% of the untransfected cells fell within the gate. The responses to TPG observed in the three clones are shown in (B) changes in eYFP positive cells and (C) the changes in the MFI of the eYFP positive cells (N=1).

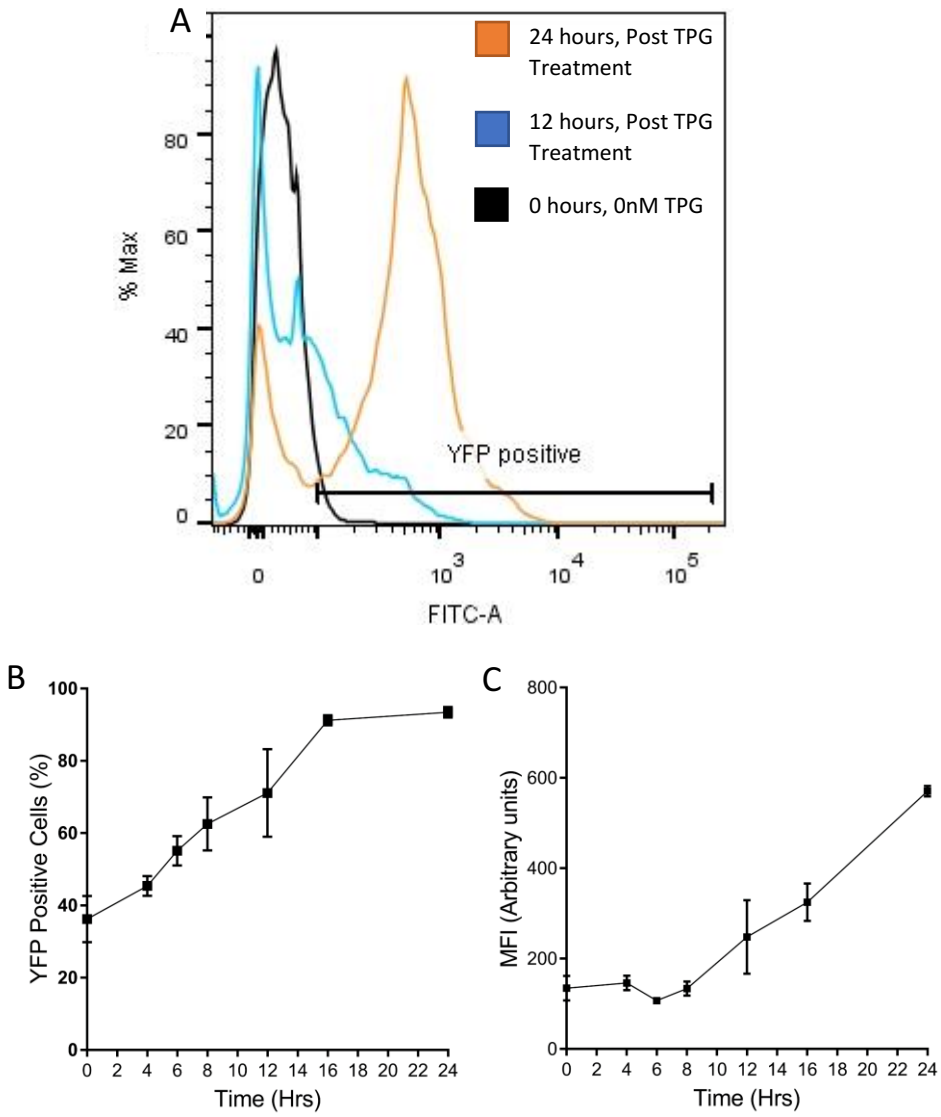

Figure 4.11: **The Activation of the ATF-4.eYFP Transcriptional Reporter over Time in the ASATF4-HeLa-IC1 Cell Line after Treatment with TPG.** ASATF4-HeLa-IC1 cells were seeded 24 hrs before treatment with 150 nM TPG. Cells were analysed by FACS 4, 6, 8, 12, 16, and 24 hours post-treatment. Intact cells were assessed for levels of eYFP expression. (A) The eYFP positive gate was set so that less than 0.1% of the untransfected cells fell within the gate. (B) The change in percent eYFP positive cells and (C) their MFI was assessed in vehicle and TPG treated cell over a 24 hour time course (N=3).

4.4: Assessment of the Effect on MIF on ER stress responses:

4.4.1: Assessment of the Effects of MIF on Activation of the ATF.ePYFP-N1 Reporter Cell Lines:

An initial set of experiments was performed to assess the effects of human MIF alone on the activity of the ATF4.ePYFP-N1 reporter. To confirm that MIF alone was not able to activate the reporter ASATF4-HeLa-IC1 and WATF4-SH-SY5Y cells were treated with a range of MIF concentrations and activation of the ATF4.eYFP-N1 reporter measured.

ASATF4-HeLa-IC1 was seeded in a 96 well plate at a density of $2.5x10^4$ cells per well. 24 hours after seeding these cells were treated with a range of MIF concentrations (75ng-1000ng). Cells were collected 8 hours post treatment fixed and the levels of eYFP assessed by FACS (Figure 4.12). A positive control was also performed where cells were treated with 150nM TPG. MIF did not cause any consistent effect in levels of background YFP expression in these cells. This experiment was repeated were cells were collected at a later timepoint 24 hours post treatment to see if these results differed from the 8hr post-treatment timepoint (Figure 4.13). Like the 8 hr post-treatment cells MIF did not cause any consistent effect in levels of background eYFP expression in these cells.

An equivalent set of experiments was also performed using the WATF4-SH-SY5Y cell line and the results for 8 hr post-treatment (Figure 4.14) showed a similar profile to the ASATF4-HeLa-IC1 cells. This data indicates that in both cell lines tested MIF alone does not significantly affect the activation of the ATF4.ePYFP-N1 reporter.

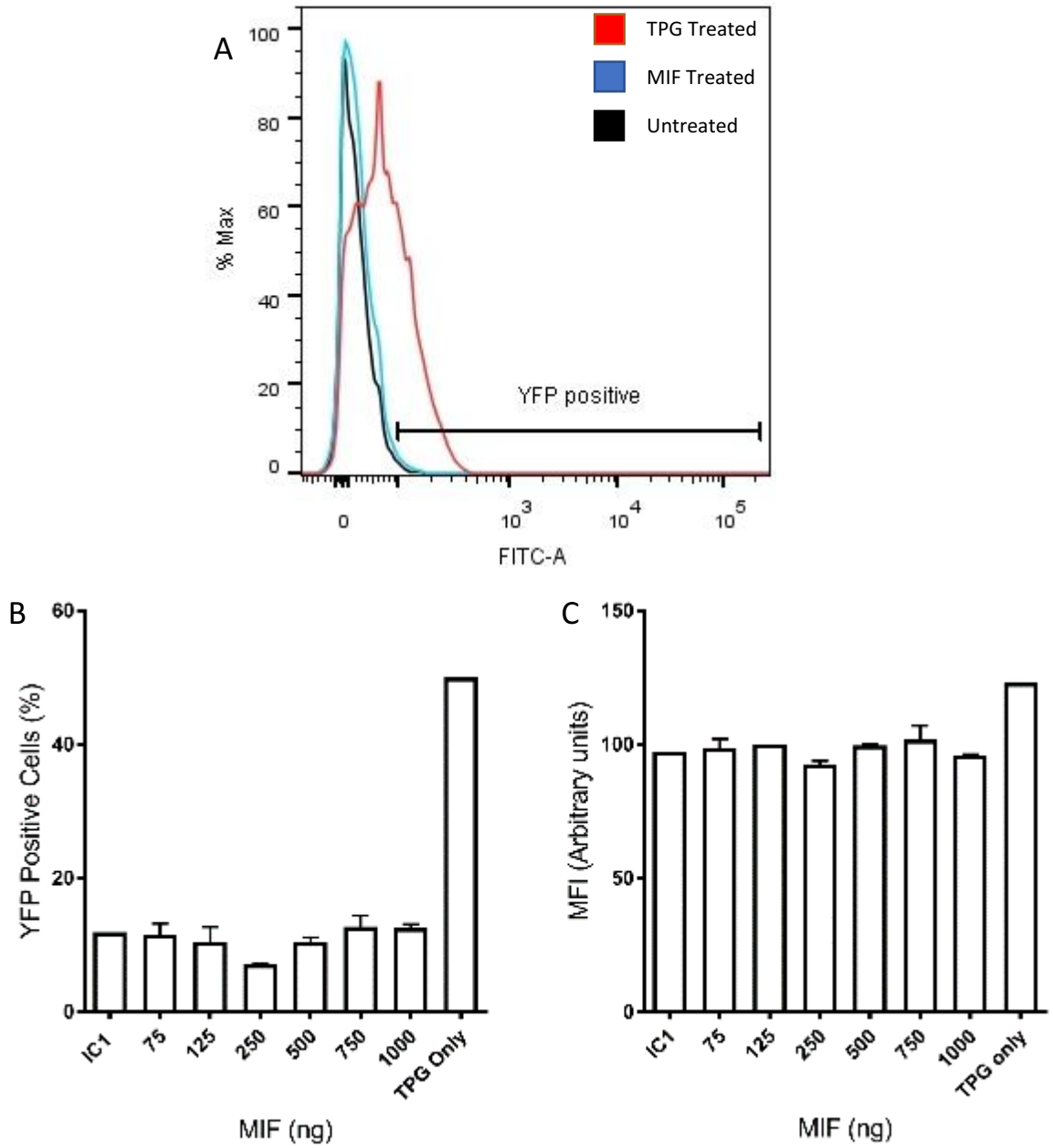

Figure 4.12: **Assessment of the Effects of MIF on HeLa ASATF4-HeLa-IC1 Cells 8hrs Post-Treatment.** Cells were seeded and allowed to recover for 24 hrs before treatment with a range of concentrations of MIF. Cells were collected fixed and analyzed by FACS 8 hours after treatment. Intact cells were assessed for levels of eYFP. (A) The eYFP positive gate was set so that less than 0.1% of the wild-type control cells fell within the gate. (B) The changes in percent eYFP positive cells (C) and their MFI was assessed over range of MIF concentrations tested. The ASATF4-HeLa-IC1 reporter cell line did not show significant responses to MIF No significant difference was found between the untreated control and the MIF only titration. Statistical analysis for both 4.12.B and 4.12.C determined with One Way ANOVA and Bonferroni Post Hoc test for multiple comparisons. (N=3).

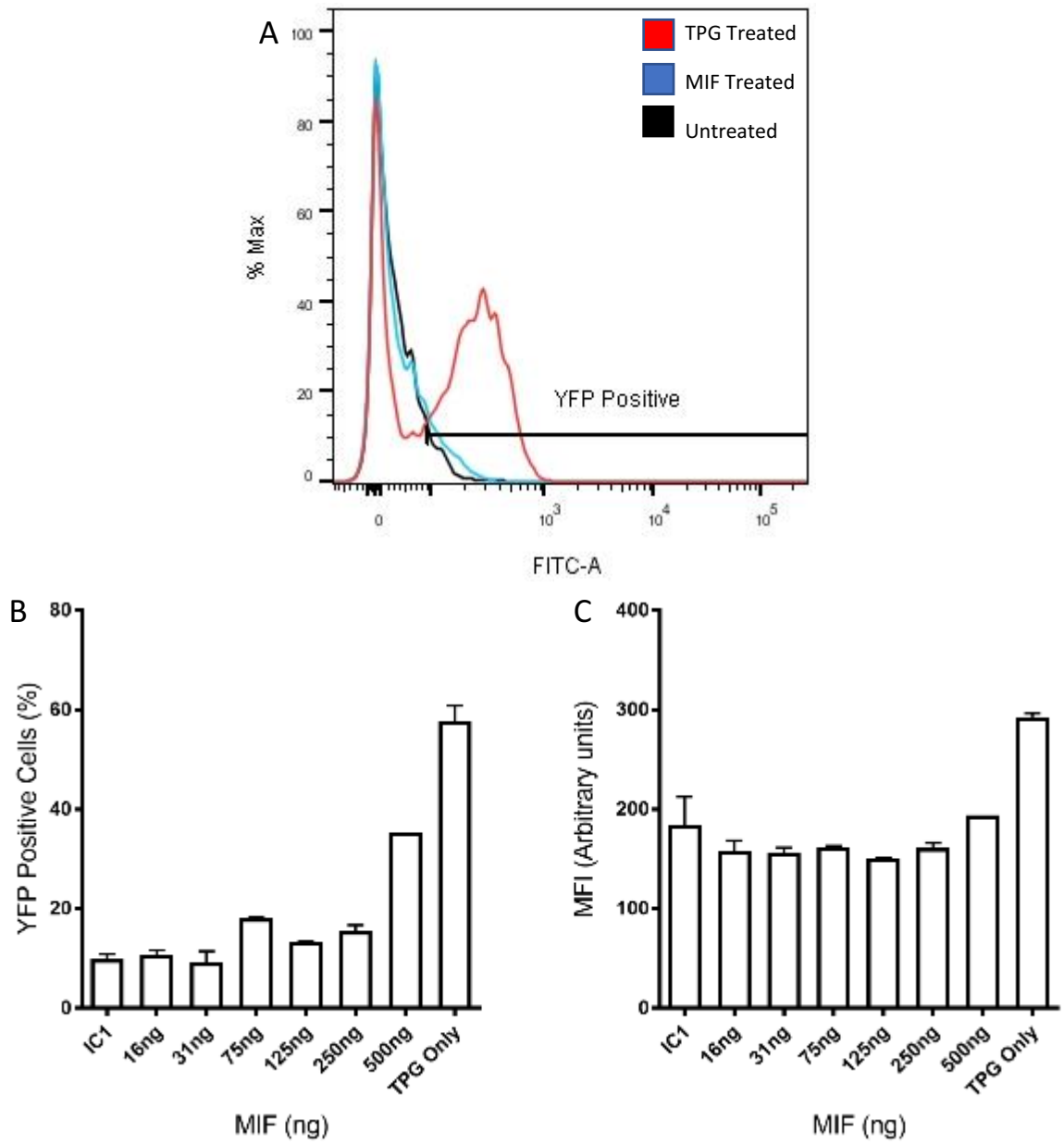

Figure 4.13: **Assessment of the Effects of MIF on HeLa ASATF4-HeLa-IC1 Cells 24 hrs Post-Treatment.** Cells were seeded and allowed to recover for 24 hrs before treatment with a range of concentrations of MIF. Cells were collected fixed and analyzed by FACS 24 hours after treatment. Intact cells were assessed for levels of eYFP. (A) The eYFP positive gate was set so that less than 0.1% of the wild-type cells fell within the gate. (B) The changes in percent eYFP positive cells (C) and their MFI was assessed over range of MIF concentrations tested. The ASATF4-HeLa-IC1 reporter cell line did not show significant responses to MIF. No significant difference was found between the untreated control and the MIF only titration. Statistical analysis for 4.13.B and C was performed with One Way ANOVA and Bonferroni Post Hoc test for multiple comparisons (N=3)

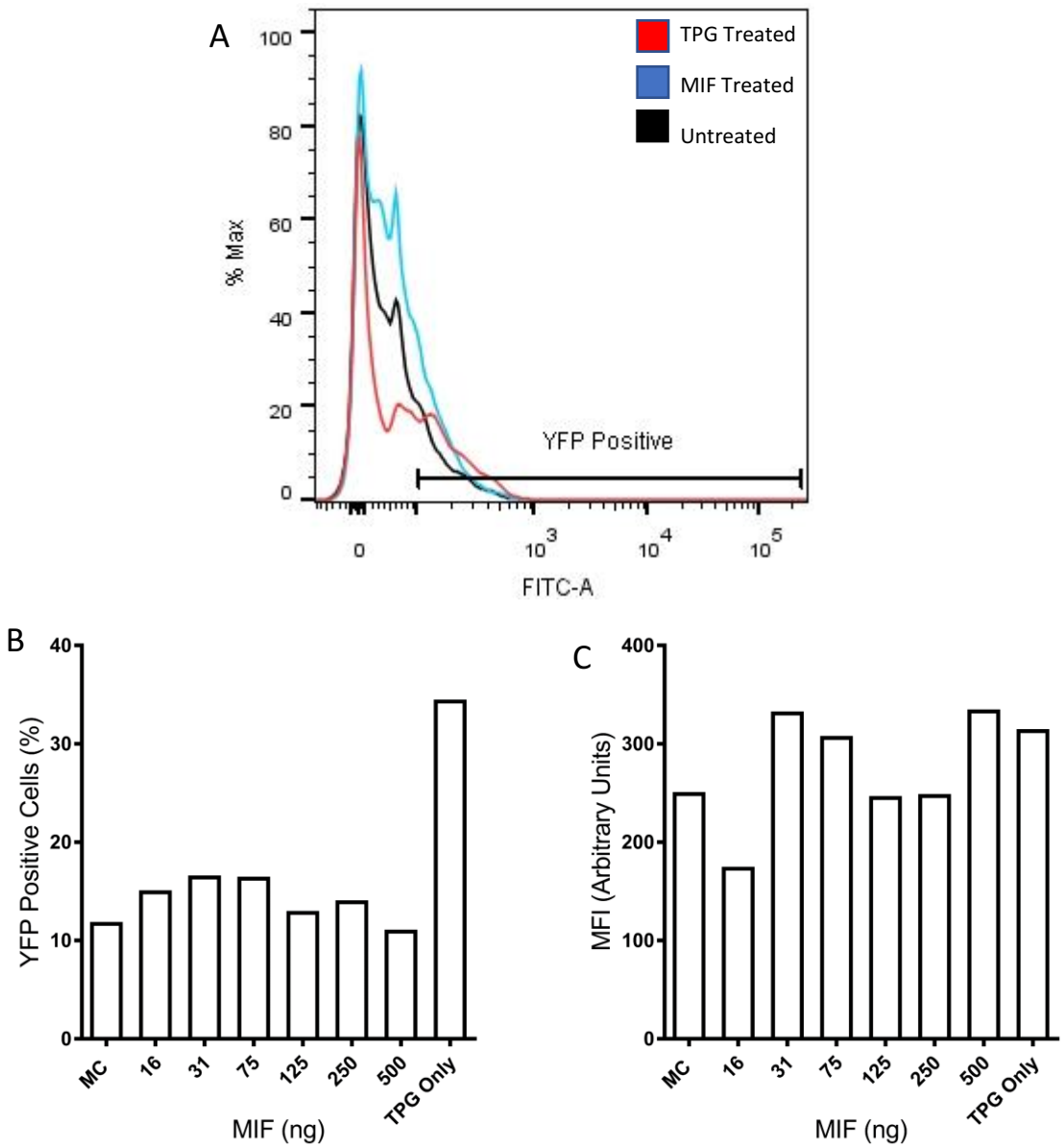

Figure 4.14: **Assessment of the Effects of MIF on WATF4-SH-SY5Y Cells 8hrs Post-Treatment.** WATF4-SH-SY5Y cells were seeded and allowed to recover for 24 hrs before treatment with a range of concentrations of MIF. Cells were collected fixed and analyzed by FACS 8 hours after treatment. Intact cells were assessed for levels of eYFP. (A) The eYFP positive gate was set so that less than 0.1% of the wild-type control cells fell within the gate. (B) The changes in percent eYFP positive cells (C) and their MFI was assessed over range of MIF concentrations tested. The WATF4-SH-SY5Y reporter cell line did not show significant responses to MIF. No significant difference was found between the untreated control and the MIF only titration. Statistical analysis for both 4.14.B and C was performed with One Way ANOVA and Bonferroni Post Hoc test for multiple comparisons (N=3).

In a subsequent set of experiments to determine if MIF could influence the activation of ATF4 during ER stress conditions cells were co-treated with MIF and TPG and the affects MIF on TPG activation of the reporter assessed 24 hrs post-treatment (Figure 4.15). This initial experiment did not suggest that MIF had any effect on activation of the reporter at this time point. However, because previous studies have shown that the timing and kinetics of the ER stress activation response are key factors influencing how it effects downstream processes in cells this experiment was repeated in both ATF4.ePYFP-N1 reporter cell lines looking at a time course of activation rather than a single time point.

Within these experiments 250ng/mL was selected for the MIF dose as this was a median dose for the range that had previously been tested in these assays and is a concentration for this cytokine that is biologically feasible *in vivo*.

The assays performed with the ASATF4-HeLa-IC1 cells showed that MIF treatment caused distinct differences in the activation profile of the ATF.ePYFP-N1 reporter (Figure 4.16). This encompassed both the number of eYFP positive cells (early time points, <36hrs post-treatment) and the MFI of the eYFP positive cells (later timepoints, >36hrs post -treatment) with MIF suppressing the effects of TPG in these cells. This difference approaches statistical significance at p=0.056 (One way ANOVA, n=3).

The WATF4-SH-SY5Y cells behaved slightly differently while there is no consistent difference in the number of eYFP positive cells at later timepoints the MFI of the eYFP positive cells is decreased in those cells that were treated with both MIF and TPG (Figure 4.17, n=2). However while this trend is promising it does not approach statistical significance when analyzed by One way ANOVA.

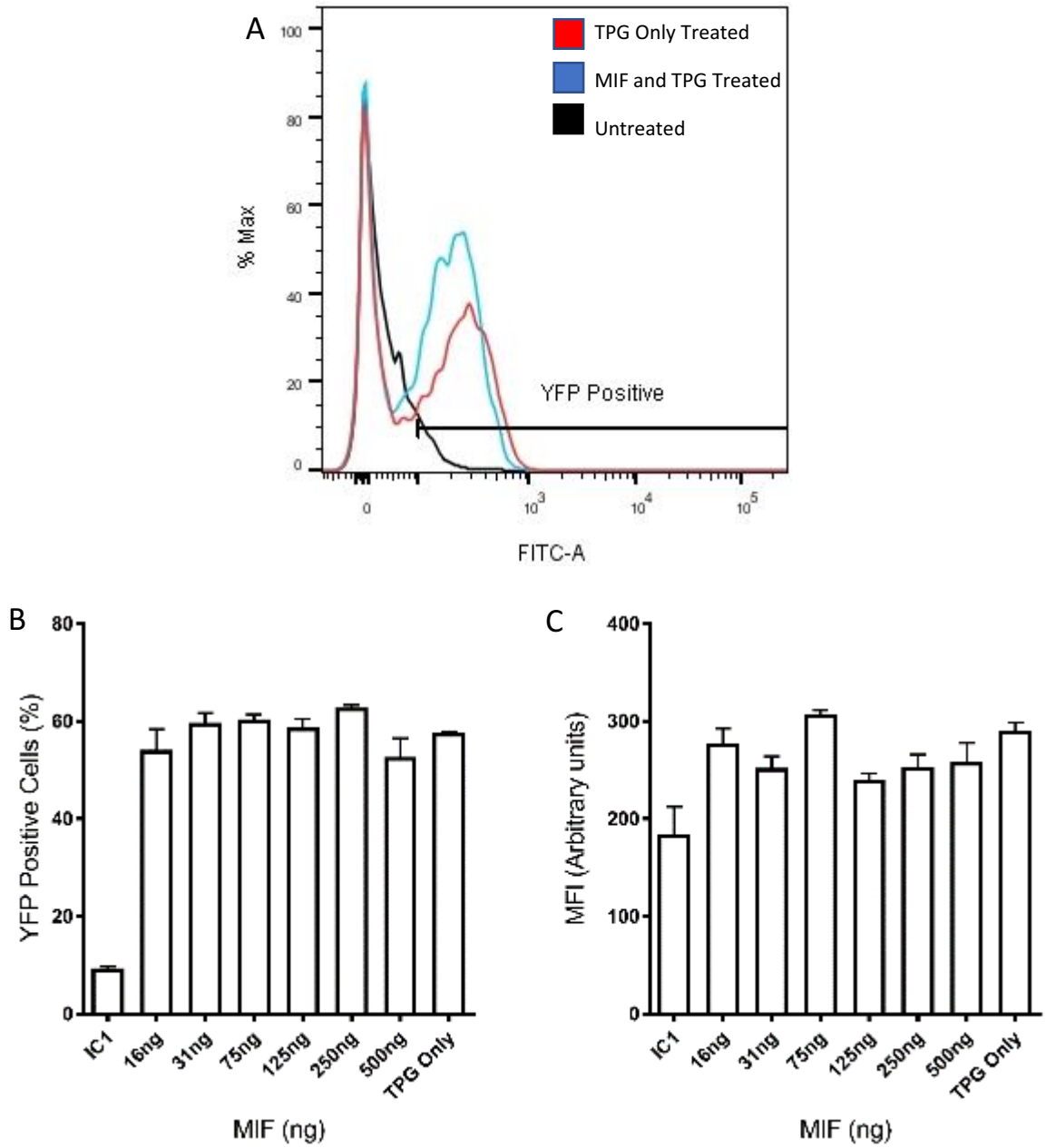

Figure 4.15: **Assessment of the Effects of MIF on ASATF4-HeLa-IC1 Cells Treated with TPG 24 hrs Post-Treatment.** ASATF4-HeLa-IC1 cells were seeded and allowed to recover for 24 hrs before treatment with a range of concentrations of MIF and 150nM TPG. Cells were collected fixed and analyzed by FACS 24 hours after treatment. Intact cells were assessed for levels of eYFP. The eYFP positive gate was set so that less than 0.1% of the wild-type cells fell within the gate. (B) The changes in percent eYFP positive cells and (C) their MFI was assessed over range of MIF concentrations tested. The ASATF4-HeLa-IC1 reporter cell line did not show significant responses to MIF. No significant difference was found between the TPG treated control and the MIF and TPG titration. No significant difference was found between the treated time course and the MIF and TPG time courses. Statistical analysis for 4.15.B and C was performed with One Way ANOVA and Bonferroni Post Hoc test (N=3).

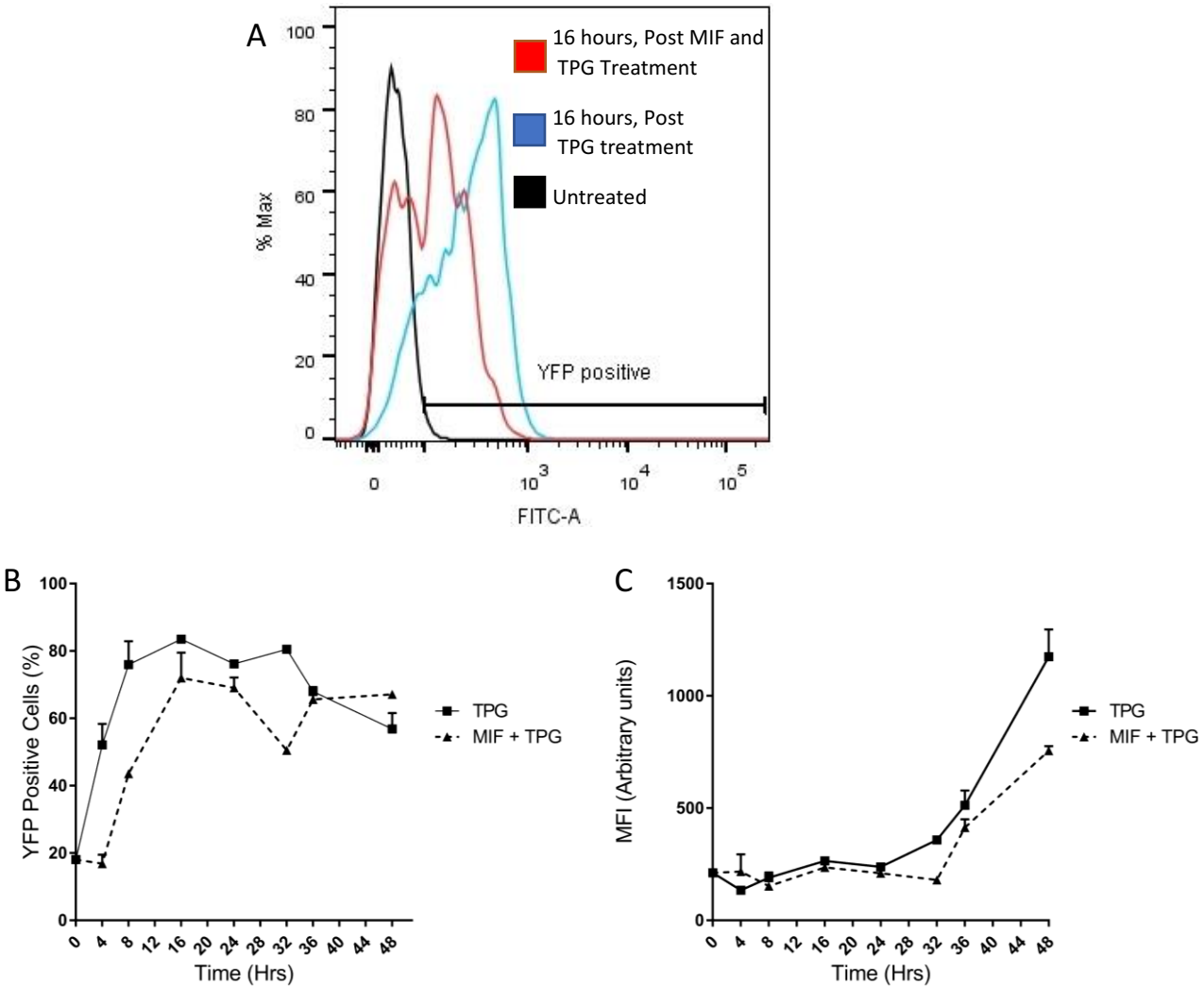

Figure 4.16: **The Analysis of the Activation of the ATF4.eYFP Transcriptional Reporter over Time in ASATF4-HeLa-IC1 Cells after Treatment with TPG and MIF.** ASATF4-HeLa-IC1 cells were seeded 24 hrs before treatment with 150 nM TPG and 250 ng/mL MIF. Cells were analysed by FACS 2-48 hours post-treatment. Intact cells were assessed for levels of eYFP expression. (A) The eYFP positive gate was set so that less than 0.1% of wild-type control cells fell within the gate. (B) The change in percent eYFP positive cells and (C) their MFI was assessed comparing cells treated TPG and those treated with TPG and MIF. No significant difference was found between the treated time course and the MIF and TPG time courses. Statistical analysis for 4.16.B and C was performed with One Way ANOVA and Bonferroni Post Hoc test (N=3).

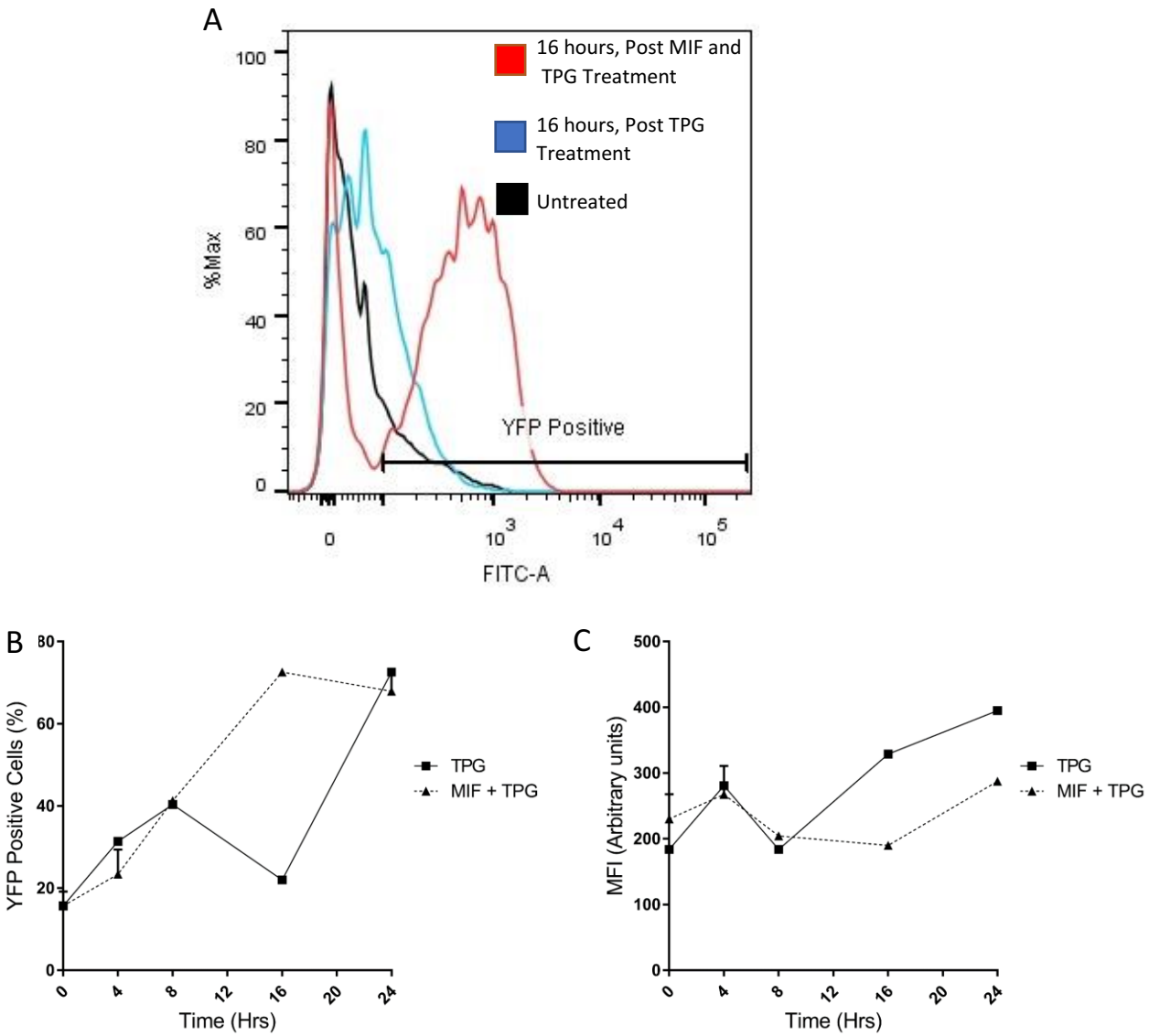

Figure 4.17: **The Analysis of the Activation of the ATF4.eYFP Transcriptional Reporter over Time in WATF4-SH-SY5Y Cells after Treatment with TPG and MIF.** WATF4-SH-SY5Y cells were seeded 24 hrs before treatment with 150 nM TPG and 250 ng/mL MIF. Cells were analysed by FACS 4-24 hours post-treatment. Intact cells were assessed for levels of eYFP expression. (A) The eYFP positive gate was set so that less than 0.1% of wild-type control cells fell within the gate. (B) The change in percent eYFP positive cells and (C) their MFI was assessed comparing cells treated TPG and those treated with TPG and MIF. No significant difference was found between the treated time course and the MIF and TPG time courses. Statistical analysis for 4.17.B and C was performed with One Way ANOVA and Bonferroni Post Hoc test (N=2).

4.4.2: Assessment of the Effects of MIF on Activation of the XBP1.ePYFP-N1 Reporter Cell Lines:

A similar set of experiments were performed with the ASXBP1-HeLa-PC2 or ASXBP1-SH-SY5Y-PC1 polyclonal cell lines to assess the effects of MIF alone or MIF in combination with TPG on the XBP1.eYFP-N1 reporter. For initial experiments 8 hour post treatment was chosen as the timepoint to analyse the effects of MIF on the reporter construct. Like the ATF4.eYFP-N1 reporter MIF alone does not appear to influence the activation of reporter in either the ASXBP1-HeLa-PC2 (data not shown) or ASXBP1-SH-SY5Y-PC1 (Figure 4.18) cell lines. However, like the ATF4.eYFP-N1 reporter cells time course experiments were performed where the effects of MIF and TPG cotreatment on these cell lines was assessed.

The results of the ASXBP1-HeLa-PC2 time course reveal that unlike the ATF4 reporter MIF treatment did not have any effect on the activation of the XBP1.eYFP-N1 reporter in terms of the number of eYFP positive cells or their MFI (Figure 4.19). Unlike the HeLa cells analysis, the ASXBP1-SH-SY5Y-PC1 cell line shows that like the ATF4 reporter MIF treatment suppresses the response to TPG. However, this effect extends into both a reduction of the number of eYFP positive cells and the MFI of those cells (Figure 4.19).

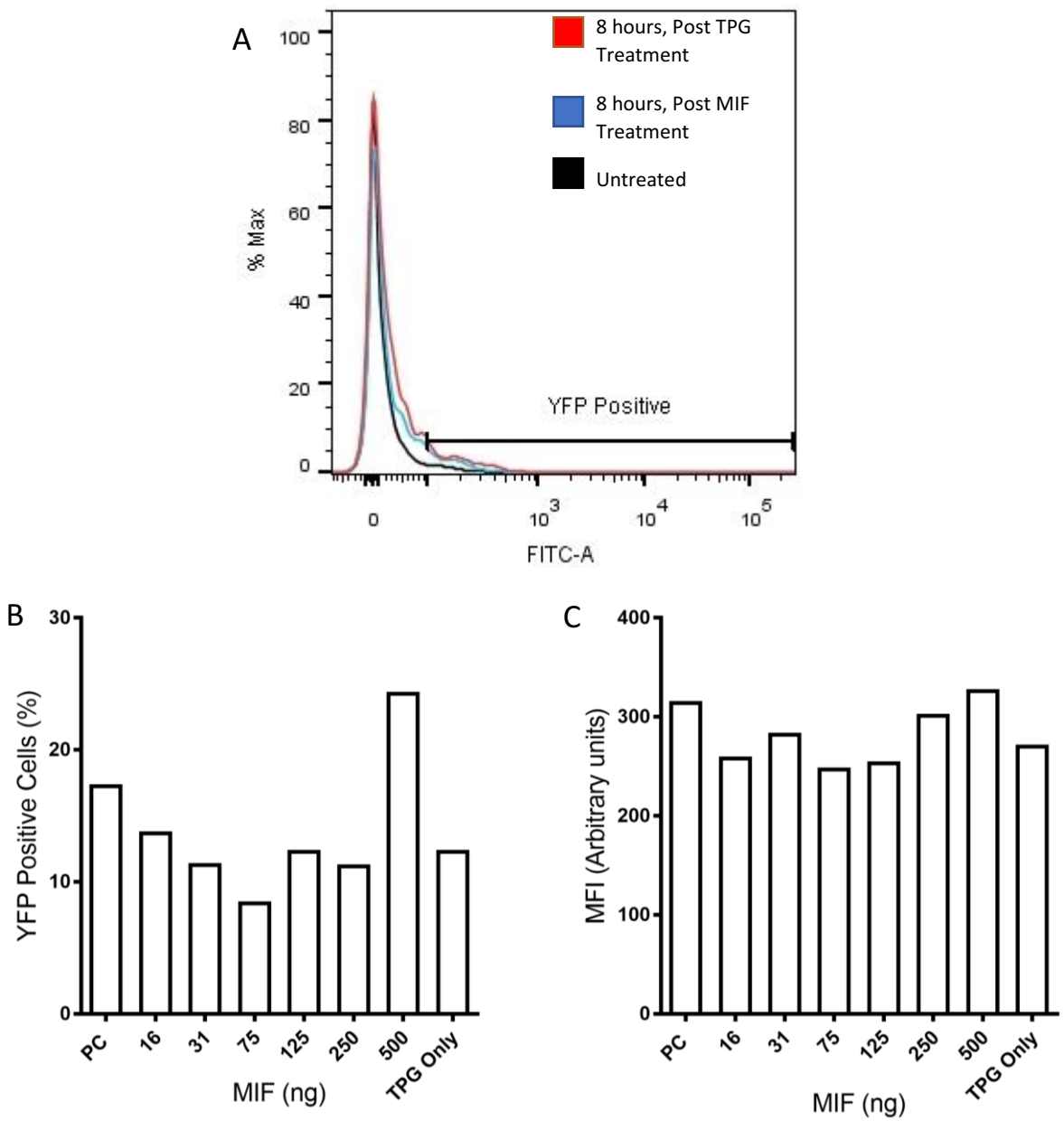

Figure 4.18: **SH-SY5Y Assessment of the Effects of MIF on WXBP1- SH-SY5Y-PC1 Cells 8hrs Post-Treatment.** ASXBP1-SH-SY5Y-PC1 cells were seeded and allowed to recover for 24 hrs before treatment with a range of concentrations of MIF. Cells were collected fixed and analyzed by FACS 8 hours after treatment. Intact cells were assessed for levels of eYFP. (A) The eYFP positive gate was set so that less than 0.1% of the wild-type control cells fell within the gate. (B) The changes in percent eYFP positive cells and (C) their MFI was assessed over range of MIF concentrations tested. The ASXBP1-SH-SY5Y reporter cell line did not show significant responses to MIF. Insufficient data collected to perform statistical analysis (N=1).

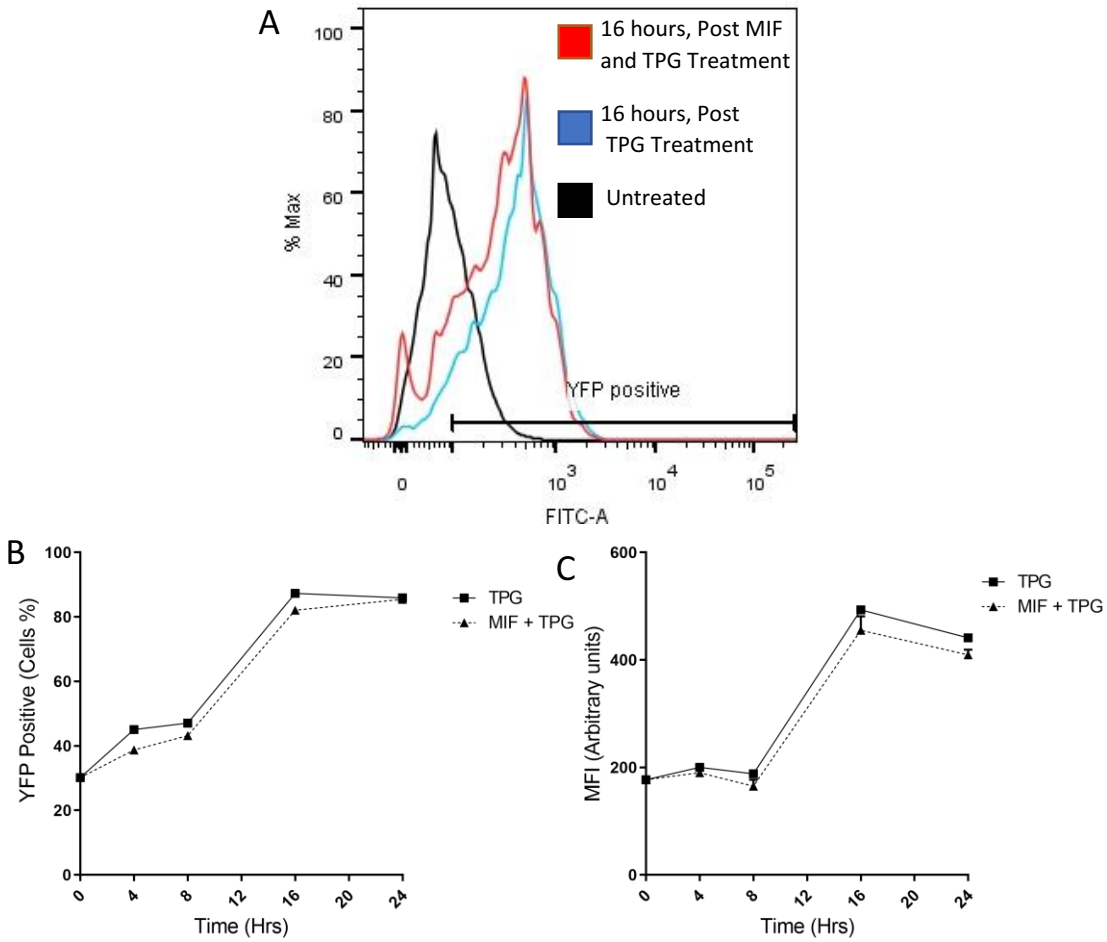

Figure 4.19: **The Analysis of the Activation of the XBP1.eYFP Transcriptional Reporter over Time in ASXBP1-HeLa-PC2 Cells after Treatment with TPG and MIF.** ASXBP1-HeLa-PC2 cells were seeded 24 hrs before treatment with 700 nM TPG and 250 ng/mL MIF. Cells were analysed by FACS 4-24 hours post-treatment. Intact cells were assessed for levels of eYFP expression. (A) The eYFP positive gate was set so that less than 0.1% of wild-type control cells fell within the gate. (B) The change in percent eYFP positive cells and (C) their MFI was assessed comparing cells treated TPG and those treated with TPG and MIF. No significant difference was found between the treated time course and the MIF and TPG time courses. Statistical analysis for 4.19.B and C was performed with One Way ANOVA and Bonferroni Post Hoc test (N=3).

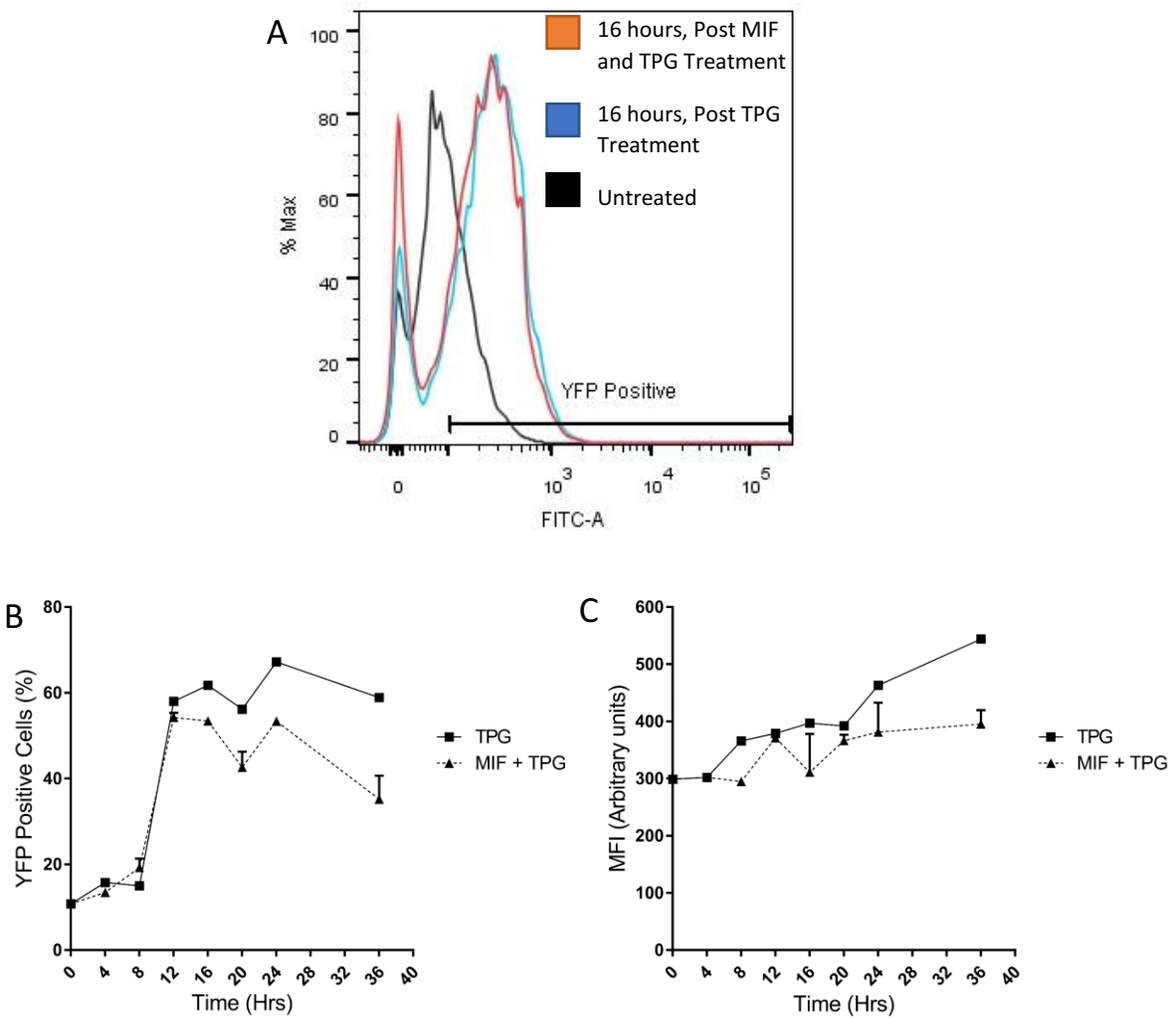

Figure 4.20: **The Analysis of the Activation of the XBP1.eYFP Transcriptional Reporter over Time in ASXBP1-SH-SY5Y-PC1 Cells after Treatment with TPG and MIF.** ASXBP1-SH-SY5Y-PC1 cells were seeded 24 hrs before treatment with 700 nM TPG and 250 ng/mL MIF. Cells were analysed by FACS 4-24 hours post-treatment. Intact cells were assessed for levels of eYFP expression. (A) The eYFP positive gate was set so that less than 0.1% of wild-type control cells fell within the gate. (B) The change in percent eYFP positive cells and (C) their MFI was assessed comparing cells treated TPG and those treated with TPG and MIF. No significant difference was found between the treated time course and the MIF and TPG time courses. Statistical analysis for 4.20.B and C was performed with One Way ANOVA and Bonferroni Post Hoc test (N=3).

4.5: Assessment of the Effects of MIF on the Downstream Targets of the UPR by RT-qPCR:

To support the results of the transcriptional reporter assays RT-qPCR was performed on wild-type HeLa and SH-SY5Y cells examining two downstream targets of the UPR response CHOP (ATF4) and ErDj4 (XBP-1). These targets were chosen because their upregulation during ER stress encompass the two endpoints for the UPR activation, attempt resolution (ErDj4) or apoptosis (CHOP).

The results of the RT-qPCR studies of the HeLa cells (Figure 4.21) partially supports the transcriptional reporter assays with MIF reducing the levels of CHOP transcript (a downstream target of ATF4) in cells experiencing ER stress relative to control cells (Figure 4.21.A). Unlike the transcriptional reporter assays which did not show any change in XBP-1 activation there was a suppression in the levels of ErDj4 transcript which mirrored that of CHOP (Figure 4.21.B).

In the SH-SY5Y cells a steady decline is seen in the levels of CHOP transcript over the time course however this decline is more acute in those cells which had been co-treated with MIF and TPG supporting the transcriptional reporter findings in the WATF4-SH-SY5Y cells which indicate a suppression of ATF4 activity 12 and 24 hours post-treatment (Figure 4.22.A). Similarly, ErDj4 transcript levels drop dramatically after TPG treatment however these partially recover in cells by 24 hrs post-treatment (Figure 4.22.B). This recover does not occur in MIF treated cells indicating a suppression in XBP activity which is consistent with the lower number of eYFP positive cells and lower MFI of eYFP positive cells observed in the transcriptional reporter assays using ASXBP1-SH-SY5Y-PC1.

A

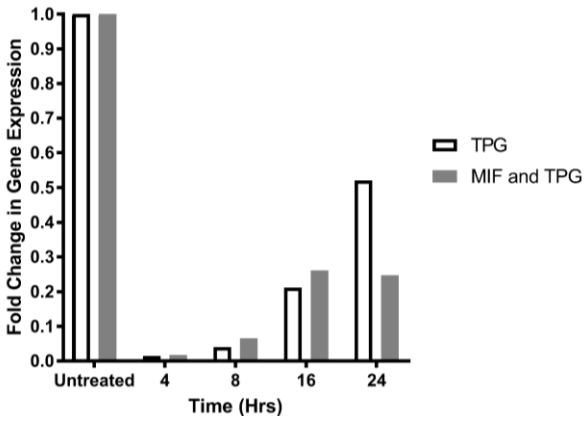

CHOP

B

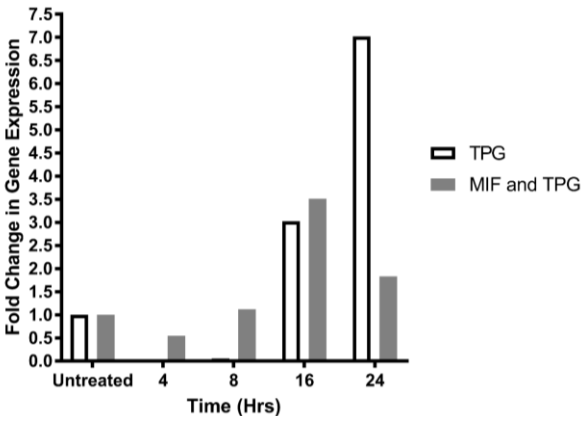

ErDJ4

Figure 4.21: **Assessment of Effects of MIF on CHOP and ErDJ4 Transcript Levels in WT HeLa Cells During ER Stress Responses.** Wild-type Hela cells were treated with TPG (150nM) or TPG and MIF (250ng/mL). RNA was isolated from these cells at 0, 4, 8, 12 and 24 hours post-treatment. RT-qPCR was performed using these RNA samples (A) assessing the levels of CHOP (B) or ErDJ4. The housekeeping gene GAPDH was used as the internal control to normalise transcript levels. The delta-delta Ct of the target transcripts were calculated to determine the relative level of each transcript at each timepoint. The relative fold change in gene expression was then calculated using the untreated control cells as the baseline level of expression for each transcript. No significant difference was found between the treated time course and the MIF and TPG time courses. Statistical analysis for 4.21.B and C was performed with One Way ANOVA and Bonferroni Post Hoc test (N=1).

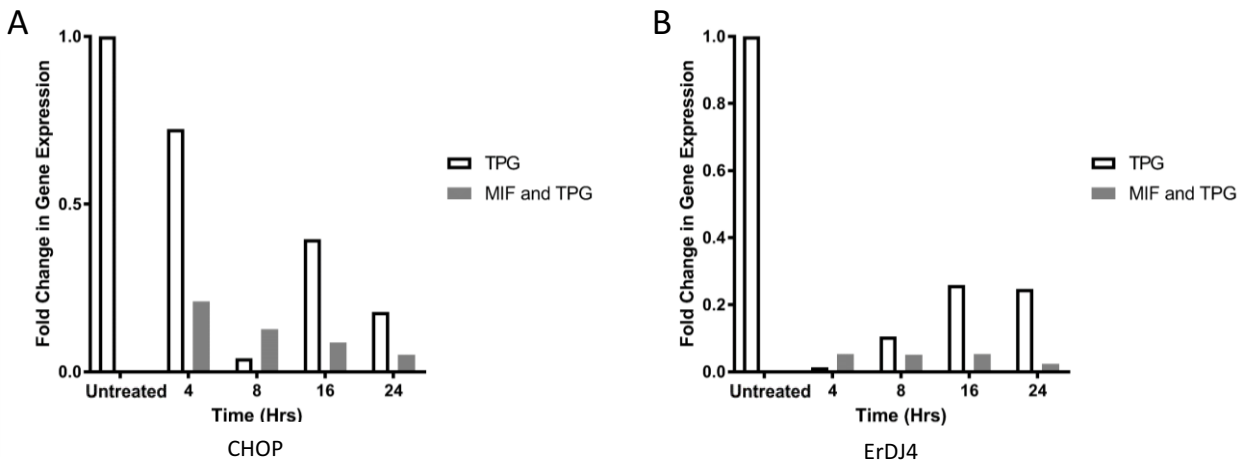

Figure 4.22: **Assessment of Effects of MIF on CHOP and ErDJ4 Transcript Levels in SH-SY5Y Cells During ER Stress Responses.** Wild-type SH-SY5Y cells were treated with TPG (150nM) or TPG and MIF (250ng/mL). RNA was isolated from these cells at 0, 4, 8, 12 and 24 hours post-treatment. RT-qPCR was performed using these RNA samples (A) assessing the levels of CHOP or (B) ErDJ4. The housekeeping gene GAPDH was used as the internal control to normalise transcript levels. The delta-delta Ct of the target transcripts were calculated to determine the relative level of each transcript at each timepoint. The relative fold change in gene expression was then calculated using the untreated control cells as the baseline level of expression for each transcript. No significant difference was found between the treated time course and the MIF and TPG time courses. Statistical analysis for 4.22.B and C was performed with One Way ANOVA and Bonferroni Post Hoc test (N=1).

5.0 Discussion:

5.1 MIF Partially Suppresses UPR responses:

A combination of fluorescent protein transcriptional reporter constructs and RT-qPCR were used to assess the effects of MIF on UPR induction after TPG treatment in cells derived from an epithelial (HeLa) and neuronal (SH-S5Y) lineages. The results of both studies support that MIF partially suppresses the induction of UPR responses in both cell lineages. In both cell lines the activity of the ATF4 transcriptional reporter were suppressed while the activity of the XBP reporter was supressed in SH-SY5Y cells but not HeLa cells. The RT-qPCR the results obtained for the HeLas show a consistent trend from the transduction pathways to the mRNA for the downstream targets with a lower mRNA transcription rate for ErDj4 and CHOP. The SH-SY5Ys show the same general trend but reasons that are not clear the post-treatment timepoints show lower level of ErDj4 and CHOP than the pre-treatment controls .

5.2: Potential signal transduction pathways that connect MIF UPR activity:

While a clear transcription effect on UPR in induction was observed in this study the defining the molecular mechanisms underlay this effect lay outside the scope of this study. However, there are several possibilities. One key regulator of UPR activity that shares common signal transduction partners with CD74 mediated MIF signalling is mTORC1. So, one possibility is that MIF signalling may somehow impinges on the mTOR pathway in a manner which depresses its activation of the UPR.

A number of recent studies have examined links between these pathways. There is some evidence that they are connected, a recent study looking at mTOR knockdown showed that it specifically depressed IRE1/XBP activation but not the PERK/ATF4 pathway (Kato *et al.*, 2012). Within this study Kato *et al.,* showed that mTOR's pro-inflammatory/pro-apoptotic activity was meditated via modulation of AKT, in which mTOR suppresses the hyperphosphorylation of AKT which in turn results in lowers IRE1 activity and suppression of Bcl-2. Similarly, a subsequent study showed that inhibition of JNK, a second potential transduction mediator, could link CD74 mediated MIF signalling caused upregulation of pro-apoptotic signals potentially via activation of mTORC1 through activating RAPTOR (Kwak *et al.*, 2012). So, it is possible that one or more transduction pathways are influenced by MIF signalling (via CD74) that would modulate downstream UPR pathways via distinct activities on IRE1 and mTORC1. This may explain some of the slightly different results that were observed between the two cell lines derived from epithelial and neuronal lineages.

It is known that MIF also has at least one non-classical, CD74 independent, signalling route for affecting cells. The most well-known of these non-classical receptors is the intracellular target JAB1 (Kleemann *et al.,* 2000). JAB1 can, under a variety of circumstances, phosphorylate JNK. However, when MIF binds to JAB1 it inhibits this activity offering another potential pathway via which MIF might indirectly influence mTORC1 and UPR transducers such as IRE1. Therefore, it reasonable to speculate that suppression of IRE1 caused by MIF might be linked to its activities on JAB1. Differences in MIF signalling via the JAB1 pathway that might be found in different cell lineages or differences in a cell's ability to respond to MIF via CD74 could lead to differences in how it influences UPR activation and downstream apoptotic and inflammatory responses.

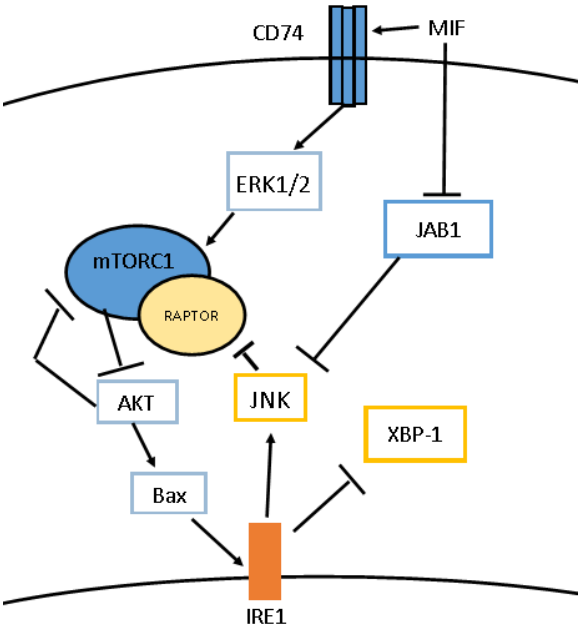

Figure 5.1: **Diagram showing the Potential Relationships Between MIF and IRE1.** Impingement of MIF on CD74 leads to an upregulation of mTORC1, this leads to a suppression of AKT leading to a change of IRE1 from endoribonuclease activity to phosphorylation of JNK. Suppression of JAB1 activity by MIF prevents JNK from being phosphorylated leading to a diminished JNK signal and causes a diminished mTOR response.

Links between PERK/ATF4 and JNK activity have been identified (Liang *et al.*, 2006)However, this paper suggests that it is caused by Ca^{2+} loss within the ER and not by blockage of Glycosylation and so it this effect might be an artefact of the use of TPG rather than Tunicamycin. This is, of course, undercut by Kato showing that only IRE1 is affected by mTORC1 activation status. So, cell lineage may also be playing a role as the Kato paper utilized NRK-52E, a Rat kidney Epithelial cell line for their study, rather than a human epithelial or neuronal cell lineage.

5.2: Downstream Targets, ErDj4 and CHOP:

Due to constraints in the time and scope of the study there are several aspects of the RT-qPCR data that is both unexpected and requires further exploration. The effects of TPG on CHOP transcript levels in both cell lines showed that there was very little difference between the treated and untreated samples in the HeLa cells (Figure 4.19 and 4.20). In addition, unexpectedly in both cell lines the control samples (0 hours) showed much higher levels of CHOP transcript relative to the subsequent time points (4-24hrs post treatment). This is possibly due to the use of only 150nm of TPG within the treatment so that there was never enough stress induced to cause a clear upregulation of CHOP. For ErDj4 there was a more consistent effect in the HeLa cells with a clear induction of the transcript after TPG treatment. The results are suggestive that MIF suppression mediates effects on both UPR pathways reducing the production of both of these key transcripts after ER stress induction however additional assays replicating these results and examining additional downstream targets of both XBP-1 and ATF4 are required.

5.3: How might MIF Suppression of UPR Influence Health and Disease?:

This study has identified a potential new role for MIF in modulating UPR during ER stress. What ramifications might this have in understanding the potential role of MIF in development and disease? Both MIF and ER stress responses have been found to be key components in normal homeostatic process and are linked to a variety diseases or disease processes. For instance, both MIF and the UPR are linked to disease aetiology in Alzheimer's and Diabetes type 2 (Casas-Tinto *et al.,* 2011, Gorasia *et al.,* 2015). Potential interventions based on MIF or UPR targets are being tested in models for both of these diseases. Previously, MIF was thought to exert its activity in these diseases by modulating recruitment or activation of pro-inflammatory immune cells. However, if MIF differentially suppresses specific elements of UPR responses this could potentially lead to apoptosis or pathological responses linked to a cells inability to successfully resolve ER dysfunction. In a recent study published by Walter *et. al.* (2015) the kinetics of activation of the different UPR pathways (IRE1/XBP-1 or PERK/ATF4) determined if a cell survived a potentially lethal ER dysfunction. If early IRE1/XBP-1 activation and delayed ATF4 translation were cytoprotective and reduced ER stress induced apoptosis. In our studies in HeLa cells MIF reduced/delayed PERK/ATF4 activation but did not affect IRE1/XBP-1 activity this should allow cells that respond to MIF to survive conditions which cause acute ER stress. MIF is found to be produced in high amounts in epithelial tissues like the GI tract. Perhaps it helps reduce apoptosis in these tissues when they experience ER stress. Interestingly in the SH-SY5Ys (the neuronal cell line) both pathways were suppressed by MIF

which could result in the inhibition of resolution of ER dysfunction and promote terminal downstream effects. A study recent study has shown that MIF (which is a biomarker for the onset of Alzheimer's pathology) exacerbates the toxicity of protein aggregates of beta amyloid or tau (Bacher *et al.,* 2010). These aggregates activate UPR responses leading to apoptosis. If MIF specifically increases the sensitivity of this cell type to these aggregates this may explain why they are selectively lost as the disease progresses and thus why MIF is a biomarker for pathology.

5.5 Future Work:

There are a number of logical extensions to this study. This would include further assessment of the potential downstream targets of MIF, mTOR and JAB1, to see one or both of them is required for mediating the UPR suppression. To complete this, XBP-1.eYFP monoclonal lines of both HeLa and SH-SY5Ys would need to be isolated. However, due to the potential toxicity problems of the full length XBP protein, making constructs that lack the DNA binding site from XBP-1 may help facilitate the isolation of stable lines. To make sure the effects of MIF on UPR induction are specific a second UPR inducer such as Tunicamycin should also be tested within this assay. Once these cells are available the specific pathway that mediates the suppression can be examined by either genetically modifying the cells to create JAB1 knockout (CRISPR/CAS), or by transiently reducing JAB1 levels using transfection with specific siRNAs. If UPR suppression is reduced in the JAB1 deficient cells, then this would suggest that MIF (via JAB1) is potentiating IRE1 phosphorylation of JNK. Lastly to confirm and expand results of the RT-qPCR data RNA sequencing (RNAseq) should be performed on cell treated with MIF during ER stress which will allow simultaneous assessment of transcript levels for a wide variety of UPR targets including BIP, Calnexin/Calreticulin, CHOP, EDEM, ErDJ3-5 and GADD34 along with genes involved in other biological process such as apoptosis.

6.0 Concluding Remarks:

To conclude, transgenic poly and monoclonal cell lines were produced that show the activation of different UPR pathways during ER stress by upregulation of a fluorescent reporter proteins. These were tested to assess whether MIF can affect basal levels or Thapsigargin-induced ER Stress. The fluorescent reporters indicated a MIF suppressed UPR activation although there was variation in which UPR pathways that were affected in different cell types. These observations were supported by RT-qPCR of specific UPR target transcripts though further work is required. This effect, if more advanced work supports it, may be important for understanding the aetiologies of a number of conditions where both MIF and ER stress are implicated as factors influencing disease development and/or pathology. It might also offer potential targets for the development of novel therapeutics strategies for the treatment of these diseases.

References:

Alexopoulou, L. *et al.* (2001) 'Recognition of double-stranded RNA and activation of NF-κB by Toll-like receptor 3', *Nature*. Macmillan Magazines Ltd., 413, p. 732. Available at: https://doi.org/10.1038/35099560.

Amin, M. A. *et al.* (2003) 'Migration Inhibitory Factor Mediates Angiogenesis via Mitogen-Activated Protein Kinase and Phosphatidylinositol Kinase', *Circulation Research*, 93(4), pp. 321–329. doi: 10.1161/01.RES.0000087641.56024.DA.

Appenzeller-Herzog, C. and Hall, M. N. (2012) 'Bidirectional crosstalk between endoplasmic reticulum stress and mTOR signaling.', *Trends in cell biology*. Elsevier, 22(5), pp. 274–82. doi: 10.1016/j.tcb.2012.02.006.

Bendrat, K. *et al.* (1997) 'Biochemical and Mutational Investigations of the Enzymatic Activity of Macrophage Migration Inhibitory Factor', *Biochemistry*. American Chemical Society, 36(49), pp. 15356–15362. doi: 10.1021/bi971153a.

Bernhagen, J. *et al.* (1993) 'MIF is a pituitary-derived cytokine that potentiates lethal endotoxaemia', *Nature*, 365(6448), pp. 756–759. doi: 10.1038/365756a0.

Bertolotti, A. *et al.* (2000) 'Dynamic interaction of BiP and ER stress transducers in the unfolded-protein response', *Nat Cell Biol*. Macmillan Magazines Ltd., 2(6), pp. 326–332. Available at: http://dx.doi.org/10.1038/35014014.

Bitko, V. *et al.* (1997) 'Transcriptional Induction of Multiple Cytokines by Human Respiratory Syncytial Virus Requires Activation of NF-κB and Is Inhibited by Sodium Salicylate and Aspirin', *Virology*. Academic Press, 232(2), pp. 369–378. doi: 10.1006/VIRO.1997.8582.

Bloom, B. R. and Bennett, B. (1966) 'Mechanism of a Reaction in Vitro Associated with Delayed-Type Hypersensitivity', *Science*, 153(3731), p. 80 LP-82. doi: 10.1126/science.153.3731.80.

Calandra, T. *et al.* (1994) 'The macrophage is an important and previously unrecognized source of macrophage migration inhibitory factor', *The Journal of experimental medicine*. The Rockefeller University Press, 179(6), pp. 1895–1902. Available at: https://www.ncbi.nlm.nih.gov/pubmed/8195715.

Calandra, T. *et al.* (2003) 'Macrophage Migration Inhibitory Factor and Host Innate Immune Defenses against Bacterial Sepsis', *The Journal of Infectious Diseases*, 187(Supplement_2), pp. S385–S390. doi: 10.1086/374752.

Calfon, M. *et al.* (2002) 'IRE1 couples endoplasmic reticulum load to secretory capacity by processing the XBP-1 mRNA', *Nature*. Macmillan Magazines Ltd., 415, p. 92. Available at: https://doi.org/10.1038/415092a.

Cao, S. *et al.* (2006) 'NF-kappaB1 (p50) homodimers differentially regulate pro- and anti-inflammatory cytokines in macrophages', *The Journal of biological chemistry*. 2006/07/11, 281(36), pp. 26041–26050. doi: 10.1074/jbc.M602222200.

Carracedo, A. *et al.* (2008) 'Inhibition of mTORC1 leads to MAPK pathway activation through a PI3K-dependent feedback loop in human cancer', *The Journal of Clinical Investigation*. The American Society for Clinical Investigation, 118(9), pp. 3065–3074. doi: 10.1172/JCI34739.

Casas-Tinto, S. *et al.* (2011) 'The ER stress factor XBP1s prevents amyloid-β neurotoxicity', *Human Molecular Genetics*. Oxford University Press, 20(11), pp. 2144–2160. doi: 10.1093/hmg/ddr100.

Clemens, M. J. (2001) 'Initiation Factor eIF2$α$ Phosphorylation in Stress Responses and Apoptosis', in Rhoads, R. E. (ed.) *Signaling Pathways for Translation: Stress, Calcium, and Rapamycin*. Berlin, Heidelberg: Springer Berlin Heidelberg, pp. 57–89. doi: 10.1007/978-3-662-09889-9_3.

Collart, M. A., Baeuerle, P. and Vassalli, P. (1990) 'Regulation of tumor necrosis factor alpha transcription in macrophages: involvement of four kappa B-like motifs and of constitutive and inducible forms of NF-kappa B', *Molecular and cellular biology*, 10(4), pp. 1498–1506. Available at: https://www.ncbi.nlm.nih.gov/pubmed/2181276.

David, J. R. (1966) 'Delayed hypersensitivity in vitro: its mediation by cell-free substances formed by lymphoid cell-antigen interaction', *Proceedings of the National Academy of Sciences of the United States of America*, 56(1), pp. 72–77. Available at: https://www.ncbi.nlm.nih.gov/pubmed/5229858.

Fan, C. *et al.* (2013) 'MIF intersubunit disulfide mutant antagonist supports activation of CD74 by endogenous MIF trimer at physiologic concentrations', *Proceedings of the National Academy of Sciences of the United States of America*. 2013/06/17. National Academy of Sciences, 110(27), pp. 10994–10999. doi: 10.1073/pnas.1221817110.

Gardner, B. M. and Walter, P. (2011) 'Unfolded proteins are Ire1-activating ligands that directly induce the unfolded protein response', *Science (New York, N.Y.)*. 2011/08/18, 333(6051), pp. 1891–1894. doi: 10.1126/science.1209126.

Gonzalez, S. and Rallis, C. (2017) 'The TOR Signaling Pathway in Spatial and Temporal Control of Cell Size and Growth ', *Frontiers in Cell and Developmental Biology* , p. 61. Available at: https://www.frontiersin.org/article/10.3389/fcell.2017.00061.

Gorasia, D. G. *et al.* (2015) 'Pancreatic Beta Cells Are Highly Susceptible to Oxidative and ER Stresses during the Development of Diabetes', *Journal of Proteome Research*. American Chemical Society, 14(2), pp. 688–699. doi: 10.1021/pr500643h.

Gordon-Weeks, A. N. *et al.* (2015) 'Macrophage migration inhibitory factor: A key cytokine and therapeutic target in colon cancer', *Cytokine & Growth Factor Reviews*. Pergamon, 26(4), pp. 451–461. doi: 10.1016/J.CYTOGFR.2015.03.002.

Han, J. *et al.* (2013) 'ER-stress-induced transcriptional regulation increases protein synthesis leading to cell death', *Nat Cell Biol*. Nature Publishing Group, a division of Macmillan Publishers Limited. All Rights Reserved., 15(5), pp. 481–490. doi: 10.1038/ncb2738http://www.nature.com/ncb/journal/v15/n5/abs/ncb2738.html#supplementary-information.

Helenius, A., Marquardt, T. and Braakman, I. (1992) 'The endoplasmic reticulum as a protein-folding compartment', *Trends in Cell Biology*, 2(8), pp. 227–231. doi: http://dx.doi.org/10.1016/0962-8924(92)90309-B.

Hetz, C. *et al.* (2011) 'The Unfolded Protein Response: Integrating Stress Signals Through the Stress Sensor IRE1α', *Physiological Reviews*. American Physiological Society, 91(4), pp. 1219–1243. doi: 10.1152/physrev.00001.2011.

Hiscott, J. *et al.* (1993) 'Characterization of a functional NF-kappa B site in the human

interleukin 1 beta promoter: evidence for a positive autoregulatory loop', *Molecular and cellular biology*, 13(10), pp. 6231–6240. Available at: https://www.ncbi.nlm.nih.gov/pubmed/8413223.

Hou, J. *et al.* (2012) 'Induction of interleukin-10 is dependent on p38 mitogen-activated protein kinase pathway in macrophages infected with porcine reproductive and respiratory syndrome virus', *Virology journal*. BioMed Central, 9, p. 165. doi: 10.1186/1743-422X-9-165.

Hoyos, B. *et al.* (1989) 'Kappa B-specific DNA binding proteins: role in the regulation of human interleukin-2 gene expression', *Science*, 244(4903), p. 457 LP-460. doi: 10.1126/science.2497518.

Jackson, R. J., Hellen, C. U. T. and Pestova, T. V (2010) 'The mechanism of eukaryotic translation initiation and principles of its regulation', *Nature reviews. Molecular cell biology*, 11(2), pp. 113–127. doi: 10.1038/nrm2838.

Jiang, S. *et al.* (2016) 'TLR10 Is a Negative Regulator of Both MyD88-Dependent and -Independent TLR Signaling', *Journal of immunology (Baltimore, Md. : 1950)*, 196(9), p. 3834—3841. doi: 10.4049/jimmunol.1502599.

Johnson, D. R. and Pober, J. S. (1994) 'HLA class I heavy-chain gene promoter elements mediating synergy between tumor necrosis factor and interferons', *Molecular and cellular biology*, 14(2), pp. 1322–1332. Available at: https://www.ncbi.nlm.nih.gov/pubmed/8289810.

Jung-Kang, J. *et al.* (2017) 'ATF6 Decreases Myocardial Ischemia/Reperfusion Damage and Links ER Stress and Oxidative Stress Signaling Pathways in the Heart', *Circulation Research*. American Heart Association, 120(5), pp. 862–875. doi: 10.1161/CIRCRESAHA.116.310266.

Kato, H. *et al.* (2012) 'mTORC1 serves ER stress-triggered apoptosis via selective activation of the IRE1-JNK pathway', *Cell death and differentiation*. 2011/07/22. Nature Publishing Group, 19(2), pp. 310–320. doi: 10.1038/cdd.2011.98.

Kim, M. J. *et al.* (2017) 'Macrophage migration inhibitory factor interacts with thioredoxin-interacting protein and induces NF-κB activity', *Cellular Signalling*. Pergamon, 34, pp. 110–120. doi: 10.1016/J.CELLSIG.2017.03.007.

Klasen, C. *et al.* (2014) *MIF promotes B cell chemotaxis through the receptors CXCR4 and CD74 and ZAP-70 signaling*, *Journal of immunology (Baltimore, Md. : 1950)*. doi: 10.4049/jimmunol.1302209.

Kleemann, R. *et al.* (2000) 'Intracellular action of the cytokine MIF to modulate AP-1 activity and the cell cycle through Jab1', *Nature*. Macmillan Magazines Ltd., 408, p. 211. Available at: https://doi.org/10.1038/35041591.

Kudrin, A. *et al.* (2006) 'Human Macrophage Migration Inhibitory Factor: A PROVEN IMMUNOMODULATORY CYTOKINE? ', *Journal of Biological Chemistry* , 281(40), pp. 29641–29651. doi: 10.1074/jbc.M601103200.

Kwak, D. *et al.* (2012) 'Osmotic Stress Regulates Mammalian Target of Rapamycin (mTOR) Complex 1 via c-Jun N-terminal Kinase (JNK)-mediated Raptor Protein Phosphorylation', *Journal of Biological Chemistry* , 287(22), pp. 18398–18407. doi: 10.1074/jbc.M111.326538.

Lee, A.-H., Iwakoshi, N. N. and Glimcher, L. H. (2003) 'XBP-1 regulates a subset of endoplasmic reticulum resident chaperone genes in the unfolded protein response', *Molecular and cellular biology*. American Society for Microbiology, 23(21), pp. 7448–7459. doi:

10.1128/MCB.23.21.7448-7459.2003.

Lencer, W. I. *et al.* (2015) 'Innate immunity at mucosal surfaces: the IRE1-RIDD-RIG-I pathway', *Trends in Immunology*. Elsevier Current Trends, 36(7), pp. 401–409. doi: 10.1016/J.IT.2015.05.006.

Leng, L. *et al.* (2003) 'MIF signal transduction initiated by binding to CD74', *The Journal of experimental medicine*. The Rockefeller University Press, 197(11), pp. 1467–1476. doi: 10.1084/jem.20030286.

Leng, L. and Bucala, R. (2006) 'Insight into the biology of Macrophage Migration Inhibitory Factor (MIF) revealed by the cloning of its cell surface receptor', *Cell Research*. Shanghai Institutes for Biological Sciences, Chinese Academy of Sciences, 16, p. 162. Available at: https://doi.org/10.1038/sj.cr.7310022.

Liang, S.-H. *et al.* (2006) 'PERK (eIF2alpha kinase) is required to activate the stress-activated MAPKs and induce the expression of immediate-early genes upon disruption of ER calcium homoeostasis', *The Biochemical journal*. 2005/12/12. Portland Press Ltd., 393(Pt 1), pp. 201–209. doi: 10.1042/BJ20050374.

Lue, H. *et al.* (2006) 'Rapid and transient activation of the ERK MAPK signalling pathway by macrophage migration inhibitory factor (MIF) and dependence on JAB1/CSN5 and Src kinase activity', *Cellular Signalling*. Pergamon, 18(5), pp. 688–703. doi: 10.1016/J.CELLSIG.2005.06.013.

Lue, H. *et al.* (2011) 'Activation of the JNK signalling pathway by macrophage migration inhibitory factor (MIF) and dependence on CXCR4 and CD74', *Cellular signalling*. 2010/08/31, 23(1), pp. 135–144. doi: 10.1016/j.cellsig.2010.08.013.

Marciniak, S. J. and Ron, D. (2006) 'Endoplasmic Reticulum Stress Signaling in Disease', *Physiological Reviews*, 86(4), pp. 1133–1149. doi: 10.1152/physrev.00015.2006.

Matsuura, T. *et al.* (2007) 'Basal and angiotensin II-inhibited neuronal delayed-rectifier K+ current are regulated by thioredoxin', *American Journal of Physiology-Cell Physiology*, 293(1), pp. C211–C217. doi: 10.1152/ajpcell.00615.2006.

Maurel, M. *et al.* (2014) 'Getting RIDD of RNA: IRE1 in cell fate regulation', *Trends in Biochemical Sciences*. Elsevier Current Trends, 39(5), pp. 245–254. doi: 10.1016/J.TIBS.2014.02.008.

Mear, J. P. *et al.* (1999) *Spondyloarthropathies Role in Susceptibility to Pocket Suggests a Novel Mechanism for Its Misfolding of HLA-B27 as a Result of Its B Misfolding of HLA-B27 as a Result of Its B Pocket Suggests a Novel Mechanism for Its Role in Susceptibility to Spondyloart*, *J Immunol References*. doi: 10.4049/jimmunol.1102711.

Merk, M. *et al.* (2009) 'The Golgi-associated protein p115 mediates the secretion of macrophage migration inhibitory factor', *Journal of immunology (Baltimore, Md. : 1950)*, 182(11), pp. 6896–6906. doi: 10.4049/jimmunol.0803710.

Merk, M. *et al.* (2012) 'D-dopachrome tautomerase (D-DT or MIF-2): doubling the MIF cytokine family', *Cytokine*. 2012/04/14, 59(1), pp. 10–17. doi: 10.1016/j.cyto.2012.03.014.

Mori, K. *et al.* (1992) 'A 22 bp cis-acting element is necessary and sufficient for the induction of the yeast KAR2 (BiP) gene by unfolded proteins', *The EMBO journal*, 11(7), pp. 2583–2593. Available at: https://www.ncbi.nlm.nih.gov/pubmed/1628622.

Okada, T. *et al.* (2002) 'Distinct roles of activating transcription factor 6 (ATF6) and double-stranded RNA-activated protein kinase-like endoplasmic reticulum kinase (PERK) in transcription during the mammalian unfolded protein response', *Biochemical Journal*, 366, pp. 585–594. Available at: https://www.ncbi.nlm.nih.gov/pmc/articles/PMC1222788/pdf/12014989.pdf.

Peeters, H. *et al.* (2004) 'Radiological sacroiliitis, a hallmark of spondylitis, is linked with CARD15 gene polymorphisms in patients with Crohn's disease', *Annals of the rheumatic diseases*, 63(9), pp. 1131–1134. doi: 10.1136/ard.2004.021774.

Pessara, U. and Koch, N. (1990) 'Tumor necrosis factor alpha regulates expression of the major histocompatibility complex class II-associated invariant chain by binding of an NF-kappa B-like factor to a promoter element', *Molecular and cellular biology*, 10(8), pp. 4146–4154. Available at: https://www.ncbi.nlm.nih.gov/pubmed/2115119.

Qi, L., Tsai, B. and Arvan, P. (2017) 'New Insights into the Physiological Role of Endoplasmic Reticulum-Associated Degradation', *Trends Cell Biol*, 27(6), pp. 430–440. doi: 10.1016/j.tcb.2016.12.002.

Roger, T. *et al.* (2005) 'Macrophage migration inhibitory factor promotes innate immune responses by suppressing glucocorticoid-induced expression of mitogen-activated protein kinase phosphatase-1', *European Journal of Immunology*. John Wiley & Sons, Ltd, 35(12), pp. 3405–3413. doi: 10.1002/eji.200535413.

Roger, T. *et al.* (2017) 'Plasma Levels of Macrophage Migration Inhibitory Factor and d-Dopachrome Tautomerase Show a Highly Specific Profile in Early Life', *Frontiers in Immunology*, 8, p. 26. Available at: https://www.frontiersin.org/article/10.3389/fimmu.2017.00026.

Romero-Ramírez, L. *et al.* (2004) *XBP1 Is Essential for Survival under Hypoxic Conditions and Is Required for Tumor Growth*, *Cancer research*. doi: 10.1158/0008-5472.CAN-04-1606.

Rosengren, E. *et al.* (1997) 'The macrophage migration inhibitory factor MIF is a phenylpyruvate tautomerase', *FEBS Letters*. John Wiley & Sons, Ltd, 417(1), pp. 85–88. doi: 10.1016/S0014-5793(97)01261-1.

Roy, B. and Lee, A. S. (1999) 'The mammalian endoplasmic reticulum stress response element consists of an evolutionarily conserved tripartite structure and interacts with a novel stress-inducible complex', *Nucleic acids research*, 27(6), pp. 1437–1443. Available at: https://www.ncbi.nlm.nih.gov/pubmed/10037803.

Rzymski, T. *et al.* (2010) 'Regulation of autophagy by ATF4 in response to severe hypoxia', *Oncogene*. Macmillan Publishers Limited, 29, p. 4424. Available at: https://doi.org/10.1038/onc.2010.191.

Sanacora, S. *et al.* (2013) 'Regulation of NFkB-dependent Interleukin-8 in Human Macrophages By Nuclear IkBa and Proteasome Inhibition', *The FASEB Journal*. Federation of American Societies for Experimental Biology, 27(1_supplement), p. 550.17-550.17. doi: 10.1096/fasebj.27.1_supplement.550.17.

Schwartz, V. *et al.* (2009) 'A functional heteromeric MIF receptor formed by CD74 and CXCR4', *FEBS letters*. 2009/08/06, 583(17), pp. 2749–2757. doi: 10.1016/j.febslet.2009.07.058.

Sha, H. *et al.* (2011) 'Stressed out about obesity: IRE1α–XBP1 in metabolic disorders', *Trends in Endocrinology & Metabolism*, 22(9), pp. 374–381. doi:

http://dx.doi.org/10.1016/j.tem.2011.05.002.

Shen, F. *et al.* (2006) 'Identification of Common Transcriptional Regulatory Elements in Interleukin-17 Target Genes', *Journal of Biological Chemistry* , 281(34), pp. 24138–24148. doi: 10.1074/jbc.M604597200.

Shi, X. *et al.* (2006) 'CD44 is the signaling component of the macrophage migration inhibitory factor-CD74 receptor complex', *Immunity*, 25(4), pp. 595–606. doi: 10.1016/j.immuni.2006.08.020.

Sica, A. *et al.* (1997) 'Interaction of NF-κB and NFAT with the Interferon-γ Promoter', *Journal of Biological Chemistry* , 272(48), pp. 30412–30420. doi: 10.1074/jbc.272.48.30412.

Son, A. *et al.* (2009) 'Direct Association of Thioredoxin-1 (TRX) with Macrophage Migration Inhibitory Factor (MIF): Regulatory Role of TRX on MIF Internalization and Signaling', *Antioxidants & Redox Signaling*. Mary Ann Liebert, Inc., publishers, 11(10), pp. 2595–2605. doi: 10.1089/ars.2009.2522.

Son, Y.-H. *et al.* (2008) 'Roles of MAPK and NF-κB in Interleukin-6 Induction by Lipopolysaccharide in Vascular Smooth Muscle Cells', *Journal of Cardiovascular Pharmacology*, 51(1). Available at: https://journals.lww.com/cardiovascularpharm/Fulltext/2008/01000/Roles_of_MAPK_and_NF__B_in_Interleukin_6_Induction.11.aspx.

Sugimoto, M. A. *et al.* (2016) 'Resolution of Inflammation: What Controls Its Onset?', *Frontiers in immunology*. Frontiers Media S.A., 7, p. 160. doi: 10.3389/fimmu.2016.00160.

Sun, H. W. *et al.* (1996) 'Crystal structure at 2.6-A resolution of human macrophage migration inhibitory factor', *Proceedings of the National Academy of Sciences of the United States of America*, 93(11), pp. 5191–5196. Available at: https://www.ncbi.nlm.nih.gov/pubmed/8643551.

Tan, T. H. *et al.* (2001) 'Macrophage migration inhibitory factor of the parasitic nematode Trichinella spiralis', *The Biochemical journal*, 357(Pt 2), pp. 373–383. Available at: https://www.ncbi.nlm.nih.gov/pubmed/11439086.

Tannous, A., Pisoni, G. B. and Hebert, D. N. (2015) 'N-linked sugar-regulated protein folding and quality control in the ER', *Seminars in Cell & Developmental Biology*. Academic Press, 41, pp. 79–89. doi: 10.1016/J.SEMCDB.2014.12.001.

Vattem, K. M. and Wek, R. C. (2004) 'Reinitiation involving upstream ORFs regulates ATF4 mRNA translation in mammalian cells', *Proceedings of the National Academy of Sciences of the United States of America*. 2004/07/26. National Academy of Sciences, 101(31), pp. 11269–11274. doi: 10.1073/pnas.0400541101.

Walter, F. *et al.* (2015) 'Imaging of single cell responses to ER stress indicates that the relative dynamics of IRE1/XBP1 and PERK/ATF4 signalling rather than a switch between signalling branches determine cell survival', *Cell Death Differ*. Macmillan Publishers Limited, 22(9), pp. 1502–1516. doi: 10.1038/cdd.2014.241.

Weiser, W. Y. *et al.* (1989) 'Molecular cloning of a cDNA encoding a human macrophage migration inhibitory factor', *Proceedings of the National Academy of Sciences of the United States of America*, 86(19), pp. 7522–7526. Available at: https://www.ncbi.nlm.nih.gov/pubmed/2552447.

Zhu, Y. X. *et al.* (1996) 'Multiple Transcription Factors Are Required for Activation of Human Interleukin 9 Gene in T Cells', *Journal of Biological Chemistry* , 271(26), pp. 15815–15822. doi: 10.1074/jbc.271.26.15815.

Zimmermann, R., Müller, L. and Wullich, B. (2006) 'Protein transport into the endoplasmic reticulum: mechanisms and pathologies', *Trends in Molecular Medicine*, 12(12), pp. 567–573. doi: http://dx.doi.org/10.1016/j.molmed.2006.10.004.

Appendix:

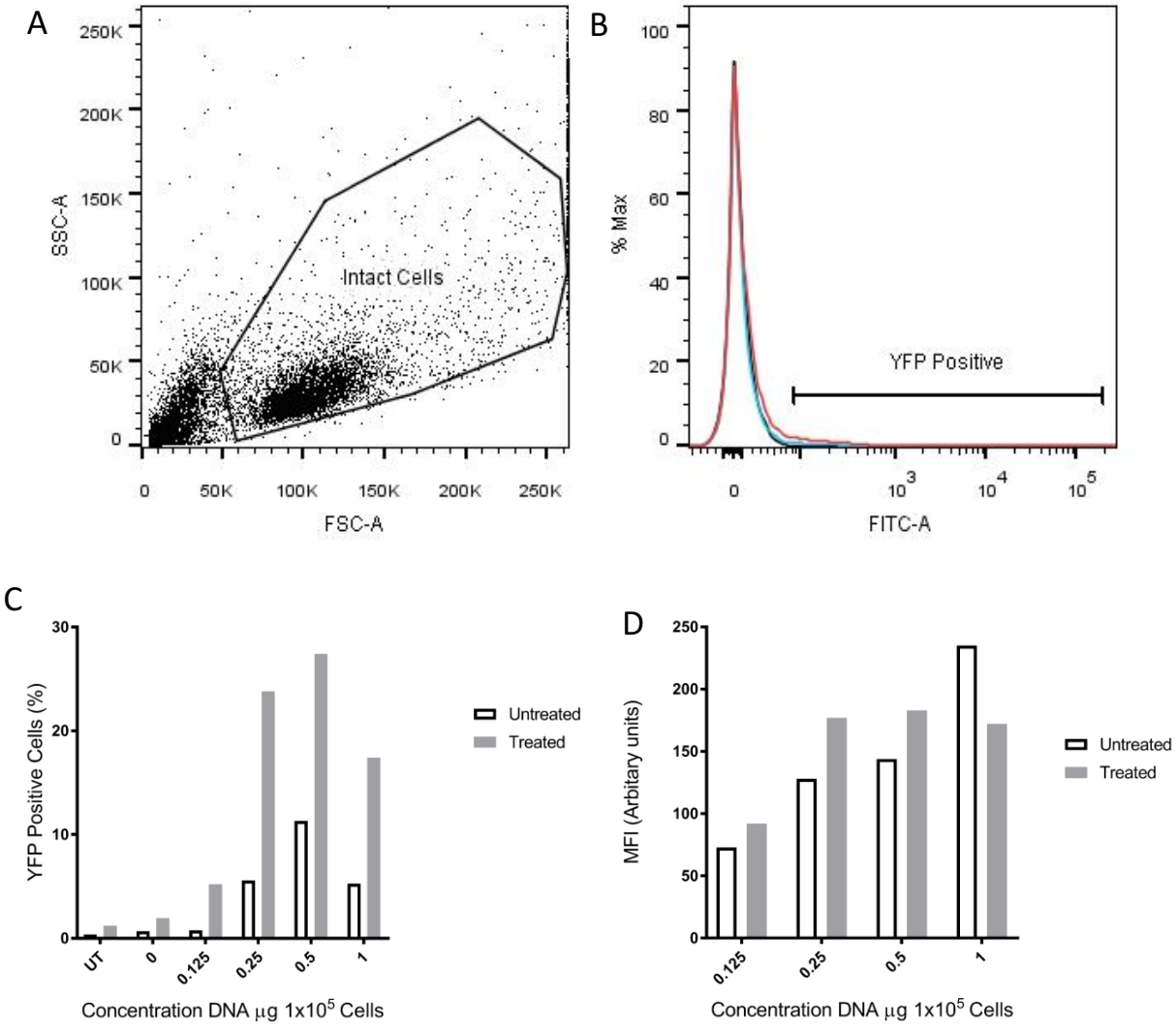

Figure S1: **Optimisation of HEK 293 Cells Transiently Transfected with Different Doses of XBP-1.eYFP Transcriptional Reporter.** HEK 293 cells were seeded 24 hrs before transfection with the XBP-1.pEYFP-N1 reporter construct and treatment with 150 nM TPG. Sixteen hours after treatment cells were collected fixed and analysed by FACS (A). Intact cells were assessed for levels of eYFP. The eYFP positive gate was set so that less than 0.1% of the untransfected cells fell within the gate. The histogram (B) shows representative results using 0.25 ug reporter DNA/10^5 cells. The graph (C) shows the percent of eYFP positive cells 16hrs after treatment with TPG in Hela cells transfected with a range of reporter plasmid DNA concentrations (ranging 0.125- 1µg DNA/1x10^5 cells, UT: Untransfected cells). The changes in the MFI of the eYFP positive cells is also shown (D).

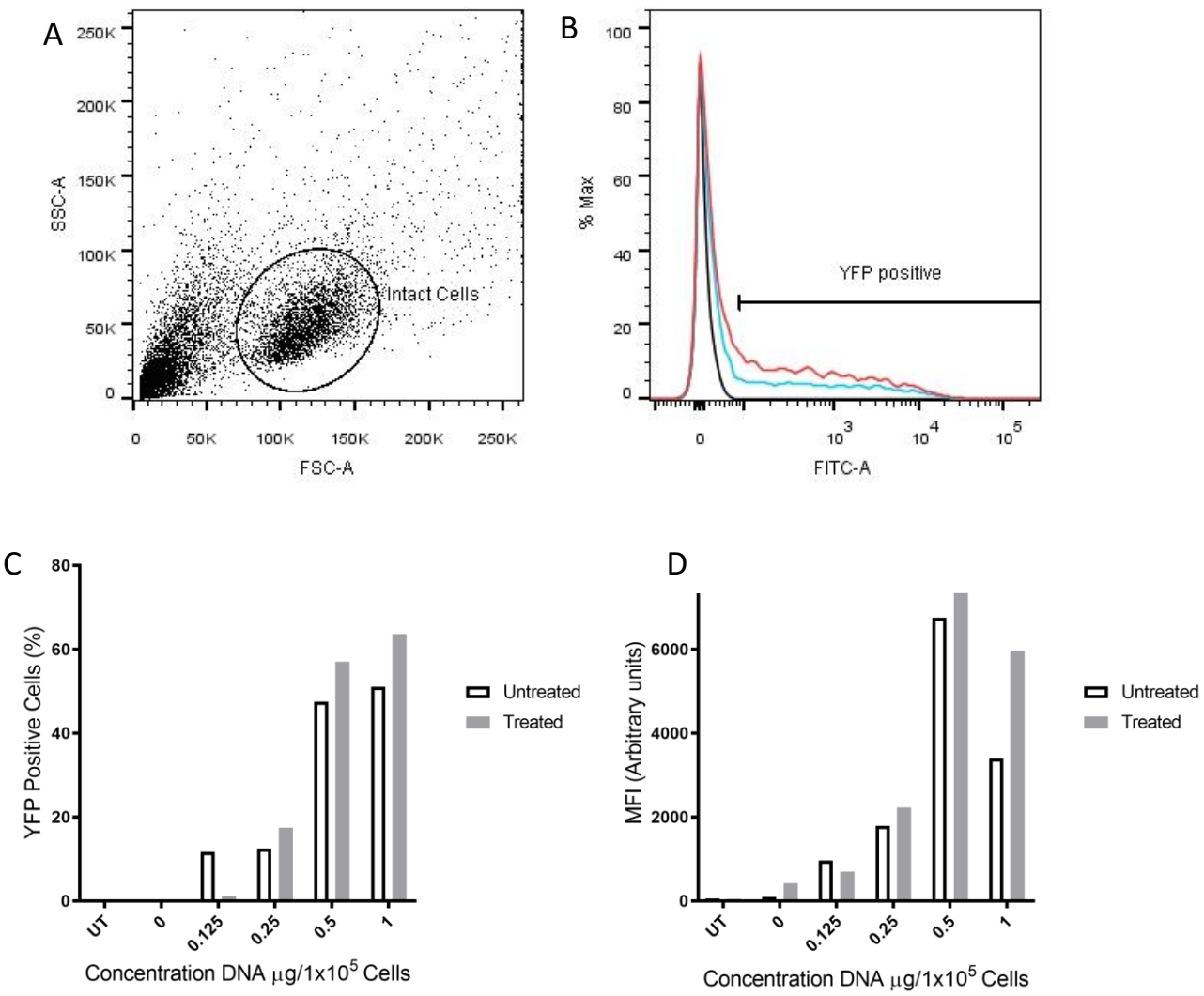

Figure S2: **Optimisation of HEK 293 Cells Transiently Transfected with Different Doses of ATF4.eYFP Transcriptional Reporter.** HEK 293 cells were seeded 24 hrs before transfection with the XBP-1.pEYFP-N1 reporter construct and treatment with 150 nM TPG. Sixteen hours after treatment cells were collected fixed and analysed by FACS (A). Intact cells were assessed for levels of eYFP. The eYFP positive gate was set so that less than 0.1% of the untransfected cells fell within the gate. The histogram (B) shows representative results using 0.25 ug reporter DNA/10^5 cells. The graph (C) shows the percent of eYFP positive cells 16hrs after treatment with TPG in Hela cells transfected with a range of reporter plasmid DNA concentrations (ranging 0.125- 1μg DNA/1x10^5 cells, UT: Untransfected cells). The changes in the MFI of the eYFP positive cells is also shown (D).

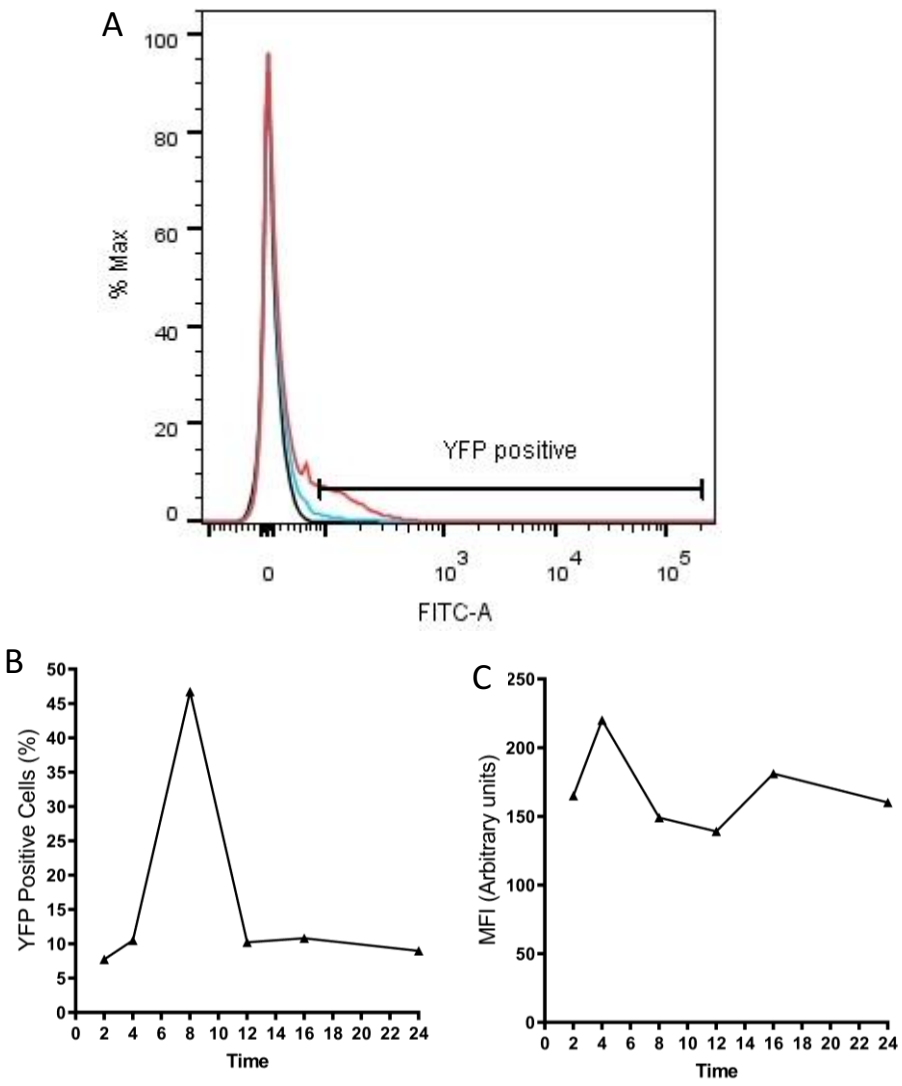

Figure S3: **The Activation of the XBP-1.eYFP Transcriptional Reporter over Time in HEK 293 Cells after Treatment with TPG.** HEK 293s cells were seeded 24 hrs before transfection with the XBP-1.pEYFP-N1 reporter construct and treatment with 150 nM TPG. Sixteen hours after treatment cells were collected fixed and analysed by FACS (A). Intact cells were assessed for levels of eYFP. The eYFP positive gate was set so that less than 0.1% of the untransfected cells fell within the gate. The histogram (B) shows representative results using 0.25 ug reporter DNA/1x10^5 cells. The graph (C) shows the percent of eYFP positive cells 16hrs after treatment with TPG in Hela cells transfected with a range of reporter plasmid DNA concentrations (ranging 0.125- 1µg DNA/1x10^5 cells, UT: Untransfected cells). The changes in the MFI of the eYFP positive cells is also shown (D).